CHEMISTRY AND SUMMER-TIME FLUXES OF SELECTED
Nr SPECIES SETTLING THROUGH DUSTFALL
IN AND AROUND DELHI

Dissertation submitted to the Jawaharlal Nehru University
in partial fulfilment of the requirements
for the award of the degree of

MASTER OF PHILOSOPHY

REEMA TIWARI

SCHOOL OF ENVIRONMENTAL SCIENCES
JAWAHARLAL NEHRU UNIVERSITY
NEW DELHI-110067
INDIA
2015

जवाहरलाल नेहरू विश्वविद्यालय
Jawaharlal Nehru University
SCHOOL OF ENVIRONMENTAL SCIENCES
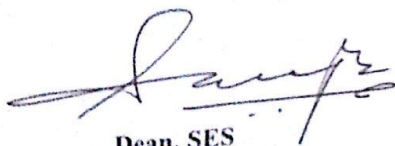New Delhi- 110 067, INDIA

Date: 27.07.2015

DECLARATION

I declare that the dissertation entitled *"Chemistry and Summer-time Fluxes of Selected Nr Species Settling through Dustfall in and around Delhi"* submitted by me for the award of the degree of **Master of Philosophy** of Jawaharlal Nehru University is my own work. The dissertation has not been submitted for any other degree of this university or any other university.

REEMA TIWARI

CERTIFICATE

We recommend that this dissertation be placed before the examiners for evaluation.

Dean, SES

Acting Dean/SES/JNU

Prof. U.C. Kulshrestha
(Supervisor)

Dedicated to
My
Parents

Acknowledgement

My dissertation would be incomplete if I do not mention a few words of gratitude towards all those have helped me cruise smoothly through my endeavours. I am highly indebted to my supervisor, Prof U.C. Kulshrestha, for providing me the opportunity of completing my dissertation under his esteemed guidance. His valuable inputs and constructive suggestions have always been of great help in the pursuance of my objectives. I have much regards for him for always providing the right shape to my thoughts, ideas and suggestions.

I would like to express my regards to Prof. A.K. Attri, Ex – Dean and Prof. I.S.Thakur, present dean, School of Environmental Sciences, for providing me the necessary facilities for the completion of my research work.

I would like to extend my heartfelt thanks to all the faculty members and staff members of School of Environmental Sciences for their kind support during the study period.

Words seem to be less to express my gratitude to Gyan sir for his constant help and valuable guidance at each and every step of my dissertation. His high tolerance and extreme patience for handling over my silly mistakes has really paid off in the end. I would also like to extend my thanks to Pallavi mam, Disha mam, Anita mam, Shabana mam, Babloo sir, Saurabh sir, Kopal, Aijaz, Saumya mam and Anshu for constantly providing that motivational zest to achieve for the excellence in life.

No written acknowledgment can express my feelings for my friend Manisha for being the pillar of support in all the ups and down throughout my dissertation work. Late night lab shifts would have been incomplete without her packed dinners and chirpy gossips. I would also like to extend my heartfelt thanks to my lovely junior Sudesh for all the time and energy she has invested in helping me out during sampling.

I would be failing my duty if I don't mention my sincere thanks to lovely Priyanka as for without her I couldn't have found a second home in the campus. I am also

thankful to Madhavi for investing a great deal of patience in making pictures and maps for my work apart from her moral support. And yes, how can I ever forget to thanks Sapna mam, Prince, Harpreet, Prabhat and Akash for their unconditional support and motivational push throughout my dissertation.

I cannot eschew to mention my family members and near ones, who deserve more than a written acknowledgement. It is primarily the sacrifices they made for my education and unconditional support, which has sustained my confidence throughout life.

Reema Tiwari

CONTENTS

LIST OF FIGURES

LIST OF TABLES

Chapter 1
Introduction

1. Introduction

Ever since the infamous episodes of the Los Angeles (photochemical) smog of 1944 and London (sulphurous) smog of 1952, there has been a growing recognition of the reactive and oxidizing species in the atmosphere. As a major driver of air pollution chemistry and climate change, reactive nitrogen species (Nr) has undergone a rapid accumulation in the environment. With the declining levels in the sulphate aerosol formation accompanied by an expected rise in the nitrate precursor gas emissions, the Nr species is gradually becoming one of the most pressing issues of the environment (Reis et al., 2009). This is clearly evident from its increased conversion rates of NO_x into HNO_3 and PAN that has gone up from <5% hr^{-1} to 24% hr^{-1} in the urban plumes (Berkowitz et al., 2004). But the tropospheric chemistry of Nr has not been able to gain much significance over the developing nations as the focus of the problems has been more on SO_x emissions.

With the growing incidences of acid rain and air borne toxins becoming a potential threat to our already fragile ecosystems, there is a need for renewing our scientific and societal understanding of the global environmental problems beyond the conventional monitoring. Therefore, the determination of atmospheric fluxes has turned out to be an indispensible tool for addressing the contemporary issues of atmospheric chemistry, acidification and eutrophication of the ecosystem. With mineral dust providing the surface reactive sites for the heterogeneous chemistry involved in the absorption and deposition of Nr from the atmosphere, there is a need for comprehensive study linking the role of dust particulates in its transport and removal of the Nr from the troposphere.

1.1 Atmospheric Dust

The solid particles in the atmosphere that eventually settle down under its own weight are known as the atmospheric dust (ISO 4225, 1994). These are usually in the size range of 1 μm up to 1000 μm with particles smaller than 40 μm constituting the suspended dust in the atmosphere (Kaushik and Khare, 2009).

Dust is considered as one of the most important atmospheric components that has adversely affected the global as well as regional atmospheric conditions. Through

the scattering and absorption of the solar radiations, it has affected the radiative balance of the earth. It's involvement as the cloud condensation nuclei has led to the modification of the cloud properties which has indirectly affected our climatic system (Zhang et al, 2003). But the most significant influence of the atmospheric dusts has been observed on the tropospheric chemistry through its involvement in various heterogeneous reactions and participation in biogeochemical cycling of various trace substances (Kulshrestha et al, 2003).

Therefore, the understanding of the chemical composition of the dust particles has become important for the purpose of not only identifying its possible source areas but also for its impact on the chemical and physical process of the atmosphere. Based on the current atmospheric aerosol research findings in India, a typical dust particulate is said to have been composed of the inorganic elements, ions, organic constituents and Black Carbon/ Elemental Carbon etc (Krishna et al, 2012).
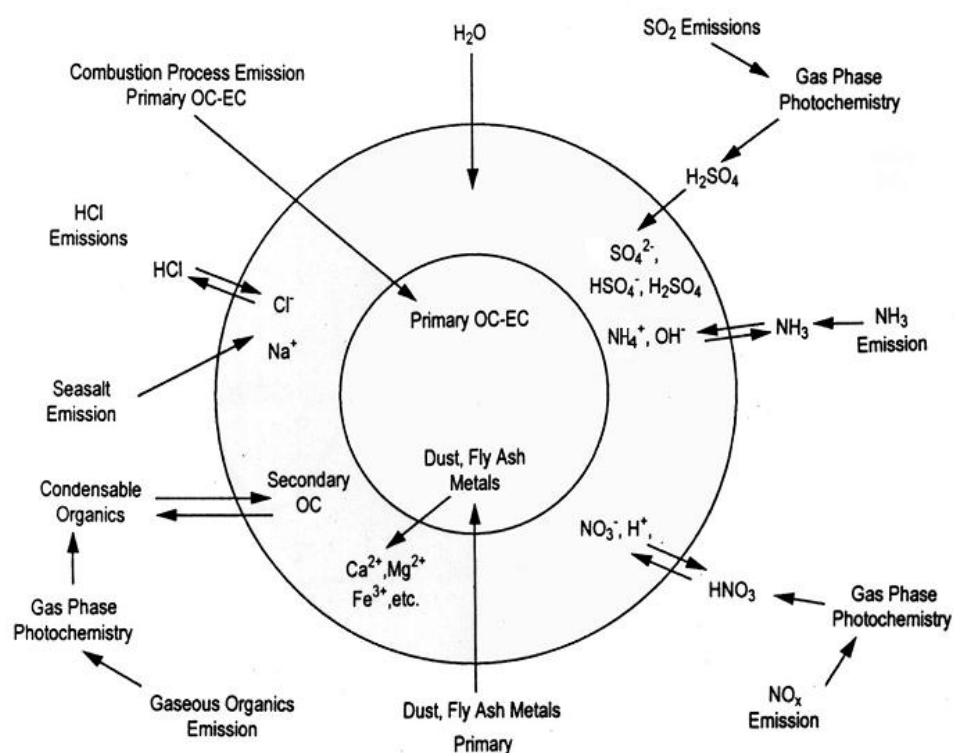
Fig.1.1. Major chemical components involved in the formation of atmospheric dust (Song et al., 2001).

1.2. Sources of atmospheric dust

Depending upon the method of introduction of the particulates into the atmosphere, the dust sources can be primary or secondary in nature. Primary sources are the ones characterized by the direct emission of the particulates in the atmosphere. Secondary sources, on the other hand, are the indirect sources that emit precursor gases into the atmosphere which via gas to particle conversion generates secondary particulates. Injection of dust to the atmosphere can also occur by a variety of natural and anthropogenic processes, where bulk of the particulates in the atmosphere (about 90% by mass) has natural origin.

Table. 1.1. Global source strength and burden of the dust aerosol (Lawrence et al., 2009).

Aerosol type		Flux (Tg/ yr)	Burden (Tg)
Natural Emissions			
Primary	Mineral dust	1678	19.2
	Sea salt	7925	7.52
Secondary	DMS	18.2	
	SO_2 from explosive volcanoes	2	
	SO_2 from degassing volcanoes	12.6	
	NO_x from soils and lightning	12	
	Biogenic organics	19.1	
Total		**9666.9**	**26.72**
Anthropogenic emissions (fossil fuel, bio fuel, wild fires)			
Primary	Particulate organic matter	66.1	1.7
	Black carbon	7.7	0.24
Secondary	SO_2	112.6	1.99
	NO_x	38	
Total		**224.4**	**3.93**

Based on the relative strength of dust sources and its contribution to the total dust budget, two major types of the atmospheric dust has been identified-carbonaceous

dust and mineral dust. Major industrial pollution regimes in Europe, Asia and North America have accounted for 85% of the global pollution sources of BC and OC. Desert regions of North Africa, Middle East and Asia, on the other hand, has contributed 90% to the mineral dust emissions with Africa contributing 60% of its emissions to the mineral dust loading (Chin et al., 2007).
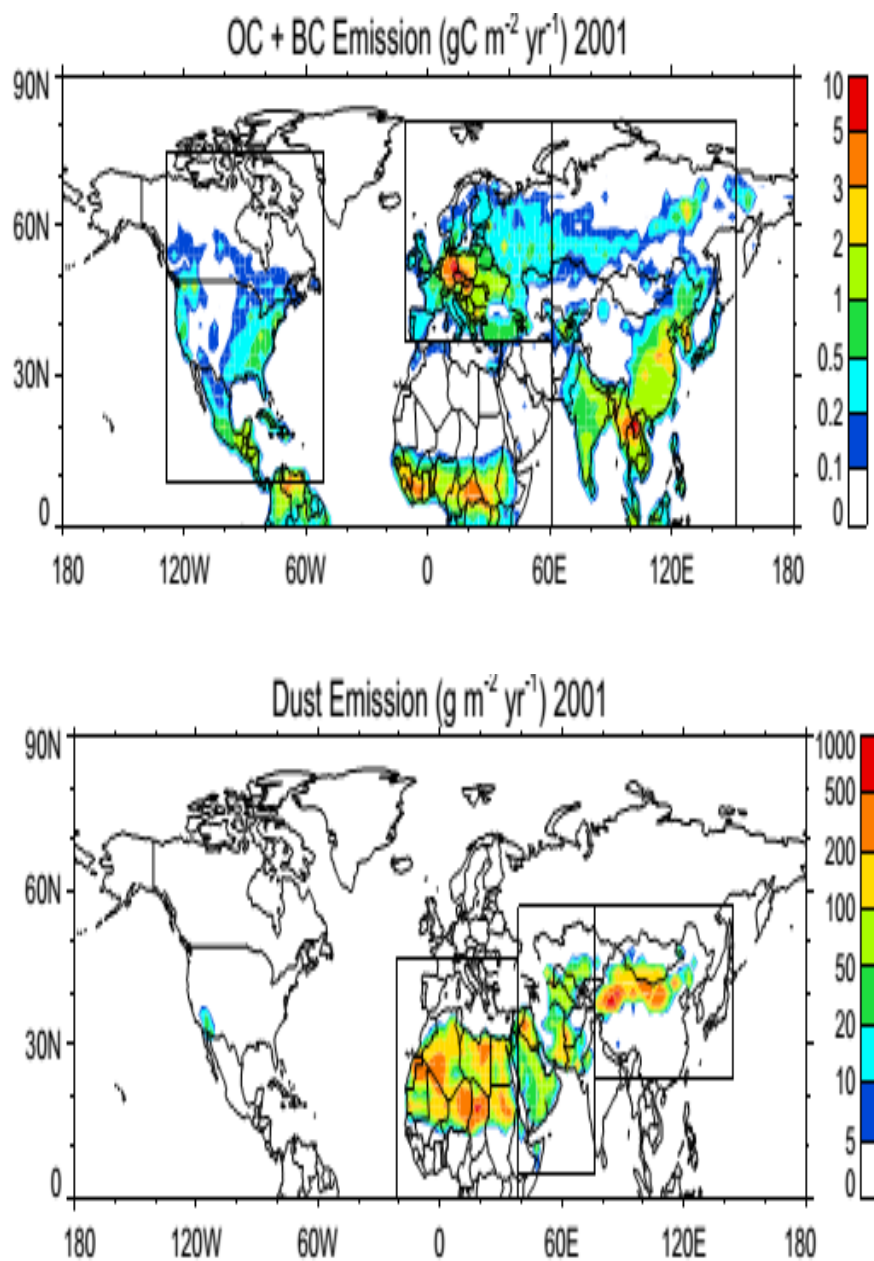
Fig.1.2. Domains of major atmospheric dust sources using GOCART model (Chin and Diehl., 2007).

1.3. Deposition of atmospheric dust

Once in the atmosphere, the dust particle starts to evolve in time and space by the way of transportation, transformation and deposition. Amongst the three processes, it is the mechanism of deposition that has provided the ultimate sinks to atmospheric dust. It is defined as the removal of particles and trace gases from the atmosphere with its subsequent collection on to some physical surface on the ground (Wallace and Hobbs, 2006)

Depending upon the solubility of the dust species in water and the amount of the precipitation received in the region, deposition is of two types:

a) Wet deposition

It is the process of scavenging and removal of the particles through the formation of rain, cloud, snow or fog which is primarily involved in the removal highly soluble gases and fine mode particulates.

b) Dry deposition

It is the process of removal of particles via gravitational settling or through atmospheric turbulence under no precipitation condition.

The relative importance of these two mechanisms shows temporal as well as spatial variation. Dry depositions are usually observed near the desert belt regions characterized by the long spells of dry conditions. As a resultant, the arid and semi arid tracts of northern India with short period of monsoon restricted to a four month period (June–September) have major dust plumes originating from the nearby Thar Desert that highly favours the mechanism of dry deposition over the wet deposition.

Based on the concept of the depositional velocities and the size range of the settling particle, the dry deposition can occur via gravitational sedimentation, impaction or interception. Brownian diffusion becomes significant for the particles less than 1 μm that falls below the size range of dust (Davidson, 1995). Removal of large particles (>10 μm) takes place via gravitational sedimentation. It involves the deposition of dust close its emission sources owing to the high depositional velocities of the settling

particles. Impaction and interception, on the other hand, involves deposition of particles lying between 1 – 10 μm size ranges (Fig. 1.3).
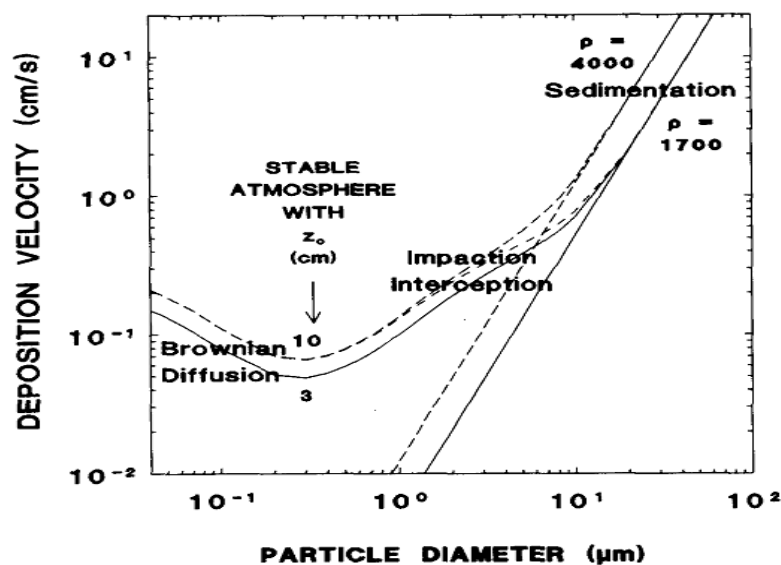
Fig. 1.3. Types of dust deposition as a function of its size (Davidson., 1995).

1.4. Global rates of dust deposition

The dust deposition has undergone major changes with fluctuation being typically attributed to the anthropogenic intrusions. Contemporary land use pattern accompanied with soil disturbance through grazing, urbanization and off road vehicle use has resulted in an increased rate of dust fluxes into the atmosphere by increasing the proneness of the surfaces to the wind erosion process (Prospero and Lamb, 2003). Dust fluxes are considered sensitive to the seasonal parameters of precipitation, meteorology, land use changes, vegetation, transport dynamics and distance from the source (Tegen et al., 1994; Arimoto et al., 1997; Bory et al., 2002 a; O'Hara et al., 2006, Lawrence et al., 2009). This has created a global variability in the dust deposition rates spanning from 0.05 g m^{-2} yr^{-1} over Penny Ice Cap in Northern Canada (Zdanowicz et al., 1998) to 450 g m^{-2} yr^{-1} over Taklimakan desert of China (Zhang et al., 1998).

The particles with larger sizes have been observed to undergo deposition deposited near its source owing to the high depositional velocity of the gravitational settling. High wind speed, on the other hand, promotes the distance up to which the

dust particles are to be transported. Deposition rates are thus, observed to be higher over the regions closer to the potential source of dust plume (Lawrence et al, 2009). Therefore, the deposition rates are generally observed to higher over the regions closer to the potential source of dust plume with frequent occurrence of dust storm events.
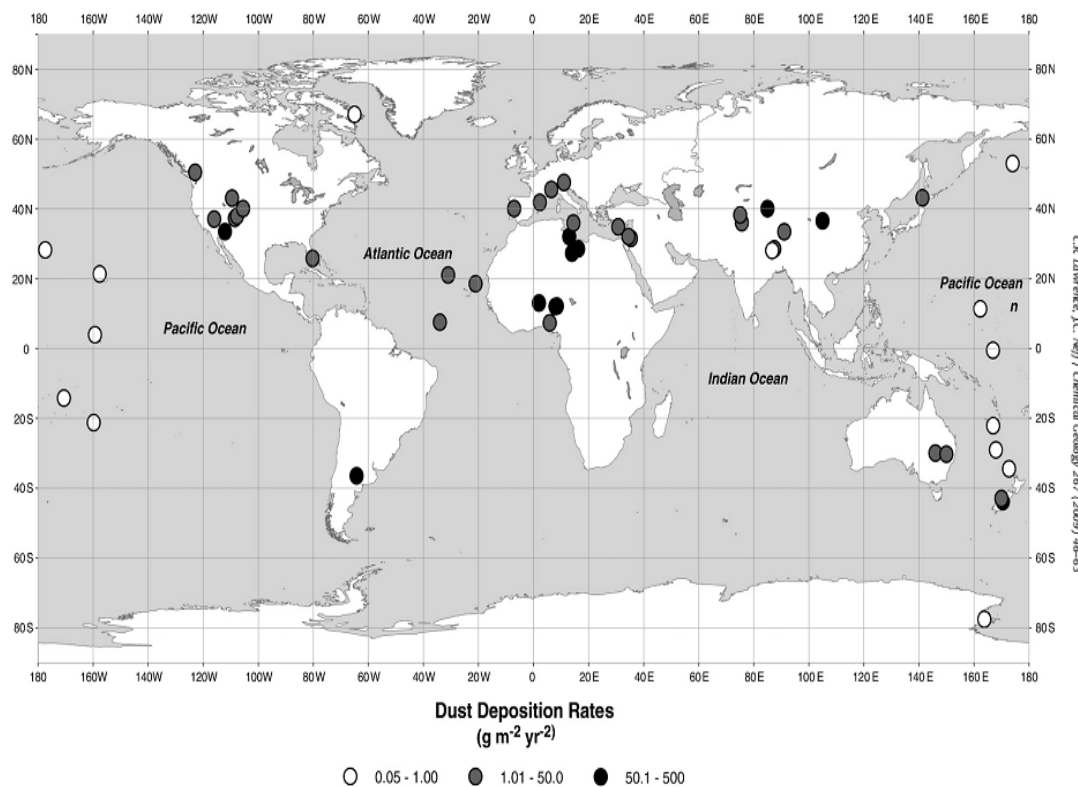
Fig.1.4. Spatial variation in the dust deposition rates (Lawrence et al., 2009).

Presence of surface features like vegetation or soil crust are known for muting the forces exerted by the wind, thereby, reduces the susceptibitly of the soil to wind erosion and dust emissions. Therefore, a dry bare soil will tend to be the largest emitter of the dust as compared to a moist vegetated soil (Okin et al., 2001). Vegetation exhibits a variety of morphologies, some of which are more effective than others in trapping the atmospheric dusts (Tegen et al., 2002). Hence, any change in the composition and morphology of the vegetation will have a direct impact on the depositional rates of the dust.

Amongst the other physical factors, the positioning of the landscape has also been observed to have a significant impact on the dust deposition rates. Leeward slope of the mountains and the valleys are known for reducing the size distribution of the dust

deposited particle grain sizes (Goosens et al., 2006). Therefore, high deposition rates of dust are usually observed over the leeward slope as compared to the windward slopes of the hills (Hoffman et al., 2008).

1.5. Significance of dust deposition

The arid and semi arid regions of India are often encountered by the frequent occurrence of dust storms owing to the shifting precipitation pattern and land use changes. These dust storm events are usually characterized by the long distance global transfer of the mineral aerosols accounting for ~ 50% of the total aerosol mass loading (Duce et al., 1991; Andreae et al., 1995). At global and local levels the mineral dusts has significantly impacted the atmospheric chemistry and geo chemical mass cycling by providing surface reactive sites for various heterogeneous reactions occurring in the troposphere (Usher et al, 2003).

Any proximity of the mineral dust sources to the industrial pollution and bio mass burning results in blend of a chemical mix of particulates with gases (Maxwell, 2004). This complex interaction, therefore, becomes indicative towards the possible role of the mineral dust in the scavenging of the gaseous pollutants from the atmosphere (Krueger et al, 2003). While the coarse mineral mass with the sizes above 10 μm tends to deposit near its source, the fine mineral dust, on the other hand, have the tendency to be transported over the oceans and across the continents (Sami et al, 2006). As a result, dust fall becomes an important mechanism for controlling the fate of the air borne pollutants at a local level.

Dustfall can be defined as the deposition of the coarse particles from the atmosphere by the process of gravitational settling. The removal rate of the gaseous pollutants through the process of dust fall depends on the uptake coefficient of the dust particles which is defined by its reaction probability or reactive sticking coefficient (γ) (Table1.2).

Table. 1.2. Uptake co efficient of various species for describing heterogeneous chemistry on mineral dust (Dentener et al., 1996).

Species	Uptake coefficient (γ)
HNO_3	0.1
N_2O_5	0.1
HO_2	0.1
O_3	5×10^{-5}
SO_2	3×10^{-4} at RH < 50% 0.1 at RH > 50%

It has been observed that the mineral dust has a high affinity for SO_2 uptake (Kulshrestha et al., 2003) and the value of the uptake co efficient is higher at high relative humidity (Usher, 2003). Therefore, the regions spanning from East Asia to Pacific Ocean have over 60% of sulphate associated with the mineral dust. But owing to the gypsiferous nature of the soil existing in the Thar, Iranian and Arabian Desert, the coarse sulphate can either come from the long range transport of the mineral dust or from the erosion of the soil itself (Dentener et al., 1996). Therefore, the origin of the coarse sulphate has always been a subject of speculation in Indian regions. According to Kulshrestha (2013), calcium carbonate rich dust acts as an efficient scavenger of atmospheric SO_2 that has eventually resulted in the formation of calcium sulphate in Indian region.
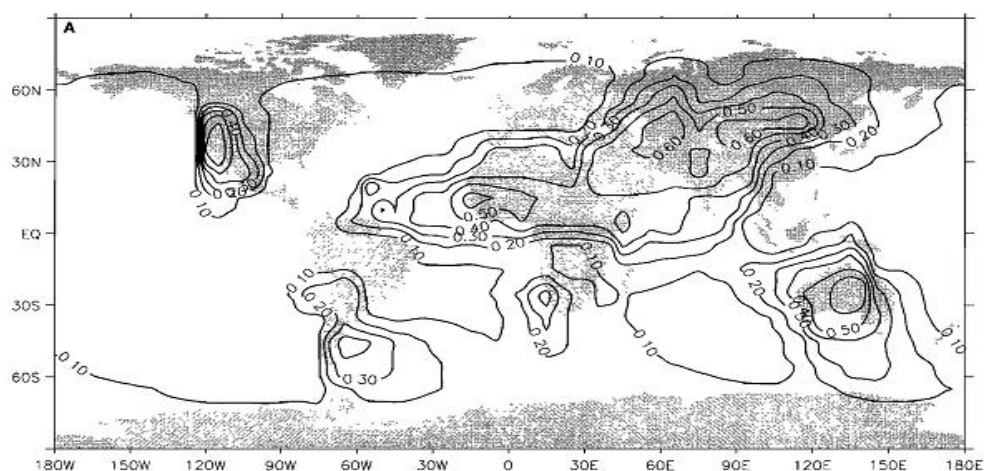
Fig. 1.5. Annual average ratio of sulphate on the mineral dust to the total sulphate (Dentener, 1996).

Mineral dust, on the other hand, shows a high uptake co efficient of nitrates from the atmosphere irrespective of the relative humidity level (Michel and Usher, 2003). This has a significant consequence of HNO_3 being present on the mineral dust which can be removed faster near the dust source regions rather than being subjected to the long range atmospheric transport.
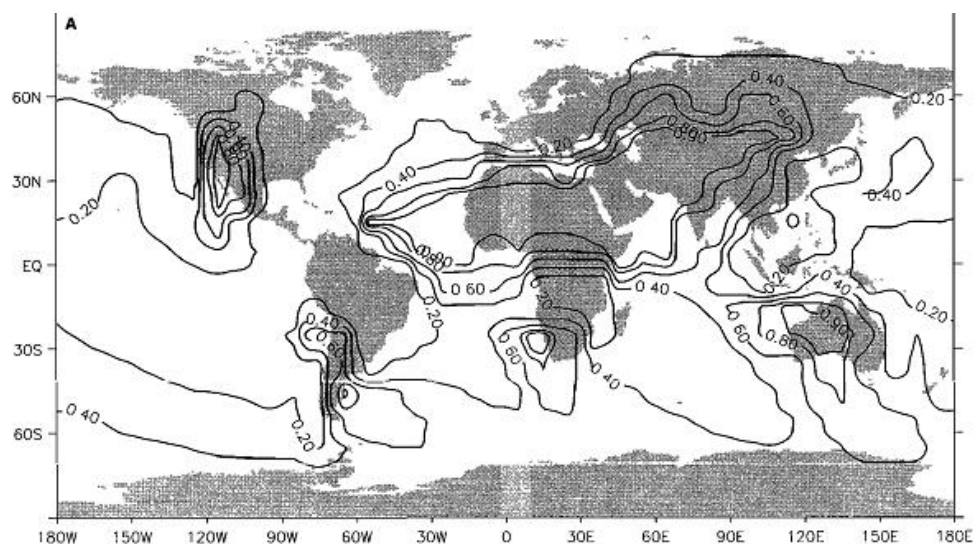
Fig.1.6. Annual average ratio of nitrates on mineral dust to the total nitrate (Dentener, 1996).

1.6. Nitrogen and reactive nitrogen in atmosphere

Nitrogen in the atmosphere is present either as "fixed" or the "non reactive" nitrogen consisting of the inert state N_2 gas that accounts for 99.99% of all the nitrogen in the atmosphere or as "reactive nitrogen" (Nr) consisting of plethora of biologically active, photo chemically reactive and radiatively active N compounds which are present at trace levels in the atmosphere (Galloway, 2004).

Since the beginning of the 19th century, humans have been altering the pace of global nitrogen cycling which is clearly reflected in their growing demand of nitrogen in agriculture and industries along with the increased combustion of fossil fuels and the pervasive inefficiencies in its use. This has accelerated the transformation rates of inert N_2 gas into Nr compounds resulting in a cascade of environmental problems. Reactive nitrogen compounds can be organic (peroxyacetyl nitrate) or inorganic (nitrates) depending upon the photochemistry involved in its formation. While PAN tends to be

abundant in the regionally polluted environment with active organic photochemistry, the inorganic nitrates, on the other hand are abundant even over the remotest areas of the troposphere. The inorganic Nr further involves reduced (NH_3, NH_4^+) and oxidized species (NO_3^-, NOx) of which NO_X are considered as the primary reactive nitrogen species that further reacts to produce other Nr species (HNO_3, NH_4^+ and NO_3^-) in the atmosphere (Kulshrestha, 2014). While ammonia is the most abundant alkaline gas responsible for neutralizing acids formed in the atmosphere, NO_X on the other hand is known to play a crucial role in the tropospheric and stratospheric chemistry (Bradshaw et al 2000).

Growth in the global population has heightened the rate of Nr accumulation in the environment but with an uneven distribution around the world (Galloway et al, 2008). Regions characterized by high energy and food production have excess Nr accumulating in its air, water and soil, moving between each compartment and causing subsequent environmental and socio economic problems. Regions with low soil fertility and scarce crop nutrients like the Sub Saharan regions, on the other hand, are grappling with a different set of challenges associated with the deficiency of Nr. Agriculture in such areas is unable to meet the basic food requirement to sustain neither its population nor its economic development (UNEP 2007).
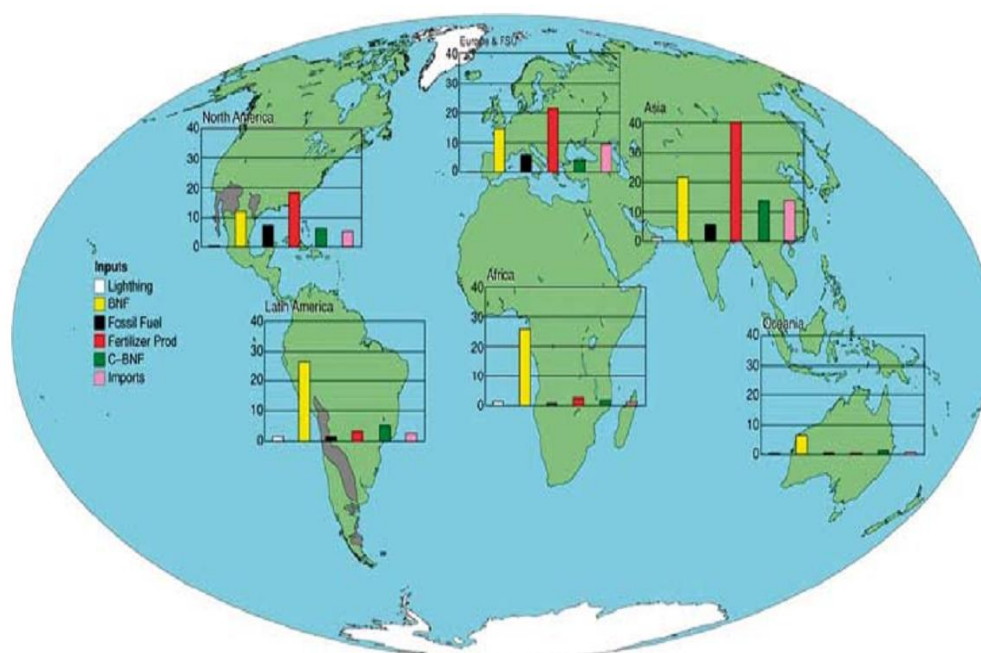
Fig.1.7. Regional Imbalances of Nr in atmosphere (UNEP, 2007).

1.7. Emission inventory of reactive nitrogen

By placing the current alteration of N cycle into historical context, the anthropogenic emission sources have surpassed over the natural sources of reactive nitrogen. The food and energy production activities have increased the Nr emission rates by a factor of 10 as compared to the late 19th century (Galloway et al., 2006). As a result the global emission of Nr have gone up from 34 Tg N yr^{-1} in 1860 to 100 Tg N yr^{-1} in 1995 and is projected to reach up to 200 Tg N yr^{-1} by 2050 (Galloway et al., 2008).

Emissions of Nr occur primarily as NO followed by its oxidation to NO_2 that together constitutes the family of NOx species (Zellwegar et al., 2003). Recent global anthropogenic NOx emission rates has been estimated to be about 40 Tg N yr^{-1} for the year 2000 with major part of the emissions originating through the fossil fuel combustion (~30 Tg N yr^{-1}) by the road transport sector (10 Tg), the energy sector (7.5 Tg), shipping and aviation (6 Tg), industries (4.5 Tg) and buildings (3 Tg) with an additional 6 Tg N yr^{-1} originating from biomass burning (Galloway et al., 2006). As the transport and power production are expected grow rapidly in terms of fossil fuel combustion, these sectors are likely to dominate NOx emissions in the future especially in the developing countries.
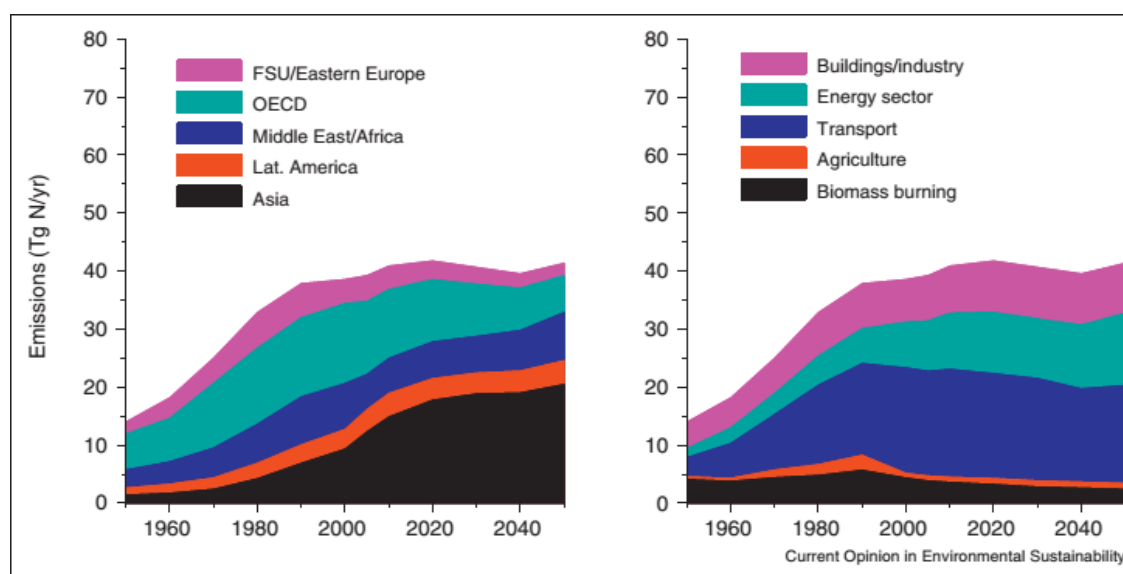
Fig.1.8. Regional and sectoral wise emissions of NOx as per IMAGE reference scenario

(Van Vuuren et al., 2011)

Therefore, the emission inventories of NO_x compiled from 16 HTAP model using fossil fuel generating units, vehicular and shipping activities, biomass burning, home heating units, soil microbial activities and lightening showed highest NO_x emissions from the regions of North America, United Kingdom, central Europe and East Asia owing to its large fossil fuel based power productions and vehicular emissions. India, South America and the western Russian federation, on the other hand, showed mid range levels in its NO_x emissions resulting from its slow economic development (Van Vuuren et al., 2011).
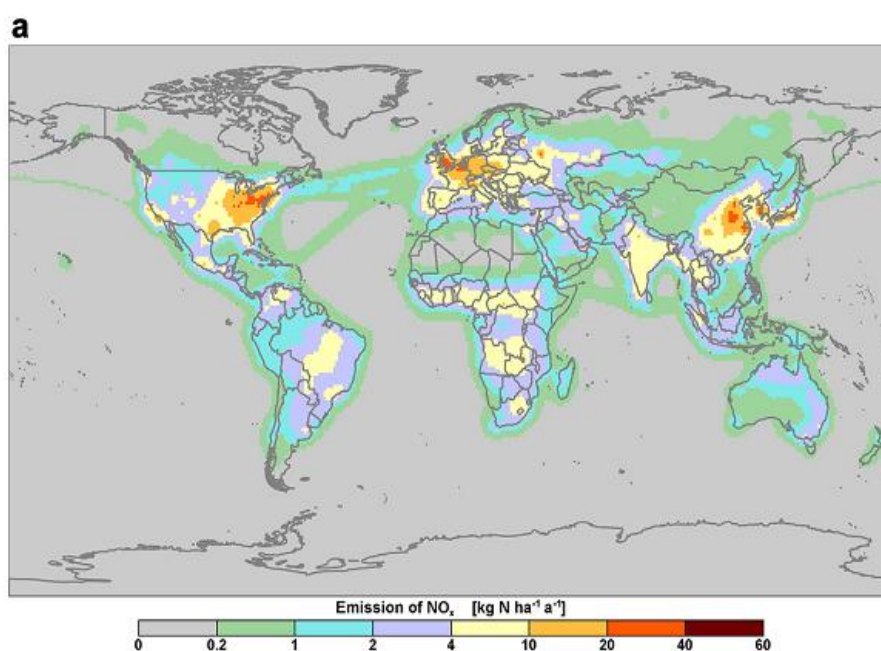
Fig.1.9.a). 2001 ensemble – mean emission of NOx using 16 HTAP NOx model

(Van Vuuren et al., 2011).

Global emissions of ammonia (NH_3) have been estimated to be nearly 40 Tg N yr^{-1} originating primarily from the agricultural activities (30 Tg N yr^{-1}) with minor emissions from light duty gasoline vehicles containing three way catalytic (Galloway et al, 2006). Any future trend in ammonia emissions is, therefore, going to depend majorly on the agricultural practices and the measures that are introduced for its control. Hence, the inventories of global NH_3 emissions that were compiled using biomass burning, animals, industries, fertilizer applications and forest fires in its 7 HTAP NH_3 model showed regions of highest emissions over Western Europe, India, Eastern China and Pakistan with intense agricultural activities (Van Vuuren et al,

2011). Lowest emissions, on the other hand, were recorded over the remote regions of the oceans with equatorial and temperate sections showing somewhat higher levels due to highly uncertain natural sources of NH_3 from the oceans (Dentener et al, 2006).
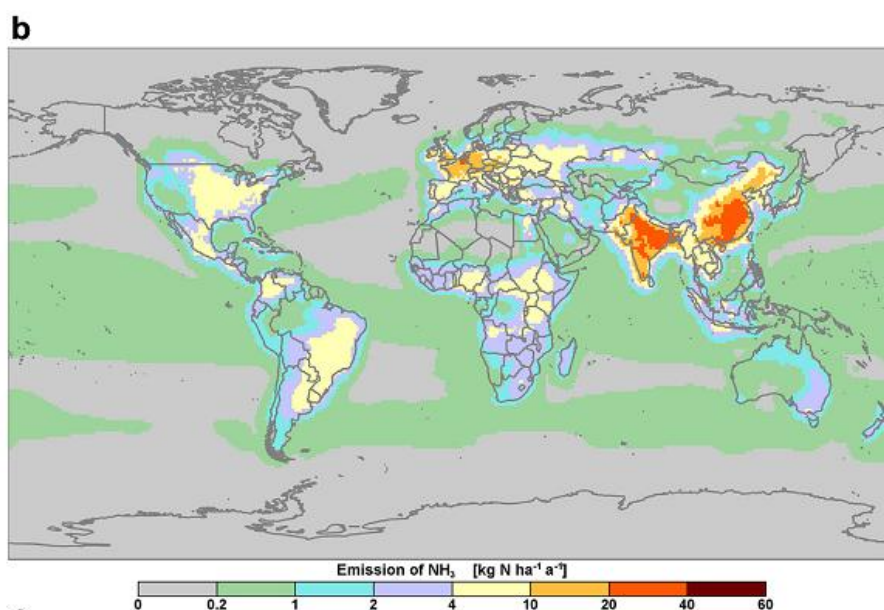
Fig.1.9.b). 2001 ensemble – mean emission of NH_3 by 7 HTAP NH_3 model (Van Vuuren et al, 2011).

1.8. Deposition inventory of reactive nitrogen

Once in the atmosphere, the Nr trace gases become central to the photochemical reactions that either stimulates the production of ozone or results in the formation of NO_y species. A typical residence time of Nr species in atmosphere is about a week. Therefore, the physio chemical transformation they undergo during their long range transport leads to its final removal by wet and dry deposition that contributes significantly to the acidification and Eutrophication of the ecosystems.

Deposition of Nr is strongly controlled by the patterns of the population and its associated activities. Keeping in sync with the emission pattern changes between the year 2000 – 2007, the median deposition values showed a declining trend over Europe (-2.7%) and North America (-4.3%) on one hand, with an increasing Nr deposition over the developing Asia (+13.6%) and Africa (+19 %) on the other (Torseth et al., 2012; IJC 2010). Therefore, the global model estimates have identified three regions of highest Nr depositions – Western Europe (Belgium, Netherlands and Germany) with 20 – 28.1 Kg N ha^{-1} a^{-1}, South Asia (Pakistan, Indian and Bangladesh) with 20.0 – 30.6 Kg

N ha^{-1} a^{-1} and East Asia with 20 – 38.6 Kg N ha^{-1} a^{-1} deposition levels (Vet et al., 2014). Deposition rates of 4–10 Kg N^{-1} ha^{-1} a^{-1} has been identified over North Atlantic, North Indian and North Pacific Ocean owing to the ship emissions as well as transport from the continental emissions off the coastlines.
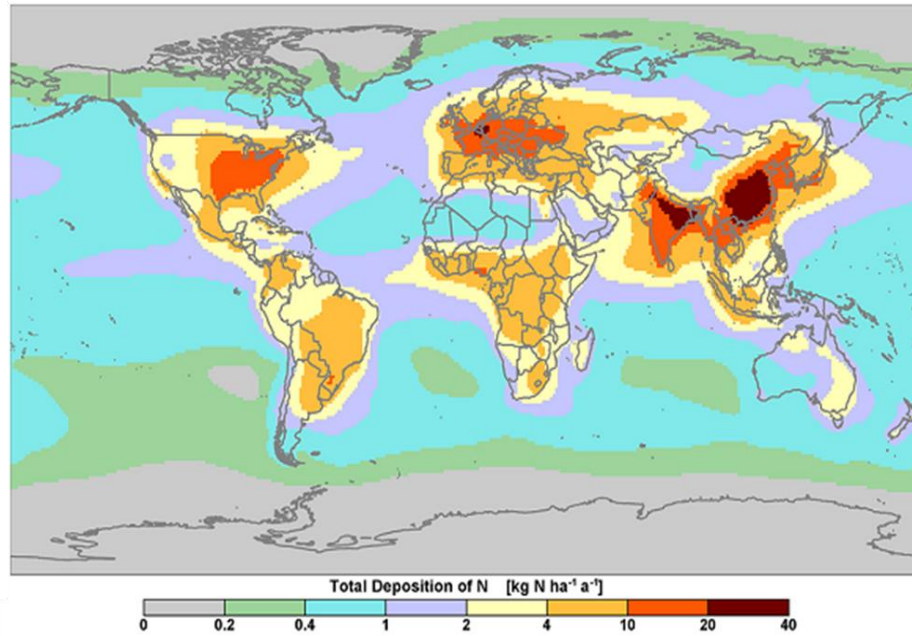
Fig.1.10 a). 2001 ensemble-mean pattern of the total deposition of Nr in Kg N^{-1} ha^{-1} a^{-1}

(Vet et al., 2014).

Though the wet deposition of Nr is considered to be the major removal process amounting to > 80% of it's scavenging in many regions, but the dry deposition of Nr was found to be dominant over the arid and semi arid regions of the world (Rengaranjan et al, 2007). Dry deposition of Nr is usually observed to be higher over the regions with greater than 2 Kg N ha^{-1} a^{-1} emissions and less than 40 cm a^{-1} precipitation depths. Therefore, parts of eastern U.S, western Europe, Northern India, Bangladesh and Eastern China have been identifies as the major regions with highest dry deposition levels reaching up to 10 – 20 Kg N ha^{-1} a^{-1}. (Vet et al., 2014)
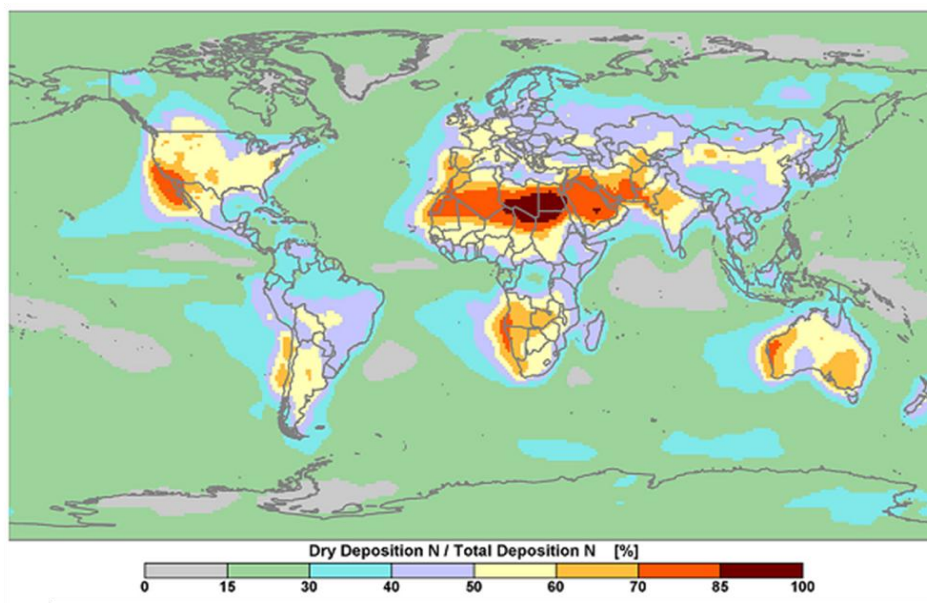
Fig.1.10 b). Percentage ratio of dry to total Nr deposition in 2001 (Vet et al., 2014).

Dry deposition of the Nr species can occur either through direct gaseous deposition or by the formation of nitrate and ammonium particulate. Since the deposition velocity of gaseous Nr species is quite slow, therefore, deposition of Nr through particulate formation is highly preferred.

1.9. Deposition chemistry of Nr

The family of oxidized tropospheric NO_y species (NO, NO_2, peroxy acetyl nitrate, HNO_3 and NO_3^- aerosol) are formed in the troposphere by the subsequent oxidation of the NO_x emissions. These are either involved in maintaining the radical balance of the troposphere by the formation of ozone or are removed from the equation of the tropospheric chemistry by the formation of nitrate particles.

Reduced Nr species like ammonia (NH_3), on the other hand, are involved in the removal of acid (HNO_3 and H_2SO_4) from the troposphere by the formation of secondary inorganic aerosols (NH_4NO_3 and $(NH_4)_2 SO_4$ respectively). As ammonia is the only common base present that is highly soluble in water, hence it provides primary removal mechanisms of NO_y and SO_x from the troposphere by the way of its neutralization reaction.

Therefore the deposition chemistry of the Nr involves formation of NO_y and its subsequent deposition which has been discussed in detail as below:

a). Formation of NO_y

The radical nature of NO_x compounds allows them to undergo series of reactions, where the primary pollutant (NO) under different environmental conditions gets ultimately oxidized to the secondary pollutants like HNO_3 and HNO_2 (NO_y) which has been discussed as follows:

- **Homogeneous gas phase reaction**:

    This reaction takes place characteristically in an oxidant rich environment during daylight hours where the NO_y compounds (HNO_3 and HNO_2) are produced photo chemically via reactions of NO_x with OH (Kondo et al., 2008).

$$NO + O_2H \longrightarrow NO_2 + OH$$
$$NO_2 + OH + M \longrightarrow HNO_3 + M$$
$$NO + OH + M \longrightarrow HNO_2 + M$$
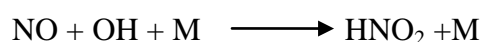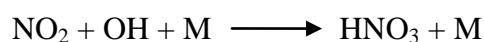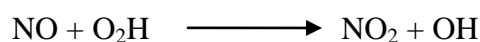
    Where M represent a third body usually N_2 or O_2.

    This reaction is relatively rapid, with an effective second order rate constant ($k=1.1\times10^{-11}$ cm^3 $molecule^{-1}$ sec^{-1}) being 10 times than that of SO^{2-} OH reaction (Lefer et al., 1999).

- **Heterogeneous aqueous phase reactions:**

    The important mechanism in the production of NO_y (HNO_3) in the absence of primary oxidant (OH) during the night time is the **heterogeneous hydrolysis of N_2O_5**. But the reaction has been regarded as too slow to be a significant source of HNO_3. (Pitts and Pitts, 1985)

$$O_3 + NO_2 \longrightarrow NO_3 + O_2$$
$$NO_3 + NO_2 \underset{M}{\longleftrightarrow} N_2O_5$$
$$N_2O_5 + H_2O \longrightarrow 2HNO_3$$
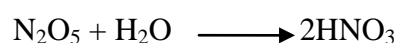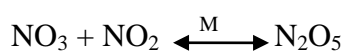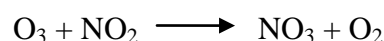
- **Heterogeneous hydrolysis of NO_2** has also regarded as another significant source of NOy (HNO_3 and HNO_2) over areas characterized by the presence of soot, sulphate or sea salt aerosols (Bari et al., 2006).

$$2NO_2 + H_2O \xrightarrow{\text{surface}} HONO + HNO_3$$
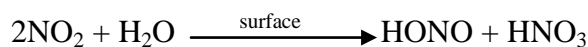
Where the gaseous HNO_3 produced by the above reactions is not observed in equivalent amounts to HONO due to its adsorption on soot surfaces.

Over the polluted urban areas, the formation of NOy by the following heterogeneous reaction occurs in parallel with the above mentioned reaction and has reported to yields of high amount of HNO_2 in the troposphere (Gerecke et al., 1998).

$$NO_2^+ \text{ surface reduced site} + H_2O \longrightarrow HNO_2^+ \text{ surface oxidized site} + OH^-$$

.
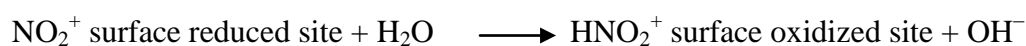
b). Removal of NO_y

Once formed, HNO_3 is most likely to be captured by the coarse mode mineral dust or sea salts that deplete the aerosol nitrate in the fine mode fraction. On the other hand, when ammonia is present in excess, nitrate aerosols are formed. Since this salt of ammonia is not thermodynamically stable, the NH_3 and HNO_3 precursor gases gets evaporated and condensed on pre existing larger aerosol particles and eventually gets removed from the atmosphere (Seinfeld and Pandis, 2006). Chemistry involved in the removal of NO_y from the troposphere involves the following reaction:

- **Uptake by sea salts (NaCl):**

Uptake of HNO_3 by the sea salt has been suggested to be an important removal pathway of NOy in marine and coastal areas (Spokes et al, 2000).

$$HNO_3 \text{ (g)} + NaCl \text{ (aq)} \longrightarrow NaNO_3 \text{ (aq)} + HCl \text{ (g)}$$
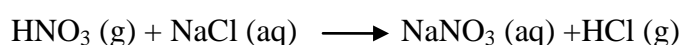
- **Uptake by mineral dusts:**

  This is the primary removal mechanism of NOy in arid and semi arid regions where uptake of HNO_3 is followed by a simple neutralization reaction by the strong base cations (Ca^{2+}) of the dust particles (Dentener et al, 1996)

  $$HNO_3 + CaCO_3 \longrightarrow Ca^{2+} NO_3^- + HCO_3^-$$
  $$HNO_3 + Ca^{2+} NO_3^- + HCO_3^- \longrightarrow Ca(NO_3)_2 + H_2O + CO_2$$
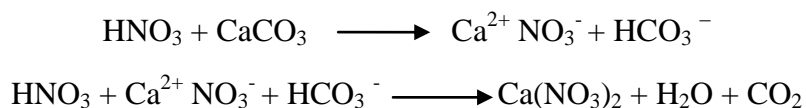
- **Uptake by reduced Nr species:**

  Amongst the reduced Nr species, ammonia is the only common base present in the atmosphere that is highly soluble in water (Bauer et al., 2007) and hence are known to play a key role in the secondary inorganic aerosol formation and its subsequent removal by either wet or dry deposition (Squizzato et al, 2013).

  $$NH_3(g) + HNO_3(g) \longleftrightarrow NH_4NO_3(s) \quad (at\ R.H < 62\%)$$
  $$NH_3(g) + HNO_3(aq) \longleftrightarrow NH_4^+(aq) + NO_3^-(aq)\ (at\ R.H > 62\%)$$
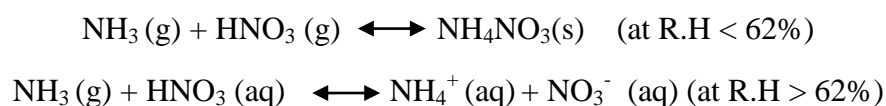
  Since it is an equilibrium reaction, these nitrate aerosols can dissociate back into HNO3 depending upon the conditions of air temperature, humidity and the level of the precursor gas present in the troposphere (Pitts and Pitts, 2000).

1.11. Factors affecting dust deposition of Nr

Dust deposition of Nr is based on the size segregated gas - particle partitioning of reactive nitrogen that subsequently affects the deposition rates and its residence time in the atmosphere. The trace gases with a short lifetime of a day or less can partition into aerosols which have a much longer lifetime of about a week depending upon its size, composition and meteorological conditions (Zellweger et al, 2003). Therefore the formation, evolution and the size dependent deposition of the inorganic particles from the atmosphere is highly dependent on the interactions of the gaseous precursors with the environmental conditions (Squizzato et al, 2013).
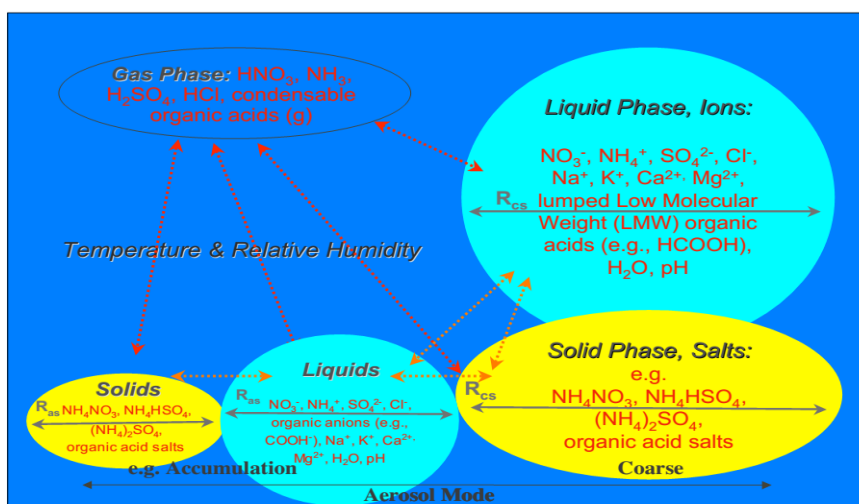
Fig.1.11. Schematic description of the factors involved in gas- particle partitioning of Nr (Metzger, 2006).

A). Chemical factors

The gas - particle partitioning is based on the assumption of the establishment of the thermodynamic and chemical equilibrium of the aerosol particles with its precursor gases. Therefore the size segregated phase partitioning is dependent on the **levels of the precursor gases** responsible for the formation of secondary inorganic aerosol as well as the **characteristic of the pre existing aerosol** on which these precursor gases are being deposited. (Squizzato et al, 2000).

The partitioning of the anions (NO_3^-, SO_4^{2-}) is based on its stoichiometric neutralization reactions with cations in such a way that the stronger acids drive the weaker acids out of the aerosol phase. Therefore, under the limiting condition of Nr precursor gas levels, the nitrate anion can be replaced by the sulphate anions from the particle phase as sulphuric acid is stronger acid than the nitric acid that inhibits the formation of nitrate aerosol (Metzger et al, 2006). Similar concept of the stoichiometric neutralization can also be applied to the cations as well, that strongly determines the particle size distribution affecting the gas – particle partitioning based on the ionic composition.

B). Meteorological conditions

Micro meteorological conditions of temperature and relative humidity has a significant impact on the gas particle phase partitioning and the mixing ratios of the

precursor NO_y species involved in the production of nitrate particulates (Forrer and Zellweger, 2003).

While the high temperature conditions are known to shift the HNO_3^- NO_3^- partitioning to the gas phase, the low temperature favours the partitioning to the particulate phase (Kondo et al, 2009). Owing to the semi volatile nature of the ammonium nitrate salt, it evaporates at high temperature whereby the precursor gases (HNO_3 & NH_3) condenses over pre existing and larger aerosol particles (Wexler et al, 1990). Therefore, high temperature favours the coarse mode particulate formation over the fine mode semi volatile particulates of reactive nitrogen compounds.

The mixing ratios of the precursor gases are also detrimental to the production of nitrate particles. High vertical mixing of the precursor gases (NO_y and NH_3) lowers its lifetime in the atmosphere by the way of deposition. As a result, stagnant atmospheric conditions are known to promote the nitrate particle formation by extending the lifetime of the precursor gases against deposition (Ellis et al, 2011). Crystallization or dissociation of the nitrate salt formed by the neutralization of its precursor gases is strongly dependent on the relative humidity of the air. At relative humidity of deliquescence (RHD), the aerosol particles are assumed to be saturated solutions with the inorganic salts being completely dissociated into anion – cation pairs (Metzger et al, 2006). Therefore, crystallization of the nitrate salt is preferred only when the relative humidity of air drops below the RHD of the salt compounds.

Since RHD of the ammonium nitrate salts (62%) are relatively higher than the RHD of the calcium nitrate salts (35%), therefore, the crystallization of calcium nitrate salts gets preferred over the ammonium nitrate salts even at low humid levels (Ansari et al, 2000)

Chapter 2
Review of literature

2. Review of literature

The rising emissions of Nr and its consequent interaction with the transport dynamics and removal mechanism from the atmosphere has led to its deposition beyond the critical threshold level. This has resulted in a growing need for the estimation of the global Nr budget along with its emissions and deposition inventories. Gaps or the uncertainties arising from the regional imbalances between the measured and modeled values of emissions and depositions are being used as a significant tool in the communication of the scientific assessments to the policy making machineries. But the level of uncertainty attached with the estimation of fluxes tends to vary from region to region depending on the methodology and input data used in its measurement. This has been rendered as a major roadblock for making any sort of comparison amongst different regional estimates. Studies done over temperate regions cannot be replicated with the same level of certainty over the tropical regions. Lack of knowledge and extensive measurement techniques in the third world countries have, thereby resulted in the creation of spatial gaps in the coverage of data estimates pertaining to Nr fluxes.

In this regard, there is a need to review the work reported by various workers on Nr deposition at national and international level in order to identify the existing gap that are required to be addressed and redressed at the same time.

2.1 International status

The growing significance of excess Nr in the acidification and eutrophication of the terrestrial as well as aquatic ecosystem has resulted in a plethora of extensive studies dealing with the deposition fluxes of Nr and its trans boundary transport from one region to another.

Importance of dry deposition of Nr over wet deposition in the coastal bays has been well established by a number of studies led by Chung et al. (1998), Russell et al. (2003), Fischer et al. (2006) and Smith et al. (2007). Based on the numerical studies,

Uno et al. (2007) has established dry to wet deposition ratio of total nitrates as 6:4 over the Eastern China Sea. Despite the dominance of particulate NH_4^+ levels (69.6 nmol N m^{-3}) over the NO_3^- particulate levels (33.1 nmol N m^{-3}), deposition fluxes of particulate NO_3^- (11 μmol m^{-2} day^{-1}) has been observed to be significantly higher than the NH_4^+ particulate fluxes (2.8 μmol m^{-2} day^{-1}) over the metropolitican Mid Atlantic Coastal Bay of U.S (Rusell et al, 2003). Significance of the size shift of the NO_3^- particulates towards the larger particles over the marine boundary layer has been well represented by the works of Matsumuto et al (2009), where the size segregated measurement of the major ions showed the dominance of NO_3^- in the coarse mode fraction (0.05 – 0.58 μg m^{-3}) subsequently resulting in a high deposition flux of NO_3^- (20.1 – 228.5 μg N m^{-2} day^{-1}) in comparison to NH_4^+ (10.1 – 47.7 μg N m^{-2} day^{-1}) over the Sea of Japan. An increase in the dry deposition flux of total nitrate (120 μmol m^{-3} day^{-1}) along the west coast of Ireland wind has been observed to be caused by the efficient scavenging of HNO_3 (g) by the sea salt resulting in its rapid deposition during the south westerly flow of the (Spokes et al., 2000). The total nitrate, therefore, tends to undergo a tremendous rapid phase change (> 85%) from the predominant gaseous HNO_3 over the continent to the particulate NO_3^- over the oceans (Lefer et al and Erikson et al, 1999). On the other hand virtually no scavenging of NH_4^+ has been observed over the ocean owing to the high pH value of the sub micron sea salt aerosol. This has subsequently resulted in the NH_3 dominating the total flux of NH_4^+ over the coastal areas as reported by the findings of Kenee et al. (2006).

However a number of studies undertaken by MINOS (Mediterranean Intensive Oxidant Study) and EANET (East Asia Acid deposition global Network) have highlighted the role of mineral dust in the chemical transformation and the transport process of the pollution plume across the continental boundaries. Numerous modelling and monitoring studies by Bauer et al. (2004), Tang et al. (2004), Seinfeld et al. (2004) and Dentener et al. (1996) highlighted the role of dust in changing the chemical composition of the troposphere. Krueger et al. (2004) stressed upon the mineralogy of the mineral dust taking a central stage in the uptake of the secondary acids with results

implying strong association of sulphate and nitrates with alumina-silicates and calcite rich dust particles repectivley.

Long range transboundary studies over the Mediterranean region have established its susceptibility to to three important sources of aerosols-deserts of North Africa and Middle East, industrialized sectors of North and North East Europe and sea salt spray (Martin et al., 1990; Kubilay et al., 2000). Annual deposition fluxes of nitrogen (0.36 Tg N yr^{-1}) over the Mediterranean as simulated by Im et al (2003) were found to be equivalent to 130 % of its regional emissions. This has been speculated to be resultant of long range transboundary transport of N_r and its subsequent deposition to the downwind regions. A further analysis into its size differentiated chemical composition by Bardouki et al. (2003) showed the dominance of NH_4^+ along with nssSO$_4^{2-}$ in the fine mode fraction (0.25-0.44 μm) and presence of NO_3^- along with Na^+, K^+, Ca^{2+}, Mg^{2+}, Cl^- in the coarse mode fraction (1.79-3.32 μm) over the east coast. Fine mode NO_3^- in the form of NH_4NO_3, on the other hand, has been observed over the west offshore Mediterranean regions owing to the transport of pollution plume arising from western Europe (Sellegri et al., 2001)

Observations from the ACE-Asia (Asian Pacific Regional Characterization Experiment) gave compelling evidences of the association of super micron nitrate and sulphate with mineral dust (70-80%) and sea salts (50-60%) during pre frontal and post frontal duration, respectively (Arimoto et al., 2006). Similar results were also obtained by Sullivan (2007) with the help of ATOFMS (Aerosol Time of Flight Mass Spectrometer) that showed a drop in the levels of nitrate and sulphate in the mineral dust before the development of dust frontal activities owing to the prior uptake of the acidifying precursor gases by the sea salt particulates present in the pre frontal air masses. Based on the linear regression method, a significant deviation in the slope of fine particulate mineral dust component (CO_3^{2-} vs. Ca^{2+} + Mg^{2+}) and pollution component (NO_3^- + SO_4^{2-} vs K^+ + NH_4^+) from unity during the frontal system passage also shed some relevant pointers towards the increasing role of mineral dust in the transboundary transport of the acidifying precursor gases (Maxwell et al., 2004).

Simulated dust and non dust column maps by Fairlie et al. (2010) also showed an increase in the fraction of nitrate in the mineral dust from ~30% in the Asiatic plume outflow to 80 – 90% over the Northern Pacific. In contrast, a sharp drop was reported for ammonium nitrate downwind to Asia owing to its volatilization into NH_3 required for the sustenance of the production of dust nitrates over the Pacific.

A comparison of ionic composition during different particulate matter event over the city of Xi'an in China as reported by Shen et al. (2009) showed lowest total ion mass concentration of TSP as well as PM $_{2.5}$ during the dust storm event in comparison to non dust and other episodic pollution events. The secondary ion concentrations (SO_4^{2-} + NO_3^-) were observed to be even lower during the dust storm than the non dust storm event which becomes indicative towards its increased scavenging by high Ca^{2+} levels accounting for 35% of TSP mass. A similar comparison of ionic composition during dust and non dust events over the semi arid Tongyu site of China by Shen et al. (2011) showed higher contribution of SO_4^{2-} and NO_3^- to the total ionic composition for the non dust samples. While the dust storm events showed Ca^{2+} > SO_4^{2-}> NO_3^-> Na^+> K^+> Cl^- > Mg^{2+} > F^- > NH_4^+, the non dust events observed SO_4^{2-} > Ca^{2+}> Na^+> NO_3^-> Cl^-> K^+> Mg^{2+}> F^-> NH_4^+ pattern of ionic dominance. Li et al (2012) specifically linked the concentration of particulate N_r with the land use pattern and meteorological conditions over Central Asia. Highest concentration of p NH_4^+ (8.23 µg N m^{-3}) and p NO_3^- (11.24 µg N m^{-3}) observed over farmlands near urban centers with significant interference from the agricultural activities as well as pollution sources. Besides the condition of low temperature and high relative humidity favouring particulate formation through poor dilution of pollutants, there are additional sources of coal combustion contributing significantly to the formation of secondary particulates during winters.

Thus, the versality and strength of the Asian sources for natural as well as pollution derived aerosols and its trans boundary transport has resulted in an increasing diversion of the research minds specially towards the Asia Pacific regions.

2.2. Indian Scenario

Ever since the inception of INDOEX programme (1996) for the monitoring of aerosol and tropospheric ozone chemistry over Indian Ocean, a number of publications have been carried out linking the role of mineral dust with the fate and transport of acidic precursor gases in India. Unlike the European and North American regions, the rain water composition over India is reported to be alkaline in nature. This has been attributed to the crustal sources contributing significantly to the dust mass loading rich in carbonates and bi carbonates of Ca and Mg (Khemani et al., 1985, 1989a, b; Naik et al., 1988; Mahadevan et al., 1989; Kulshrestha et al., 1990; Saxena et al.,1991 and Kumar et al., 1993). Abundance of soil resuspended dust in the Indian atmosphere has already been well established for its role in combating the acidification of the environment through SO_2 scavenging (Kushrestha et al., 2015). This has resulted in the low pH range of rain water samples (4.8-5.4) over the Indian ocean owing to the declining trend in the concentration of nss Ca^{2+} in the the trajectories of the air masses moving out of the Indian subcontinent (Granat et al., 2002).

While Kulshrestha et al. (1996) reported high neutralization factor of NH_4^+ over Ca^{2+} in Delhi, Parashar et al. (1996), on the other hand, reported the dominance of Ca^{2+} over NH_4^+ as the major neutralizing agent in the rain water sample of Goa and Pune. Such disparity in neutralization factor was found to be in agreement with the relative abundances of Ca^{2+} and NH_4^+ as the major neutralizing agent over the selected regions. An insight into the size distribution of the water soluble fraction of aerosols over the semi arid tracts of India showed a bi modal distribution, with the NH_4^+ salts of nitrate and sulphate constituting the fine mode fraction and Ca/Mg salts of nitrate and sulphate forming the coarse mode fraction (Kulshrestha et al., 1998). Thus, a higher neutralization factor of NH_4^+ is expected at high altitudes in comparison to the coarse mode Ca aerosols that are expected to dominate the neutralization at lower heights.

However, Singh and Kulshrestha et al. (2012) has reported 33.33% of the total NHx partitioning as particulate NH_4^+ over Delhi which has been observed to highest

during monsoons owing to the high relative humidity levels favoring its partitioning to the aerosol phase. The abundance of gaseous Nr species over the urban – rural land use pattern, on the other hand, showed high concentration of NH_3 (51.57 ± 22.8 µg/m^3) over the rural site and high concentrations of NOx over the urban land use pattern (24.4 ± 13.5 µg/m^3) depending on the emission sources of the different land use pattern (Singh and Kulshrestha, 2014).

A strong correlation of NO_3^- with the molar ratio of NH_4^+/SO_4^{2-} over Agra (Satsangi et al., 2013) and Hisar (Rengarajan et al., 2007) showed the essentiality of a high NH_4^+/SO_4^{2-} ratio for the formation of NO_3^- particulates. However, a relatively stronger correlation of NO_3^- with Ca^{2+} (r= 0.91, p> 0.01) than NH_4^+ (r = 0.74, p > 0.01) suggested the relative dominance of Ca^{2+} over NH_4^+ as the major neutralizing agent. Furthermore, NH_4^+/SO_4^{2-} molar ratio of 0.2 indicates towards the incomplete neutralization of SO_4^{2-} by NH_4^+ , thereby suggesting the limiting role of NH_4^+ in the neutralization reactions over the semi arid tracts of the Indo Gangetic Plains (Satsangi et al., 2013).

The water soluble ions over Ahmedabad and Mt Abu were also observed to be dominated by the mineral dust that maintained a uniform distribution throughout the annual seasonal cycle. Data plot between (nss K^+ + NH_4^+) and (NO_3^- + SO_4^{2-}) clearly suggested towards the abundance of excess acid represented as [(NO_3^- + SO_4^{2-}) – (nss K^+ + NH_4^+)]. The values of excess acid were observed to vary between 13-90% up to 98% of the total acid during dry and wet periods respectively, thereby, suggesting its neutralization with the mineral dust over the vast tracts of Western Indian regions (Rastogi et al., 2005). Besides, the distribution of NO_3^- was observed to be dominant for coarse mode rather than fine mode fraction which also invokes the plausible role of the mineral dust in the neutralization mechanism (Kumar et al., 2010).

The sum of the dust fall deposition flux rate of Ca^{2+} and Mg^{2+} (35 meq/m^2/a) were observed to be nearly double the sum of $NO^{3-} + SO4^{2-}$ (19 meq/m^2/a), thereby suggesting the addition of significant alkalinity through mineral dust over Pune (Pillai

et al., 2001). The percentage of alkalinity contribution (Ca^{2+}, Mg^{2+} and K^+) over Bhubaneshwar through dust varied from 15-30% over the rural site to 80-90% over the suburban regions. This was observed to affect the acidity of the atmosphere with the resulting nns SO_4^{2-} in dustfall ranging from <10% over the rural site to about 43% over the suburban regions, (Das et al., 2005). Norman et al. (2001) reported substantial difference in the chemical composition of the continental trajectories over the west and east coast of India. Observance of high levels of Ca^{2+} and nss SO_4^{2-} over Goa and Pune as compared to Bhubaneshwar indicates towards the contribution of continental and local sources of emissions over the west coast stations than the Bhubaneshwar sites. High molar ratio of NH_4^+/ $nssSO_4^{2-}$ (2.29) over Bhubaneshwar, on the other hand, suggested towards the location of some of the major NH_3 emission source regions in the North eastern part of India (Norman et al., 2001).

Based on the different land use patterns in India, high deposition fluxes of NO_3^- has been reported from the urban sites owing to the traffic emissions with NH_4^+ fluxes showing peaks over industrial areas (Kulshrestha et al., 2003). While the rural sites showed high fluxes of NO_3^- preferably due to soil resuspension, the suburban areas on the other hand reported minimum levels of both NO_3^- and NH_4^+ owing to minimum ineterference of nitrogen emission sources. Similar results were also observed over Hudegadde (rural) and Hyderabad (urban) by Kulshrestha et al as part of a RAPID CAD programme showing an increasing trend of NH_4^+ fluxes over Hudegadde (4, 7 and 8 Kg ha^{-1} yr^{-1} during 2006, 2007 and 2008, respectively) and NO_3^- fluxes over Hyderabad (18, 44, 52 and 63 Kg ha^{-1} $year^{-1}$ during 2005, 2006, 2007 and 2008, respectivley).

Keeping in tune with the continental trajectories, high particulate NH_4^+ along with NO_3^- and SO_4^{2-} over the oceans has been attributed to the growing anthropogenic influences (Rengarajan et al., 2010). While the flux of NH_4^+ has been reported to be higher over Bay of Bengal (0.101 N mg m^{-2} day^{-1}) than Arabian Sea (0.087 N mg m^{-2} day^{-1}) by Reddy et al., 2008, NO_3^- flux on the other hand, are reported to be higher over Arabian sea (78 N µg m^{-2} day^{-1}) than Bay of Bengal (14 N µg m^{-2} day^{-1}) by

Kumar et al. (2008). But contribution of NO_3^- deposition is minor to the nitrogen cycling in the Arabian Sea owing to the nitrogen enrichment resulting from the upwelling events during south west monsoon. It is only during inter monsoon and north east monsoon that the NO_3^- deposition makes a significant contribution in the southern part of the Arabian sea.

2.3. Significance of the study

The widespread problem of Nr has been well documented by the developed nations in their vastly publicized assessment reports and comprehensive budget inventories (Galloway et al., 2004; Dentener et al., 2006; Simpson et al., 2006; Erisman et al., 2007; Reis et al., 2009; Vet et al., 2014). This has paved the way for a number of quantification studies dealing with the determination of perturbations existing in their nitrogen cycling. India, on the other hand, is still constrained with the limited availability and reliability of its data set values pertaining to Nr estimates. With the rising emission trends of Nr resulting from the expanding industrial and agricultural sectors of India, the need of having a qualititative and a well established national budget inventory of Nr has therefore, become an indispensible tool in the implementation of various policy action plans.

Presence of mineral dust along the semi arid tract of the India has been instrumental in providing ultimate sinks to the excess Nr acidity in the troposphere.The estimation of Nr deposition fluxes through dustfall has, thus, gained quite a significance in recent years for the determination and quantification of the fate of Nr in the troposphere. The present study can, therefore, be used to strengthen the present estimates of the dust fluxes in the estimation of excess Nr loading in the atmosphere with a direct implication in the alteration of tropospheric chemistry.

2.4. Objectives

Keeping into account the gaps that are existing in the estimates of Nr budget, following objectives have been taken into consideration with the sole aim of providing regionally representative summer time Nr deposition fluxes -

- To determine the physical and chemical composition of dustfall at the selected sites in Delhi-NCR.
- To estimate the dustfall flux of inorganic Nr speices at sites of different characteristics.
- To calculate the ratios of different Nr species in order to find their relative sources.
- To find out the relationship of dustfall fluxes of Nr species with meterological parameters.

Chapter 3
Methodology

Methodology

3.1. Description of sampling sites

Stretched over a mere area of 1,483 km with a population holding of 16 million, Delhi has become the epitome of growing population and pollution problem over the northern region in the past few decades. It is located between the latitude of 28°-24'-17" and 28°-53'-00" North and longitude of 76°-50'-24" and 77°-20'-37" East, with neighbouring states of Uttar Pradesh, Haryana and Rajasthan sharing its border and constituting the National Capital Territory of Delhi. Situated at the periphery of the Gangetic plains with the Great Thar Desert lying to the west, the capital has become increasingly susceptible to the changing precipitation pattern and frequent dust storm events.

Based on the distribution of pollution sources along with the changing dynamics of urban–rural composition with different land use pattern, following six sites were selected for sampling from Delhi and its national capital regions:

3.1.1. Mukherjee Nagar (MN)

Located in a highly populated district of North East Delhi, this site is a typical representative of high density residential land use pattern. It is characterized by unplanned sprawling of residential colonies with a number of unauthorized colonies spurting along its fringe. This has eventually resulted in the problem of poor sewage conditions and open drains. There are some growing clusters of 2 -3 storied buildings which are intercepted by the scattered grassy patches of the residential parks. Owing to illegal encroachment of street vendors to the already narrow lanes, the area is often subjected to traffic jams especially during the evenings.

3.1.2. S.M.A Industrial Estate (SMA)

The area is a typical industrial estate with Co - operative Industrial Society involved in its development. It is located at a km distance from the bustling Azadpur

Mandi in the Northern district Zone of Delhi. Clutters of small scale industries here are involved in re rolling, annealing and pickling of stainless steel products and enamel wares with automobile service stations mushrooming at every nook and corner of the estate. The area is also characterized by its poor road condition with the regular movement of diesel fuelled trucks resulting in its total breakage.

3.1.3. Peeragarhi Chowk (PC)

The site is a well recognized transport hub located at the major intersection connecting the outer ring road and Rohtak Road (NH- 10). The area therefore witnesses a regular inflow of heavy traffic comprising of diesel fuelled heavy duty goods and passenger vehicles providing interstate connectivity. At half a kilometre distance to the sampling site is the Udyog Nagar Industrial Estate consisting of various small scale industries majorly involved in the foot wear manufacture and engineering related products.

3.1.4. Jawaharlal Nehru University campus (JNU)

The campus is located in the south district of Delhi with mini forest cover to its surrounding. No major industrial areas are present to its surrounding. Except for the few vehicles used by the students and the faculty for their daily purpose, the area is relatively free from traffic emissions, thereby making it a typical urban forest land use pattern. However, dust emissions from the activities involved in time to time construction and renovation of the campus cannot be ruled out.

3.1.5. Noida phase-II (N – II)

Located in the Gautam Buddh District of NCR – Delhi, the area has become a typical representative of semi urban land use pattern with urbanization spreading rapidly into the already fertile hinterlands of the western Uttar Pradesh. The site is characterized by its proximity to the Noida Export Processing Zone (NEPZ) with well established industrial and business enterprises involved in engineering, textiles, economics and software development. Within a few km distance is the Barolla village

characterized by its rural land use pattern. Owing to the frequent power cuts and failures, the area has also become accustomed to the use of diesel fuelled heavy duty generators for restoring normalcy in the daily functional activities of its people.

3.1.6. Chhuchhakwas village (CV)

The sampling area is a small village located in the Jhajjar district of Haryana constituting the National Capital Territory of Delhi. The land use pattern is typically agricultural characterized by the harvesting of wheat and mustards during summers and barley during winters. But the changing demography and socio economic patterns have resulted in the reduction of many agricultural fields to fallow lands. The site is easily accessible by the roads from Dadri and Beri and is therefore subjected to traffic as well as road dust emissions.
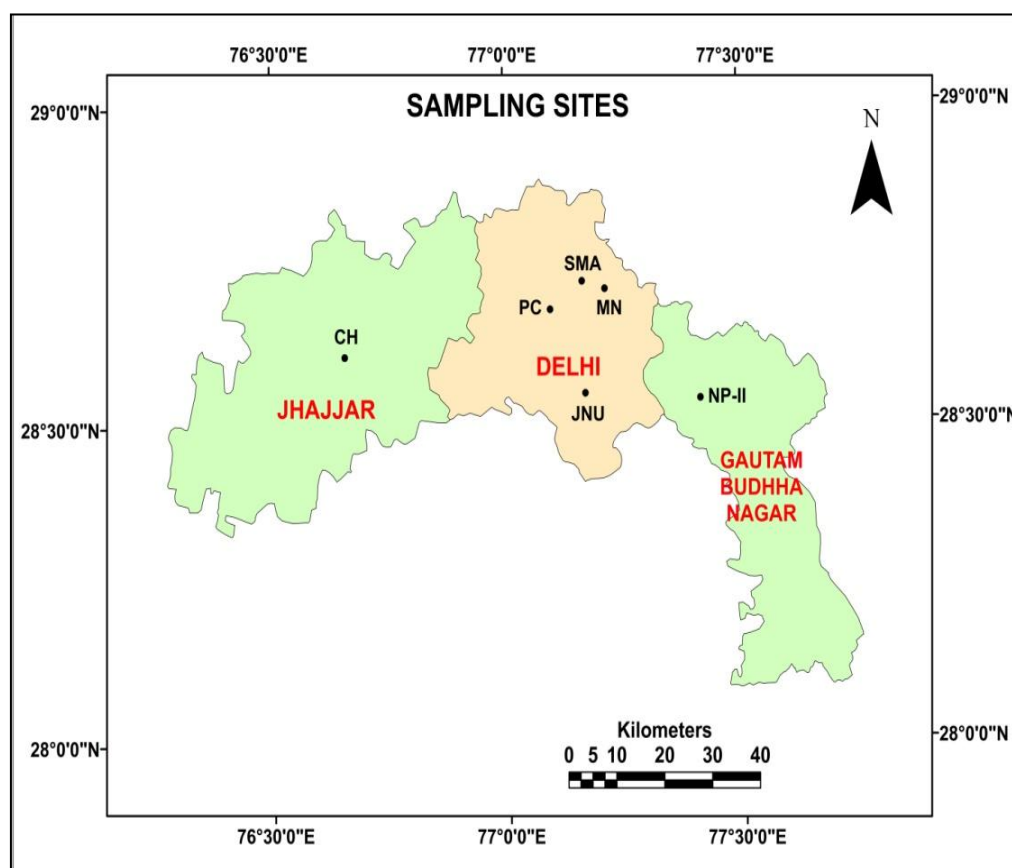
Fig.3.1. Map of Delhi-NCR showing the sampling sites

3.2. Wind direction over Delhi-NCR

Wind rose was plotted for the duration of sample collection (April-June, 2015) with the help of meteorological data (wunderground.com) using WR software. Dominant wind directions of south east and south west were observed in the form of western disturbances during the sampling period of April - June (Fig.3.2.). Wind rose, therefore, indicates towards the transport of mineral dust from western and eastern directions of Delhi which along with the urban emissions could be attributed for its altered composition.
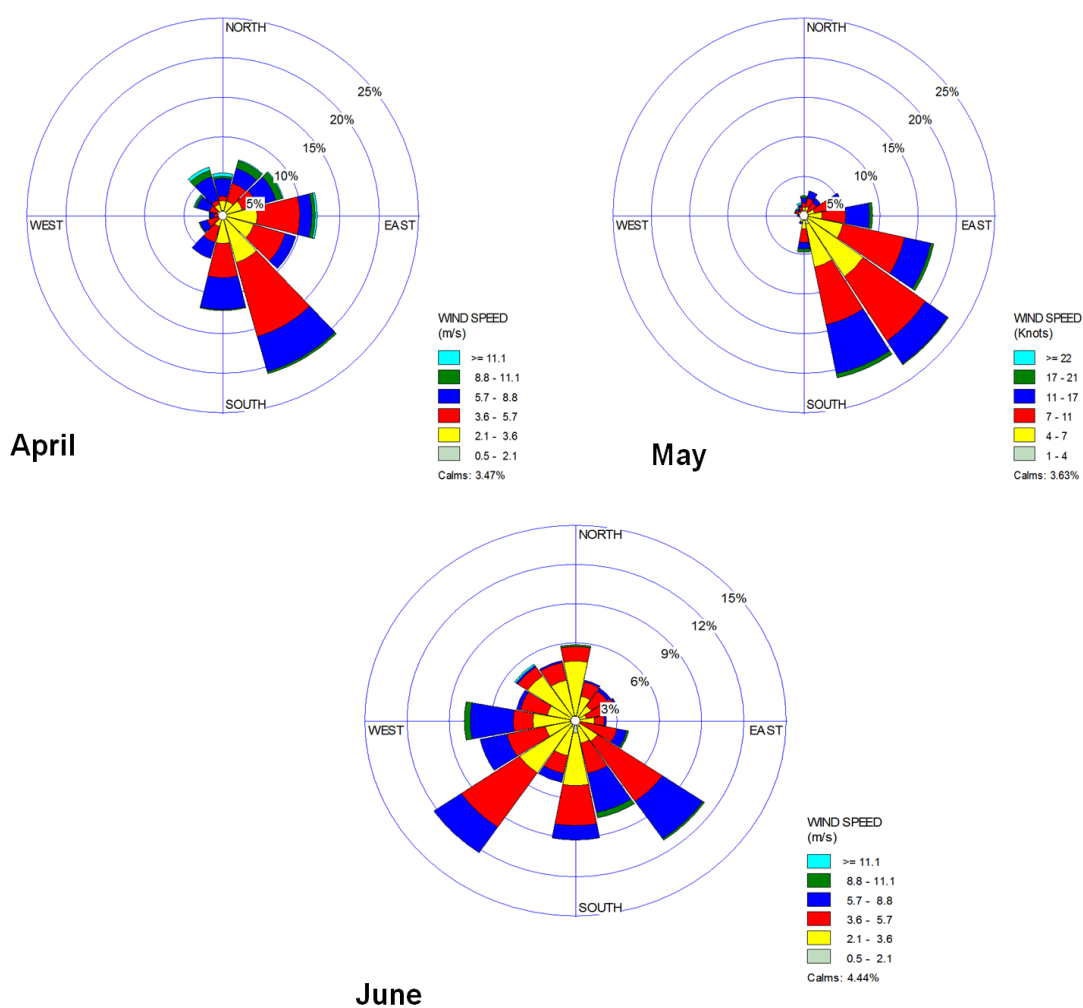
Fig.3.2. Wind rose pattern at Delhi-NCR during the sampling period (April-June, 2015)

3.3. Sample collection

Dust samples were collected during the summer season from April – June, 2015 using surrogate surfaces. The suitability of this approach increases with the increasing particle sizes of the dust and is best used under conditions of dominant aerodynamic resistance. Presence of any other form of resistances like canopy resistance is likely to hinder its representation of a natural surface and its effectiveness in the measurement of dust deposition. Owing to the chemical inertness of the polystyrene to the organic and inorganic components of the dustfall fluxes, the petri plates of dimension 140 mm were used for the collection of atmospheric dust. The plates were kept on the roof top of the buildings for the purpose of providing significant aerodynamic resistance and were changed after every 5 days of ambient exposure.

For soil sampling, two spots were chosen from each site within a distance of 1 km. Surface soil samples (1-5 cm) were collected in duplicates with the help of metal paddles and were subjected to air drying for a couple of days. The samples were eventually sieved through a 60 mesh size so as to finally obtain a composite mixture of homogenized soil sample.

3.4. Sample extraction

The collected dust samples were subjected to dissolution by washing the petri plates with 30 ml of ultra pure Milli Q water for pH, conductivity and ion chromatographic analysis. Water soluble fractions were then extracted by placing the sample in an ultra sonic water bath for 30 minutes at a working frequency of 1 Hz. The extract was finally collected in a centrifuge tube by filtering the sample through 0.2 μm nylon syringe filter.

Similar to the dust samples, soil samples of 0.5 g each were also dissolved in 30 ml of Milli Q water which was eventually subjected to sonication and filtration to obtain a final filtered extract of water soluble fraction.

3.5. Sample Analysis

3.5.1. pH measurement

pH is the molar concentration of hydrogen ion in the solution that is used for the determination of the acidity and basicity of the sample. Conductivity, on the other hand, is used in the determination of the dissolved ions in the sample by measuring the amount of electric current that could pass through it. The pH and conductivity of the dissolved extracts of the dust and soil samples were determined using an Eutech model pc 510 model. The instrument was calibrated using pH buffer standards of 4.0, 7.0 and 10.0 and conductivity standard of 1413 µS/cm at 25^0C. Electrodes were washed with distilled water and wiped after every analysis for maintaining the accuracy and correctness of the results.

Fig.3.3.pH meter (Eutech pc 510 model)

3.5.2. Ion Chromatographic analysis

The water soluble extracts of the dust and soil samples were analyzed for major cations (K^+, NH_4^+, Na^+, Ca^{2+}, Mg^{2+}) and anions (F^-,Cl^-,NO_3^-, SO_4^{2-}) with the help of Ion Chromatography (Metrohm–883 basic plus model). IC is best known for the efficient separation and determination of ions by combining the principles of ion

exchange, liquid chromatography and eluent suppression. Therefore, its analytical system comprises of a sample injection valve and a pump for introducing sample and eluent into the sample loop respectively, an ion exchange separator column, a background ion suppressor and a conductivity detector.

Fig.3.4. Ion Chromatography (Metrohm-883 basic plus)

The principle of IC is based on the exchange equilibria existing between the ions in the mobile phase and ions of like sign on the surface of a high molecular mass solid forming the stationary phase. It is the differential affinity of the analyte ions with the functional groups present on the ion exchange resins that results in the separation of the components into different peaks. This results in the monovalent ions showing early peaks owing to its fast elution from the column in comparison to the polyvalent ions.

Based on the type of the surface active sites of the resin involved in ion exchange, the chromatography can be further divided into cation exchange and anion exchange types. The active sites for the cation exchange resin are the strong acids of sulphonic acid group (- SO_3^- H^+) or weak acids of carboxylic group (-COO^-H^+) that are able to retain a positively charged cation.

$$RSO_3^- H^+ (s) + M^+(aq) \rightleftharpoons RSO_3^- M^+(s) + H^+ (aq)$$
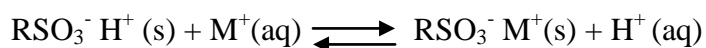
Anionic exchangers, on the other hand, contain strongly basic tertiary amine group ($-N(CH_3)_3^+ OH^-$) or a weakly basic primary amine group ($-NH_3^+ OH^-$) that are capable of retaining a negatively charged anion from the eluent.

$$RN(CH_3)_3^+OH^- (s) + A^- (aq) \rightleftharpoons RN(CH_3)_3^+ A^- (s) + OH^- (aq)$$
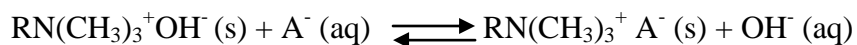
Table.3.1. Operating conditions of Ion chromatography

Cation Exchange chromatography	Anion Exchange chromatography
Column-Metrosep C4 (silica gel with carboxylic group) of 100×4 mm dimension	**Column**-Metrosep A SUPP 4 (polyvinyl alcohol with quaternary ammonium group) of 250×4 mm dimension
Flow rate – 0.9 ml/min	**Flow rate** – 1 ml/min
System Pressure – 5.22M Pa	**System Pressure** – 4.6 M Pa
Sample volume - 20 μl	**Sample Volume** - 20 μl
Eluent – 1.7 mmol/L Nitric Acid + 0.7 mmol/L Dipicolinic acid Supressor – 50mM H_2SO_4	**Eluent** – 1.8 mmol/L Na_2CO_3 + 1.7 mmol/L $NaHCO_3$

The columns were equilibrated for 30 mins before analysis. Standards were used after every eight analytical run in order to check the calibration of the instrument for its variation that should not be more than ± 5%. Chromatogram of 2ppm standard solution of anions and cations has been shown in Fig. 3.5a and 3.5b, respectively. Fig.

3.6a and 3.6b shows the typical chromatogram of sample for anions and cations, respectively.

Chromatogram of standard
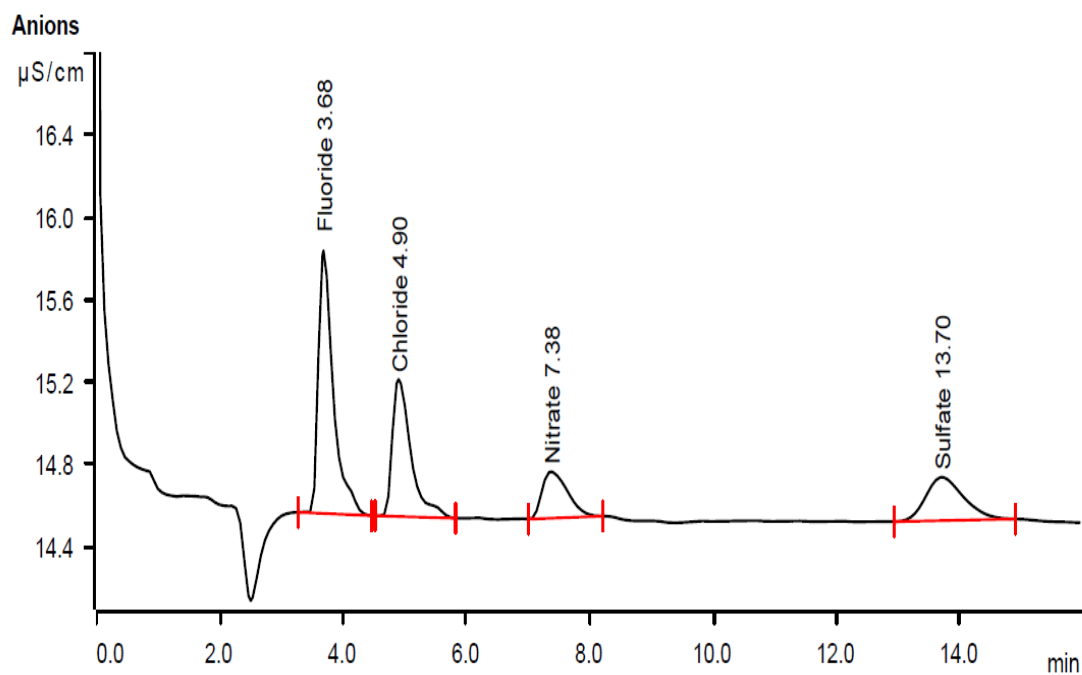
Fig. 3.5a.Chromatogram of anions for standard (2ppm). (Retention time is shown above the peak)
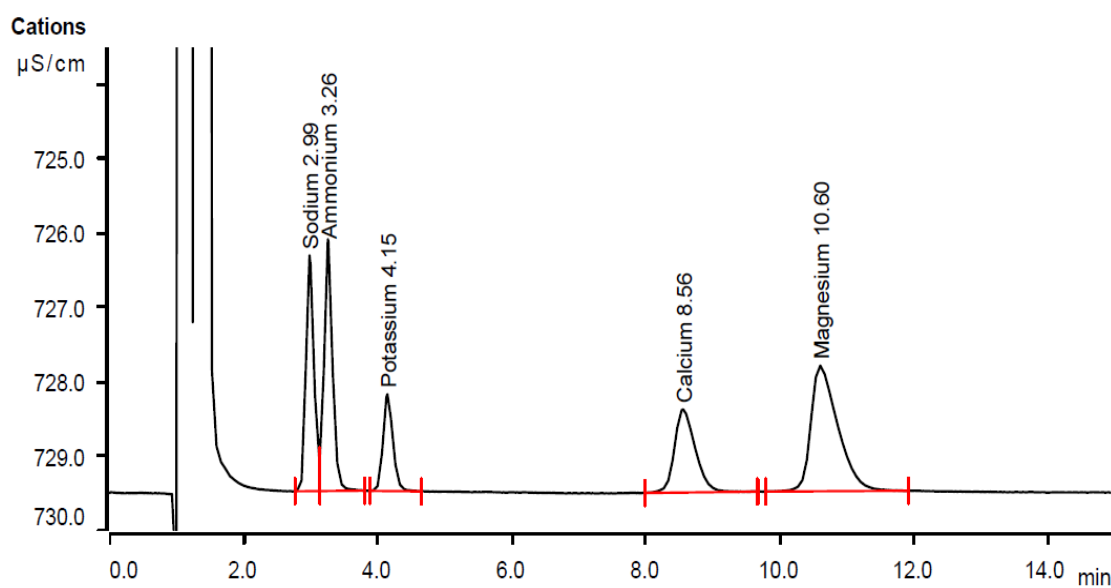
Fig. 3.5b.Chromatogram of cations for standard (2ppm). (Retention time is shown above the peak)

Chromatogram of samples
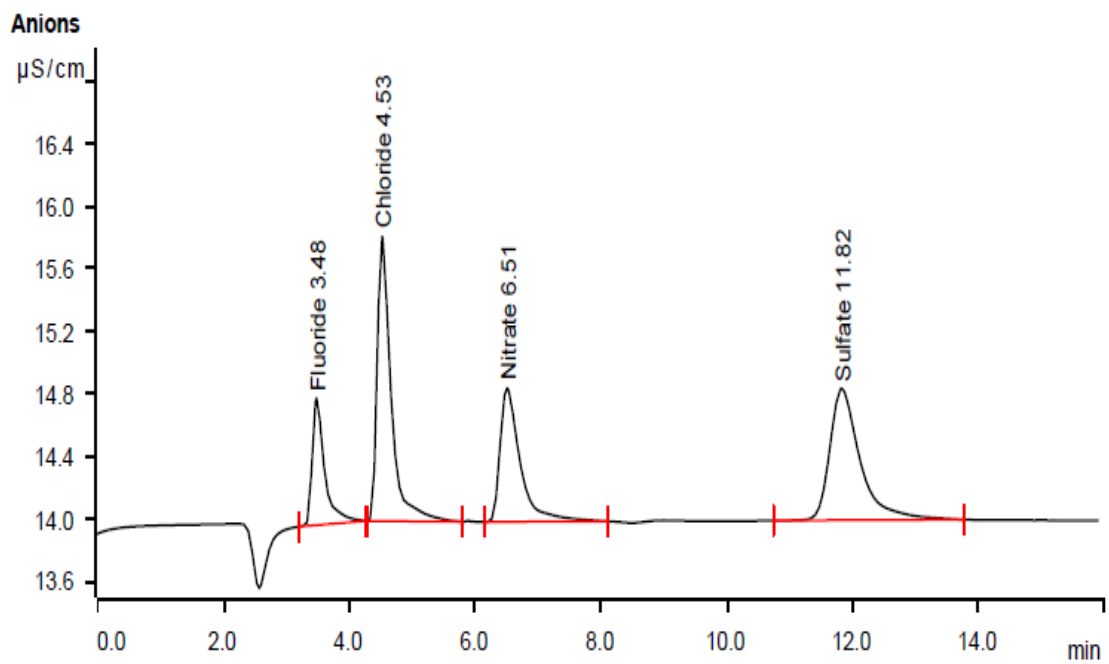
Fig.3.6a. Chromatogram of a sample (anions)
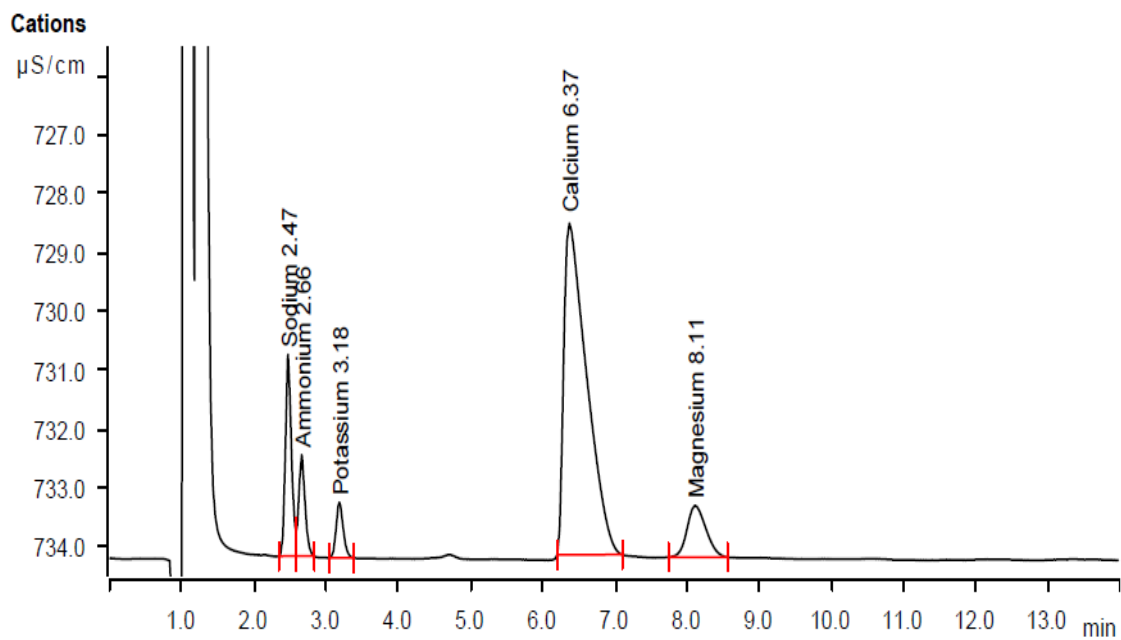
Fig.3.6b. Chromatogram of a sample (cations)

3.5.4. Scanning Electron Microscopic (SEM) and Energy Dispersive X–Ray Spectroscopic (EDX) analysis

Qualitative analysis of the dust samples for its morphological and micro structural features was done with the help of Scanning Electron Microscope (Carl Zeiss AG-Evo 40 series model) (Fig. 3.7). The technique is based on the principle of sample-electron interaction that involves the dissipation of the incident beam energy into the signals of secondary and backscattered electrons. As the kinetic energy of the emitted secondary electrons is low, these can be used for imaging the morphology and topography of the sample only. Emissions from the deeper regions of the samples are absorbed by the overlying surface layer and therefore results in its heightened sensitivity to the surface of the sample. Back scattered electrons, on the other hand, are produced from the back scattering of the primary electron beam from the sample that suffer a minor loss in its energy levels. Therefore, signals from these electrons can be used for illustrating contrasts in the composition of the multiphase layers as they are able to carry information from the even the deepest regions of the sample.

For the purpose of deriving quantitative results of the samples for its elemental composition along with their relative proportion, Energy dispersive X–ray spectroscopy (X–Flash 310 model with Bruker EDX detector) was used in conjugation with the SEM. Based on the principle of inelastic interaction of the electron beam with the constituent atoms of the sample, characteristic X–rays of particular wavelength are emitted for balancing the energy differences created by the bombardment of the samples with the high energy electrons. The resulting spectrum of the X– ray emissions has, therefore, been considered as the characteristic fingerprint of every individual atom that has been encountered. Owing to their penetrative abilities, the X-rays can escape easily from the surface as well as subsurface regions with intensities that are directly proportional to the quantity of the parent atoms scanned from the sample. The resulting evaluation of the X-ray spectrum energies verses its total counts are represented in the form of individual peaks imposed on the background of continuum X–rays from which the quantitative determination of the elemental analysis can be easily derived.

Fig.3.7. SEM–EDX instrument

Samples for SEM–EDX analysis were directly mounted on the carbon tape pasted on the metallic stubs and was subjected to a thin film coating of gold deposition with the help of a Sputter loader. At 20 kV SEM images were obtained at four magnifications of 500x, 1500x, 3000x and 6000x with 11 mm of working distance. The EDX analysis, on the other hand, was carried out for the samples placed in bulk over the other corner of the carbon tape. A total of 13 elements were selected for the determination of its weight percentage with the subsequent normalization of each element with the weight % of oxygen fraction in the sample. Frequency diagrams and probability density plots were prepared with the help of Image J software for the purpose of analyzing particle size distribution in three size bins viz, less than 2.5 µm, between 2.5 and 10 µm and greater than 10 µm.

Chapter 4
Results and discussion

4.1. Dustfall fluxes

The dust fluxes were calculated for the selected sites in the Delhi- NCR region using the following equation given by Katz et al (1969)

$$DF = \quad M_2 - M_1/A \times T$$

Where, M_1 = weight of the petri plates before dust collection (mg)

M_2 = weight of the petri plates after dust collection (mg)

A = area of the petri plates (m^2)

T = duration for which the petri plates were exposed for dust collection (days)

DF = Dustfall flux ($mg/m^2/d$)

Table 4.1 gives the average fluxes of the dustfall along with its minimum, maximum and standard error values for all the sites. The highest average dustfall flux was observed at the SMA site (1157 ± 345 $mg/m^2/d$) and lowest at the N-II site (429 ± 96 $mg/m^2/d$). The order of average dustfall fluxes was noticed as SMA>CV>JNU> MN>PC>N–II.

Table.4.1. Dustfall fluxes at each sampling sites

Dustfall flux ($mg/m^2/d$)	Sampling Sites					
	MN	SMA	PC	JNU	N -II	CV
Average	556	1157	548	664	429	1030
Min.	212	244	276	109	81	400
Max.	1645	5584	1260	3766	1120	2690
Std. Error	115	345	72	264	96	216

For all the samples, the results showed that the average values of the dustfall fluxes varied in the range of 81 to 5584 mg/m^2/d. As given in Table 4.2, 44% samples had the dustfall flux in the class interval of 0–200 mg/m^2/d while 15% of the samples were observed with dust flux values greater than 3000 mg/m^2/d. 92%, 92%, 90%, 84%, 79% and 70%, of the samples had dustfall fluxes below 1000 mg/m^2/d at PC, JNU, N–II, MN, SMA and CV respectively.

Table 4.2. Frequency distribution of dust flux data set at each sampling sites

Dust flux class interval (mg/m^2/d)	Sampling sites					
	MN	SMA	PC	JNU	N-II	CV
0 - 200	-	-	-	8%	36%	-
201 - 400	38 %	13%	23%	54%	9%	10%
401 - 600	31%	13%	38%	15%	36%	20%
601 - 800	15%	20%	31%	8%	9%	-
801 - 1000	-	33%	-	7%	-	40%
1001 - 1200	8%	-	-	-	10%	-
1201 - 1400	-	7%	8%	-	-	10%
1401 - 1600	-	-	-	-	-	10%
1601 - 1800	8%	-	-	-	-	-
1801 - 2000	-	-	-	-	-	-
2001 - 2200	-	-	-	-	-	-
2201 - 2400	-	-	-	-	-	-
2401 - 2600	-	7%	-	-	-	-
2601 - 2800	-	-	-	-	-	10%
2801 - 3000	-	-	-	-	-	-
>3000		7%	-	8%	-	-

4.1.1. Mukherjee Nagar (MN)

The dustfall flux at the MN site ranged from 212 to 1645 mg/m^2/d with a mean value of 556±115 mg/m^2/d. Pre monsoon showers maintained a constant trend in the flux values in April. However, the strong winds and dry conditions of the atmosphere during May and June provided a rather upward trend with minor fluctuations arising from the construction and soil re–suspended dust emissions from its high density residential land use. Occurrence of dust storm event on 19th May resulted in a sharp peak for the samples collected during 29th May–1st June (1654 mg/m^2/d).
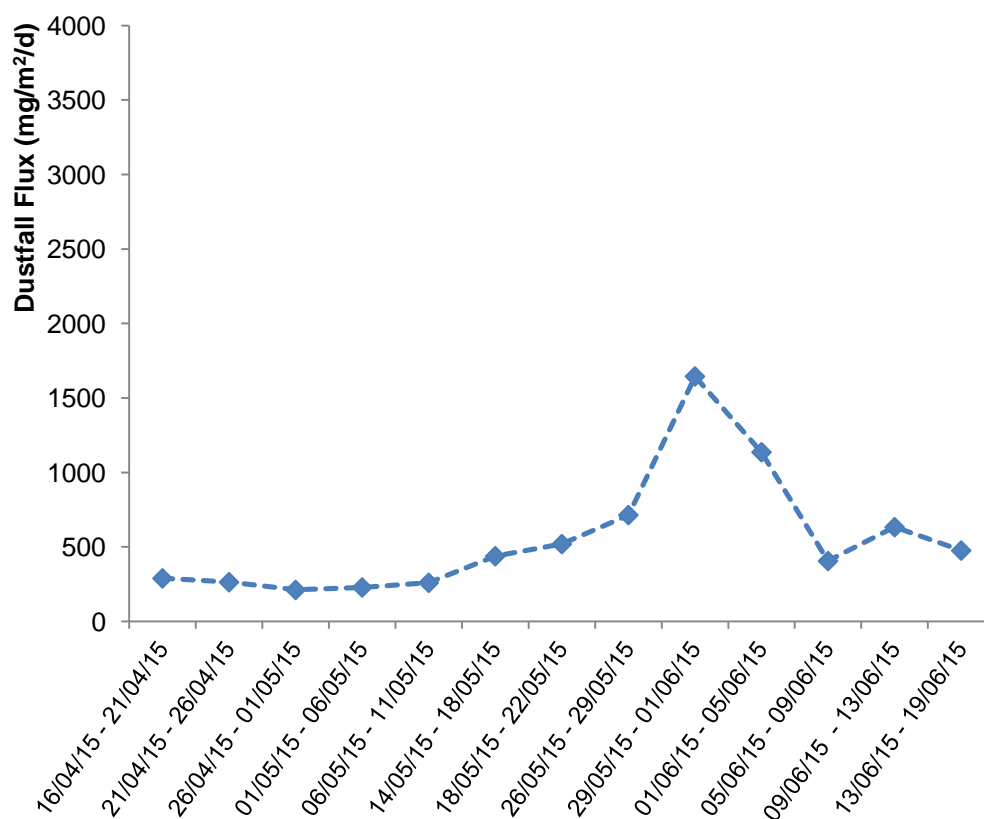
Fig.4.1. Time series of the dustfall flux variations (mg/m^2/d) at MN site

4.1.2. SMA Industrial estate (SMA)

Being a typical representative of an industrial estate, the values of dustfall fluxes ranged from 244 to 5584 mg/m^2/d with a mean of 1157±345 mg/m^2/d. Dust emissions from the industrial activities and constant movement of heavy duty vehicles over the deteroiting road conditions has resulted in a relatively higher trend of the dustfall fluxes with minor fluctuations. Corresponding to the occurrence of dust storm event on 19th May, a sharp peak in the dust fluxes were observed for the samples collected during 29th May–1st June (5584 mg/m^2/d)
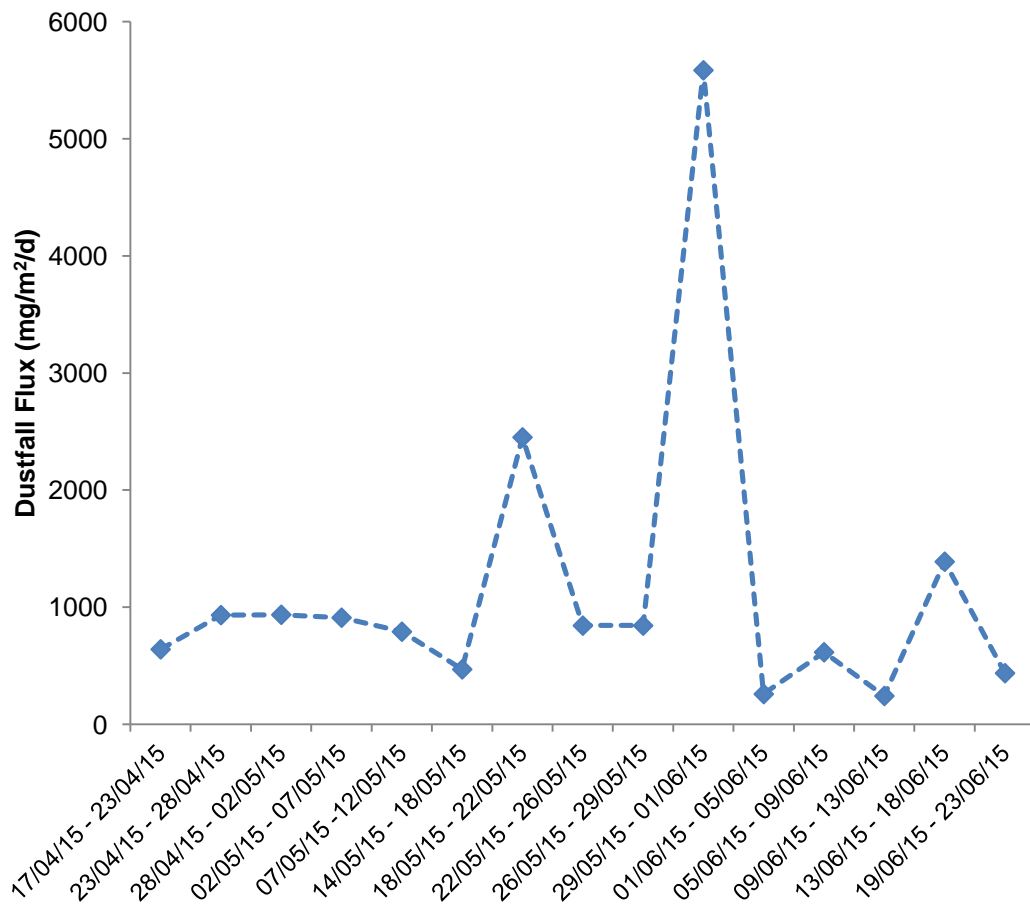
Fig.4.2. Time series of the dustfall flux variations (mg/m^2/d) at SMA site

4.1.3. Peeragarhi Chowk (PC)

At the PC site, the dust fluxes showed a range from 276 to 1260 mg/m^2/d with a mean value of 548±72 mg/m^2/d. The site being a major transport hub showed a rather constant trend in its data set with regular fluctuation depending on the flow of the traffic and congestion of the road. However, with the occurrence of a dust storm event on 19th May, a sharp peak in the dustfall fluxes were observed for the samples collected that were during 18th –22nd May (1260 mg/m^2/d).
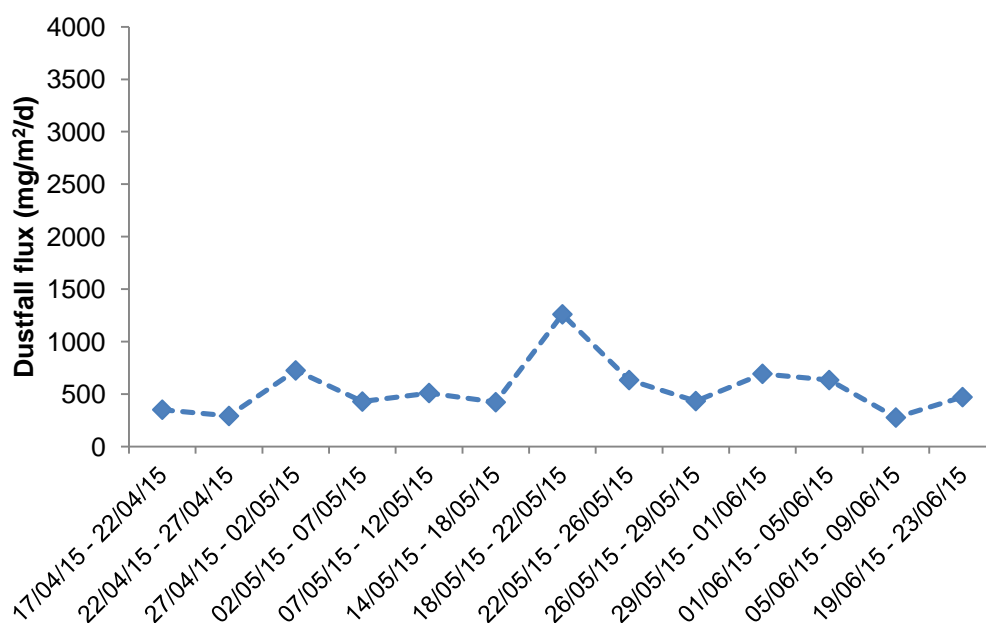
Fig.4.3. Time series of the dustfall flux variations (mg/m^2/d) at PC site

4.1.4. JNU campus (JNU)

The dustfall fluxes at the JNU site ranged from 109–3766 mg/m^2/d with a mean value of 664±264 mg/m^2/d. Presence of an extensive green cover around the sampling site provided a rather low but a constant trend to its data values. Minor fluctuations in the dustfall fluxes with a peak at 866 mg/m^2/d were led by the dust storm event on 19th May. However, a sharp peak in the values of dust fluxes were observed for the samples that were collected between 6th and 10th June (3766 mg/m^2/d) owing to the heavy dust emissions arising from the untimely construction and renovation activities of the campus during the sampling period.
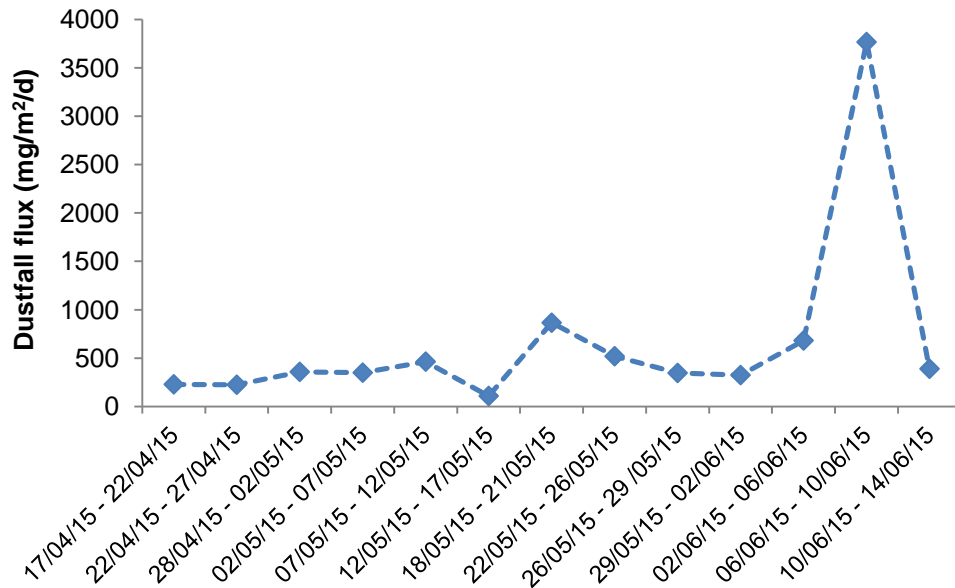
Fig.4.4. Time series of the dustfall flux variations (mg/m^2/d) at JNU site

4.1.5. Noida Phase-II (N-II)

The dustfall fluxes at the N–II site ranged from 81 to 1120 mg/m^2/d with a mean of 429 ± 96 mg/m^2/d. Presence of a well built concrete area near the sampling site has subsequently lowered its dustfall fluxes in comparison to others. However, the summer time atmospheric conditions of strong winds and low humidity provided an upward but a fluctuating trend to the data set with a peak in the dustfall flux at 1120 mg/m^2/d (29th May–2nd June).However, an untimely pre monsoonal showers on 3rd June resulted in its sharp decline of the values.
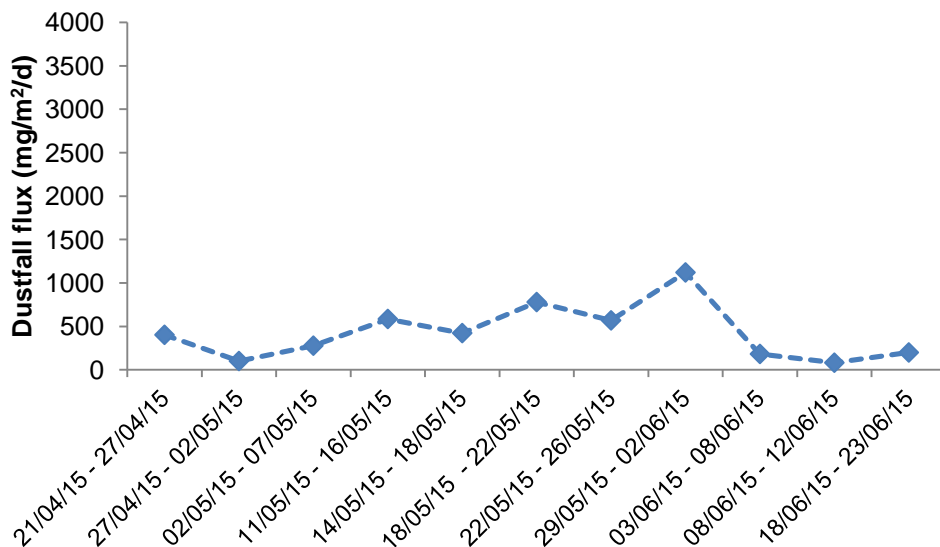
Fig.4.5. Time series of the dustfall flux variations (mg/m^2/d) at N–II site

4.1.6. Chhuchhakwas village (CV)

The dustfall fluxes at the CV site ranged from 398 to 2690 mg/m^2/d with a mean value of 1030±216 mg/m^2/d. Heavy events of dustfall fluxes were observed during the first half of the sampling duration which unlike the other sites, showed peaks at 2690 mg/m^2/d (17th-24th April), 1416 mg/m^2/d (4th-9th May) and 823 mg/m^2/d (1st-16th June). This could be attributed to the prevalence of conventional agricultural practices resulting in the soil re-suspended dust emissions from the ploughing and erosion of agricultural fields and abandoned fallow lands in addition to the road dust emissions from the movement of tractors on unpaved road surfaces
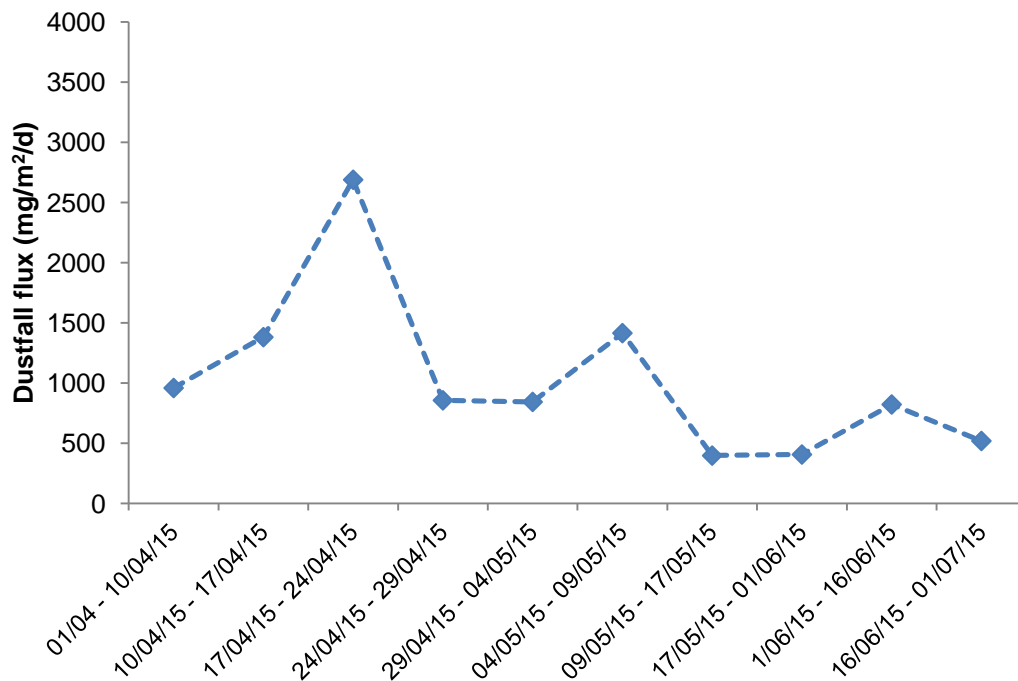
Fig.4.6. Time series of the dustfall flux variations (mg/m^2/d) at CV site.

4.2. Ionic composition of the dustfall fluxes

The fluxes of major cationic and anionic species in the dustfall were estimated for all the sites. It was observed that the contribution of the ionic composition to the dustfall fluxes varied with the changing dynamics of the pollution source across the sampling sites (Fig. 4.7).
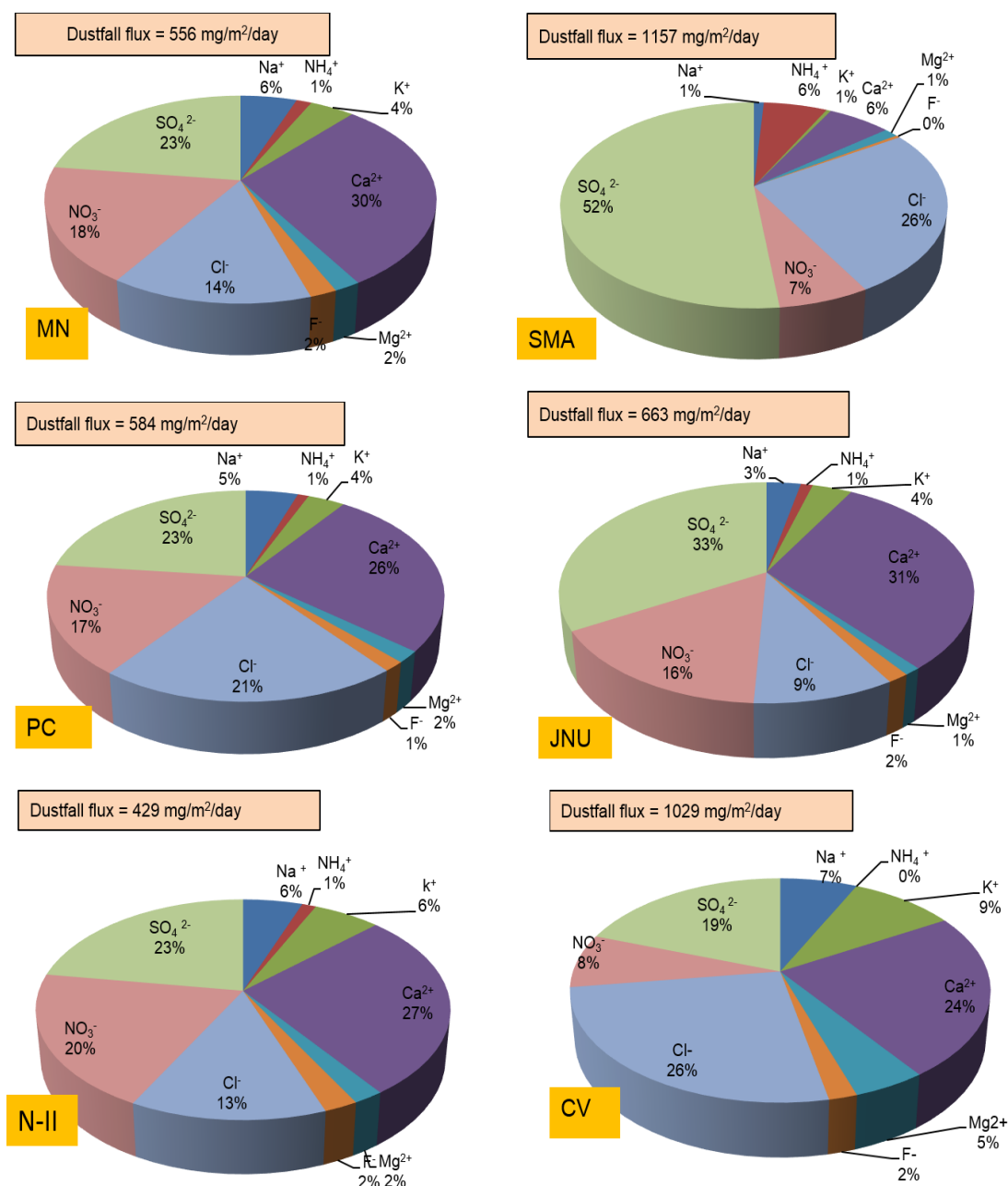
Fig.4.7. Pie diagram showing contribution of ionic species to the water soluble extract of the dustfall flux at each site.

Heavy industrial emissions resulted in the highest contribution of ions to the dust fluxes at the SMA site, while minimum anthropogenic disturbance over the CV site resulted in its lowest contribution to dustfall. The summer time meteorology of strong winds and high dust conditions maintained high Ca^{2+} fluxes from the crustal sources (Kulshrestha et al., 1996; Khemani et al., 1998) over all the sites except for SMA where industrial activities dominated the ionic flux composition. Strong neutralizing affinity of the Ca^{2+} for SO_4^{2-} in comparison to NO_3^- has resulted in the dominance of SO_4^{2-} fluxes at every site (Metzger et al., 2006). Atmospheric dust has been reported as a significant scavenger of SO_2 in India. The affinity of SO_4^{2-} with Ca^{2+} can be explained by the reaction proposed by Kulshrestha (2013).

$$CaCO_3 + SO_2 + 2H_2O \longrightarrow CaSO_4.2H_2O + CO_2$$
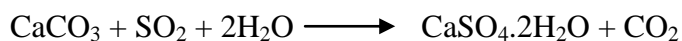
Interestingly, the SO_4^{2-} fluxes at a relatively pollution free JNU site, were observed to be higher than the traffic site PC. The anomaly could be attributed to the extensive use of the Portland cement (gypsum) during the untimely construction and renovation of the campus during the sampling period. With the exception of SMA site, NH_4^+ contributed least to the ionic composition owing to the dominance of the Ca^{2+} in the dustfall fluxes (Metzger et al, 2006).

Despite the wide disparity in the land use pattern existing between the industrial SMA site and rural CV site, similar contribution of Cl^- fluxes were observed. This could be attributed to the prevalent acidic fluxes from steel manufacturing industries resulting in high Cl^- fluxes over the SMA site on one hand, and dominating crustal sources contributing to the high Cl^- fluxes over the CV site on the other.

4.2.1. Mukherjee Nagar (MN)

MN site showed 3.5 % of its ionic contribution to the dust fluxes of which 57% consisted of the major anionic species and 43% consisted of the major cationic species. The average flux of the ions in the dustfall composition was observed as $Ca^{2+} > SO_4^{2-} > NO_3^- > Cl^- > Na^+ > K^+ > Mg^{2+} = F > NH_4^+$. The relative dominance of crustal sources (Ca^{2+},

Cl^-) has resulted in the high scavenging of acidic precursor gases in the form of SO_4^{2-} and NO_3^- in the dustfall fluxes (Kulshrestha et al., 2009; Pillai et al., 2001)

4.2.2. SMA Industrial estate (SMA)

Industrial nature of the SMA site has resulted in the highest contribution of its ionic fluxes (22.2%) to the dustfall composition in comparison to the other sites. The order of ionic fluxes was observed as $SO_4^{2-}>Cl^->NO_3^->Ca^{2+}=NH_4^+>Na^+=K^+>F^-$ with SO_4^{2-} (132.7±107.7 mg/m²/d) and Cl^- (66.4±59.2 mg/m²/d) contributing to the maximum flux values. This could be attributed to active industrial emissions rich in acidic precursor gases that have eventually resulted in the dominance of anionic acids in the dust fluxes (Budhavant et al., 2012).

4.2.3. Peeragarhi Chowk (PC)

The ionic fluxes at PC site contributed 3.7% to the dust flux composition in the order $Ca^{2+}>Cl^->SO_4^{2-}>NO_3^->Na^+>K^+>Mg^{2+}>NH_4^+=F^-$. The site being a major traffic juncture showed highest flux of Ca^{2+} (5.35±0.59 mg/m²/d) and Cl^- (4.19±0.76 mg/m²/d) resulting from the track out soils from the unpaved roads (Chakraborty et al., 2010).

4.2.4. JNU campus (JNU)

The ionic fluxes at JNU showed 2.9% of its contribution to the dust flux composition in the order of $SO_4^{2-}>Ca^{2+}>NO_3^->Cl^->K^+>Na^+>F^->Mg^{2+}=NH_4^+$. The anomaly of high SO_4^{2-} (6.30±2.77 mg/m²/d) as well as high Ca^{2+} (5.85±1.57 mg/m²/d) fluxes over an otherwise pollution free JNU campus could be attributed to the intensive use of Portland cement in construction and renovation of the campus done during sampling period.

4.2.5. Noida Phase–II (N- II)

The dust fluxes at N − II site showed 3.9 % of its fraction contribution to the ionic fluxes with $Ca^{2+}>SO_4^{2-}>NO_3^->Cl^->Na^+=K^+>Mg^{2+}=F^->NH_4^+$. Strong winds and dry condition of the sampling duration resulted in a high flux of Ca^{2+} (4.59 ± 0.70 mg/m^2/d) which on comparison with other sampling site was observed to be the lowest owing to the well built nature of its commercial land use pattern.

4.2.6. Chhuchhakwas village (CV)

The dust flux composition at CV site showed lowest (1.55%) contribution by the ionic fluxes in the order $Cl^->Ca^{2+}>SO_4^{2-}>NO_3^->K^+>Na^+>Mg^{2+}=F^->NH_4^+$. The composition clearly indicated towards the crustal source contribution with high Cl^- (4.13 ± 0.55 mg/m^2/d) and Ca^{2+} (3.77 ± 0.55 mg/m^2/d) fluxes arising from the soil re suspended dust of the rural land use pattern (Kumar et al., 2014).

4.3. Reactive nitrogen species (Nr) in the dustfall fluxes

The dustfall fluxes of NO_3^- as well as NH_4^+ Nr species were determined for the selected sampling sites as shown in Fig.4.8.
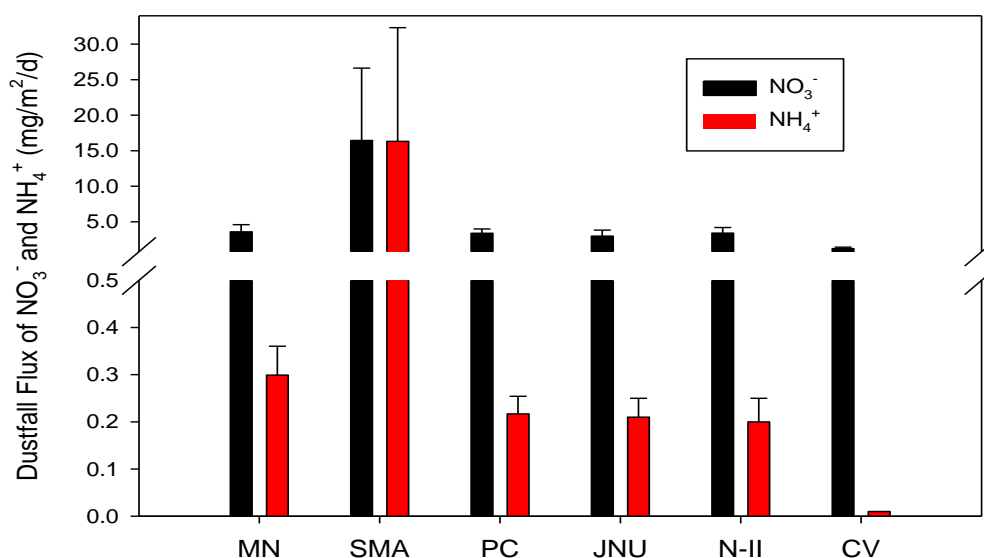
Fig.4.8. Bar diagram showing reactive nitrogen dustfall fluxes $(mg/m^2/d)$ at each site

Lowest fluxes of NO_3^- $(1.2\pm0.2$ $mg/m^2/d)$ were observed at the rural site CV owing to its minimum disturbance from the anthropogenic influence. However, with the agricultural fields being a constant emission source of ammonia near the sampling site, a rather non- detectable flux of NH_4^+ was observed (Aneja et al., 2014). This could be attributed to the high pH of the soil and dust that has resulted in its repelling behaviour with NH_3 due to its alkaline nature. High ambient temperature during the sampling could also be implicated for the rapid volatilization of NH_4^+ from the coarse mode particulates. Delay in the analysis could also be one of the reasons for the loss of NH_4^+ during storage of the samples. Highest fluxes of NO_3^- $(16.5\pm10.2$ $mg/m^2/d)$ and NH_4^+ $(16.3\pm16$ $mg/m^2/d)$, on the other hand, were observed over the SMA site where the diesel emissions from trucks and industrial activities resulted in the constant NOx emissions (Galloway et al., 2006). Also the losses from industrial refrigeration units are

known for contributing significantly to the high ammonia levels over the industrial estates (EPA, 2004).

Regular flow of traffic has resulted in a constant flux of NO_3^- (3.4 ± 0.6 mg/m^2/d) and NH_4^+ (0.2 ± 0.04 mg/m^2/d) at PC site. However, its values were relatively lower than the NO_3^- (3.6 ± 1.00 mg/m^2/d) and NH_4^+ (0.30 ± 0.06 mg/m^2/d) fluxes observed at high density residential MN site. The unusual disparity could be attributed to the high NO_3^- fluxes arising from the narrow road conditions of the MN site that has been heavily encroached by the street vendors and eatery joints resulting in its bottleneck situation of traffic congestion. Poor sewage conditions and prevalence of light duty vehicles at MN site, on the other hand, could be implicated for its relatively high NH_4^+ fluxes than PC site (Reis et al., 2009).

N–II being a typical sub urban site, showed a similar pattern of its NO_3^- (3.36 ± 0.78 mg/m^2/d) and NH_4^+ (0.22 ± 0.05 mg/m^2/d) fluxes in comparison to the other urban sites of PC and MN. High NO_3^- along with SO_4^{2-} fluxes could be attributed to the frequent use of power generators for meeting the requirements of the daily power cuts. Biomass burning from the nearby Barolla village along with the biogenic emissions from the highly fertile soil of the sampling site could be speculated for high NH_4^+ fluxes at N- II site (Anderson et al., 2003; Calvo et al., 2013). However, the JNU site showed the lowest values of the NO_3^- (3 ± 0.8 mg/m^2/d) and NH_4^+ (0.2 ± 0.04 mg/m^2/d) fluxes in comparison to the other urban sampling sites of our study area.

On comparison of our results with the other case studies (Table.4.3.) a higher Nr deposition flux pattern was observed for our urban study area. The fluxes of NO_3^- over Pune showed comparatively higher values than the urban and suburban site of the present study. Nr fluxes at the rural site, on the other hand, were observed to be even lower than the Gopalpura rural site of Agra. But with the summer time meteorology of strong winds and unstable atmospheric conditions being maintained throughout the sampling duration, a rather constant flux of Nr species were observed with an insignificant difference ($\alpha < 0.05$) in its inter site variability.

Table.4.3. Comparison of dry deposition fluxes of reactive nitrogen species measures at different sites from South East Asian region

Site	Category	NO_3^- flux (mg/m2/d)	NH_4^+ flux (mg/m2/d)	Reference
Delhi (MN)	Residential	3.59 ± 1.00	0.30 ± 0.06	Present study
Delhi (SMA)	Industrial	16.45 ± 10.17	16.33 ± 16	
Delhi (PC)	Traffic	3.39 ± 0.61	0.22 ± 0.04	
Delhi (JNU)	Urban forest	2.98 ± 0.84	0.21 ± 0.04	
Noida(N– II)	Suburban	3.36 ± 0.78	0.22 ± 0.05	
Haryana (CV)	Rural	1.24 ± 0.16	ND	
Other studies				
Delhi	Urban	0.66	ND	Parashar et al., 2001
Ahmedabad	Urban	0.41	0.03	Rastogi et al., 2006
Mumbai	Urban	0.92	ND	Venkatraman et al., 2002
Dhaka (Bangladesh)	Urban	0.71	0.12	Salam et al., 2003
Pune	Sub urban	4.73	0.03	Budhavant et al., 2012
Hisar	Semi urban	2.60 ±1.3	0.43 ± 0.28	Rengarajan et al., 2007
Chhattisgarh	Semi urban	0.749 ± 0.48	0.74 ± 0.36	Verma et al., 2010
Agra	Semi urban	1.63	0.44	Kulshrestha et al., 1998
Gopalpura	Rural (summers)	1.7 ± 0.6	2.7 ± 1.1	Satsangi et al., 2002
Manora peak	High altitude (remote)	0.10 ± 0.06	0.03 ± 0.02	Rengarajan et al., 2007
Mt. Abu	High altitude (remote - summers)	0.07 ± 0.09	ND	Kumar et al., 2010

4.3.1. Mukherjee Nagar (MN)

NO_3^- flux at MN site ranged from 0.2–8.2 mg/m^2/d with a mean value of 3.6±1.00 mg/m^2/d. Summer time meteorology of strong winds and high mixing ratios of the atmosphere resulted in its upward trend irrespective of the minor fluctuations in the temperature conditions (Fig.4.9). The highest average fluxes of NO_3^- were observed for the month June (Table 4.4) owing to the high humid levels (~ 40%) that are known for shifting the gas–particle phase partitioning of the nitrates to its crystallized phase (Metzger et al., 2006).

Table.4.4. Nr fluxes along with the meteorological parameters at MN site

Sampling (n = 13)	NO_3^- flux (mg/m^2/d)	NH_4^+ flux (mg/m^2/d)	Mean temp (^{0}C)	Mean relative humidity (%)	Mean wind speed (km/hr)
April (n = 3)	1.6 ± 1.4	0.4 ± 0.2	30.5	36.3	10.7
May (n = 6)	3.4 ± 1.2	0.2 ± 0.08	34.3	28.8	7.8
June (n = 4)	5.5 ± 1.1	0.3 ± 0.11	33.8	40.6	9.5

NH_4^+ fluxes, on the other hand, ranged from 0 – 0.7 mg/m^2/d with a mean value of 0.30 ± 0.06 mg/m^2/d. With April showing the highest NH_4^+ flux (0.4 ± 0.2 mg/m^2/d) throughout the sampling duration, it could be speculated that the rising temperature conditions resulted in a declining trend in the NH_4^+ fluxes (Table 4.4).Minor fluctuations in an otherwise declining flux trend could be attributed to the dust storm event of 19th May that resulted in its increased dust scavenged levels in the dust fluxes (Fig. 4.9).
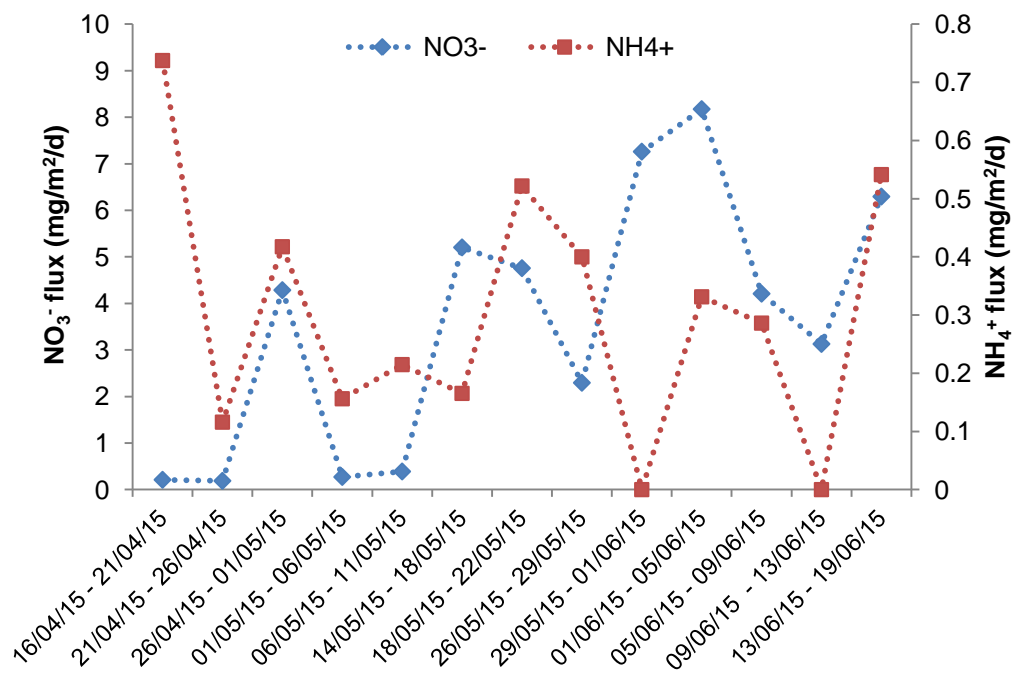
Fig.4.9. Time series of Nr flux variations at MN site

4.3.2. SMA Industrial Estate (SMA)

The nitrate flux at SMA site ranged from 0.04–156.5 mg/m^2/d with a mean value of 16.5±10.2 mg/m^2/d. The industrial emissions maintained a constant trend of high nitrate fluxes throughout the sampling period irrespective of temperature and relative humidity levels (Fig. 4.10). But with the dust storm event of 19th May, the NO_3^- showed an exponential spike in its average flux values during May (Table.4.5)

Table.4.5. Nr fluxes along with the meteorological parameters at SMA site

Sampling (n = 15)	NO$_3^-$ flux (mg/m^2/d)	NH$_4^+$ flux (mg/m^2/d)	Mean temp (^{0}C)	Mean relative humidity (%)	Mean wind speed (km/hr)
April (n = 3)	1.9±1.8	0.5±0.03	31	30.5	10.7
May (n = 7)	26.4±21.7	34.5±34.3	34.3	28.7	8.5
June (n = 5)	11.2±4.9	0.4±0.08	33.5	43.7	9.9

NH_4^+ fluxes, on the other hand, showed its value range from 0–379.5 mg/m^2/d with a mean of 16.3±16 mg/m^2/d (Table.4.5). Similar to the NO_3^- flux, a constant trend was also observed for the NH_4^+ fluxes with the dust storm event resulting in a sudden spike to its average flux values for the month of May (Fig 4.10).
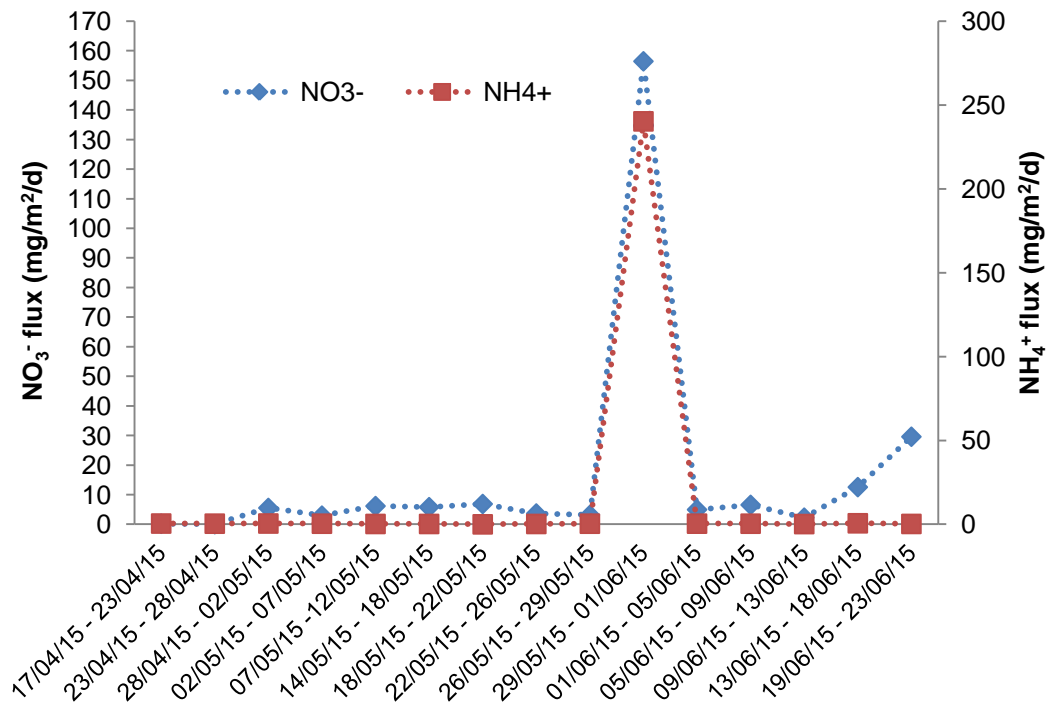
Fig.4.10. Time series of Nr flux variation at SMA site

4.3.3. Peeragarhi Chowk (PC)

The NO_3^- fluxes at PC ranged from 0.1-7.6 mg/m^2/d with a mean value of 3.4±0.6 mg/m^2/d (Fig.4.11). A constant trend was observed in the NO_3^- fluxes (Table. 4.6) owing to its continuous emissions from the heavy duty vehicles. Changing conditions of temperature and relative humidity resulted in some minor fluctuations in the data set values with the dust storm event of 19th May producing high variability in the data set of May.

Table.4.6. Nr fluxes along with the meteorological parameters at PC site

Sampling (n = 13)	NO_3^- flux $(mg/m^2/d)$	NH_4^+ flux $(mg/m^2/d)$	Mean temp (^0C)	Mean relative humidity (%)	Mean wind speed (km/hr)
April (n = 3)	2.6 ± 2.5	0.2 ± 0.1	30.9	36	10.3
May (n = 7)	3.6 ± 0.7	0.2 ± 0.06	34.3	28.7	8.5
June (n = 3)	3.6 ± 0.09	0.2 ± 0.06	33.5	43.7	9.9

Keeping in sync with the NO_3^- fluxes, a constant trend was also observed for NH_4^+ fluxes that ranged from 0–0.5 $mg/m^2/d$ with a mean of 0.2 ± 0.04 $mg/m^2/d$ (Fig 4.6). Its continuous emissions from light duty vehicles has resulted in its fluxes being independent of temperature and relative humidity conditions (Table 4.11)
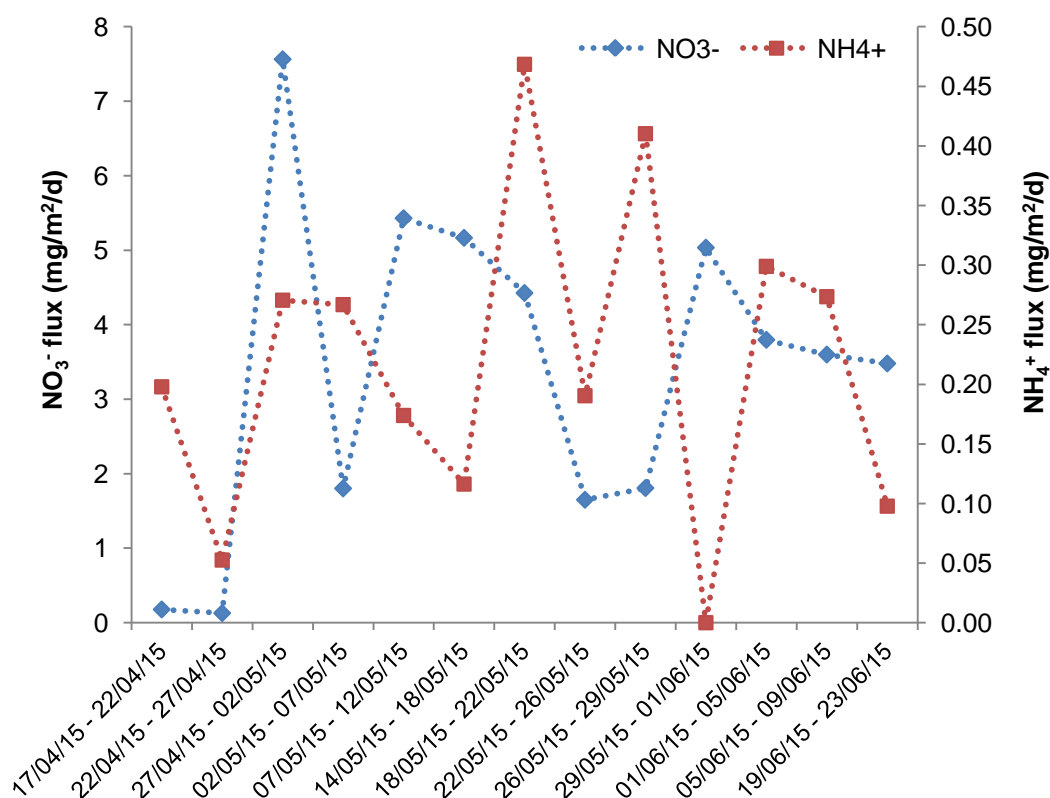
Fig.4.11. Time series of Nr flux variation at PC site

4.3.4. JNU

Nitrate fluxes at JNU ranged from 0.1–8.9 mg/m^2/d with a mean of 3.00±0.8 mg/m^2/d (Fig.4.12). Minimum emission sources of nitrates near the sampling site has resulted in a constant variability in the data set values with high relative humidity levels resulting in high average fluxes as observed for the month of June (Table 4.7).

Table.4.7. Nr fluxes along with the meteorological parameters at JNU site

Sampling (n = 13)	NO$_3^-$ flux (mg/m^2/d)	NH$_4^+$ flux (mg/m^2/d)	Mean temp (^{0}C)	Mean relative humidity (%)	Mean wind speed (km/hr)
April (n = 3)	1 ± 0.7	0.2 ± 0.1	30.9	36.5	10.3
May (n = 7)	1.9 ± 0.7	0.3 ± 0.04	34.3	28.7	8.5
June (n = 3)	7.6 ± 0.8	0.1 ± 0.1	33.6	40.6	10.6

The fluxes of NH$_4^+$ ranged from being not detected to 0.4 mg/m^2/d with a mean value of 0.2 ± 0.04 mg/m^2/d (Fig 4.12). Under the limiting condition of its minimum source emissions, the values of NH$_4^+$ showed fluctuation with the meteorological condition of the region (Table. 4.7). Despite the high temperature conditions, a average flux of NH$_4^+$ was observed during May owing to the occurrence of dust storm event resulting in its high scavenging.
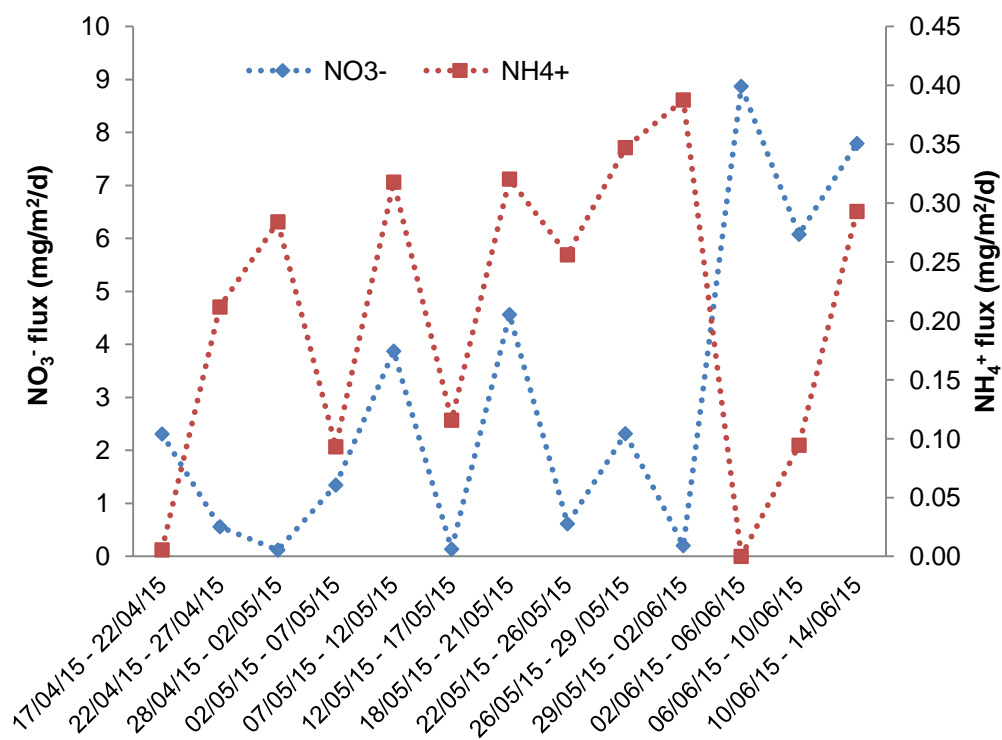
Fig.4.12. Time series of Nr flux variations at JNU site

4.3.5. Noida Phase–II (N-II)

Nitrate flux at N–II ranged from 0.02–7.6 mg/m^2/d with a mean value of 3.4±0.8 mg/m^2/d (Fig. 4.13). The highest average flux of NO$_3^-$ was observed during May irrespective of its high temperature and low humid conditions (Table.4.8). This could be attributed to the dominant emission source of NO$_3^-$ arising from extensive use of power generators during summers which have already become quite prevalent over the NCR regions for meeting the daily requirement of electric supplies due to frequent power cuts.

Table.4.8. Nr fluxes along with the meteorological parameters at N–II site

Sampling (n = 11)	NO_3^- flux (mg/m^2/d)	NH_4^+ flux (mg/m^2/d)	Mean temp (^{0}C)	Mean relative humidity (%)	Mean wind speed (Km/hr)
April (n = 2)	2.9 ± 2.9	0.5 ± 0.03	31.2	33.3	10.3
May (n = 6)	4.6 ± 0.9	0.2 ± 0.04	34.3	28.8	8.5
June (n = 3)	1.30 ± 0.8	0.1 ± 0.001	33.5	40.6	9.9

NH_4^+ fluxes, on the other hand, showed values that ranged from 0.03–0.5 mg/m^2/d with a mean of 0.2±0.05 mg/m^2/d (Fig 4.13). With the rise in temperature condition, a decline in average flux value of NH_4^+ was observed, therefore, indicating towards the significant role of meteorological parameters under limiting emission source conditions (Table 4.8)
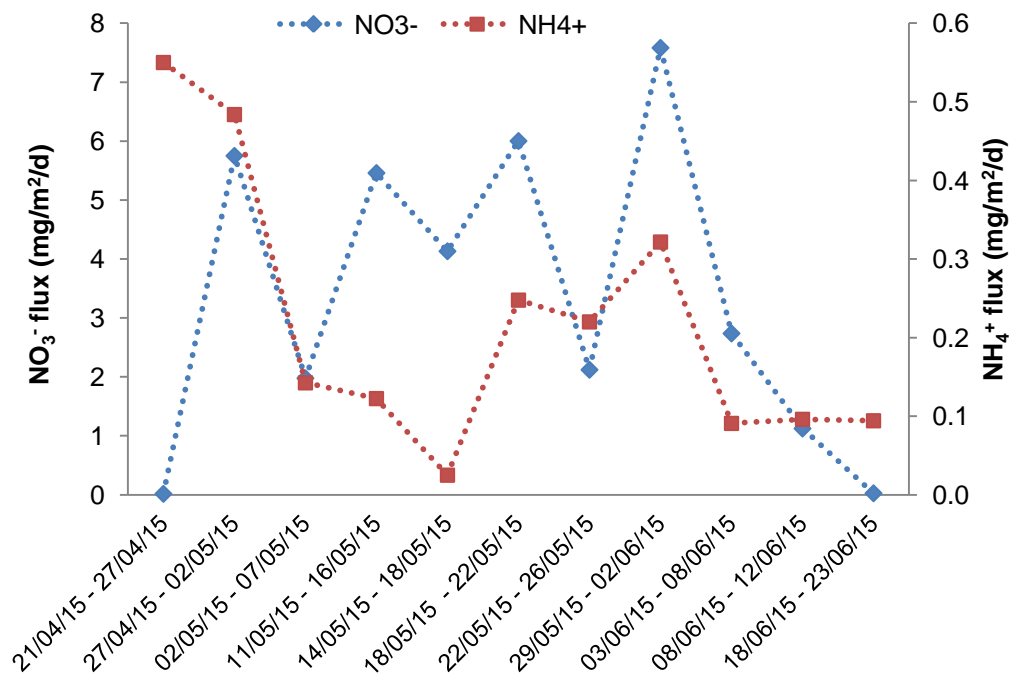
Fig.4.13. Time series of Nr flux variation at N–II site

4.3.6. Chhuchhakwas village (CV)

Nitrate flux at CV site ranged from 0.4–2.1 mg/m^2/d with a mean value of 1.2±0.2 mg/m^2/d (Fig. 4.14). A combination of strong winds and high temperature resulted in a mixing ratio of nitrate with the effect of high average fluxes of NO_3^- being observed during the month of May (Table 4.9).

Table.4.9. Nr fluxes along with the meteorological parameters at CV site

Sampling (n = 11)	NO$_3^-$ flux (mg/m^2/d)	NH$_4^+$ flux (mg/m^2/d)	Mean Temp (^{0}C)	Mean relative humidity (%)	Mean wind Speed (km/hr)
April (n = 5)	1.3 ± 0.2	ND	31.9	32	8.9
May (n = 3)	1.4 ± 0.4	ND	34.5	28	10.5
June (n= 2)	0.9 ± 0.50	ND	33.5	40	9.9

Non–detectable levels were observed in the case of NH$_4^+$ fluxes despite the rural backdrop of the sampling site (Fig 4.14). This could be attributed to the lack of constant source of emissions with high temperature conditions resulting in the rapid volatilization of NH$_4^+$ in the dustfall fluxes (Table 4.9).
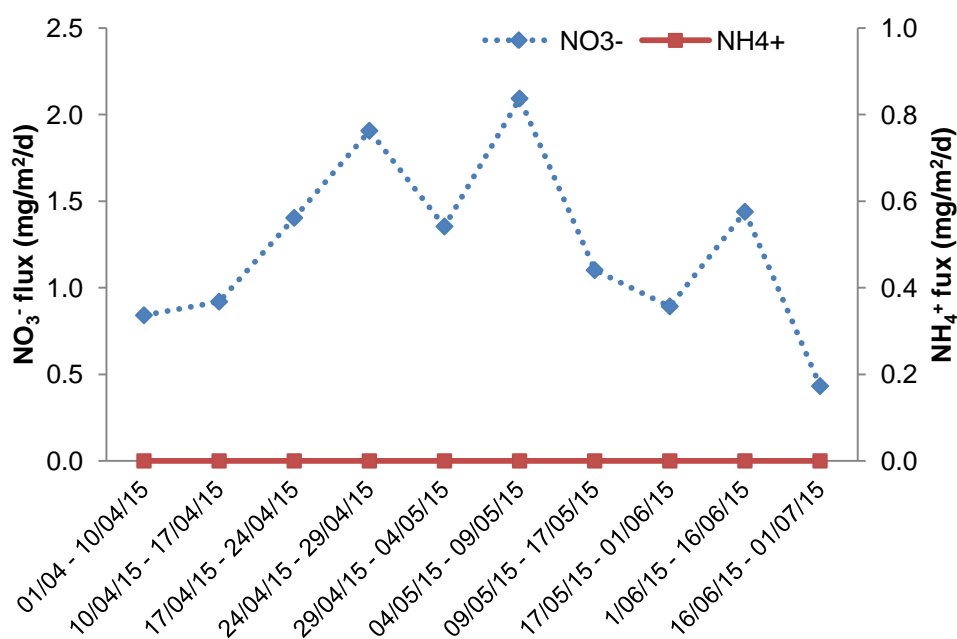
Fig.4.14. Time series of Nr flux variations at CV site

4.4. Interaction of Nr species with the dustfall components

The fluxes of Nr were analyzed for its possible interaction with the pre existing ionic composition of the dust fluxes with help of correlation graphs and ion balance ratios. Deciphering of such interactions could be used for providing an insight into the stoichiometric reactions that were involved in the scavenging of excess Nr acidity from the atmosphere.

NO_3^- being an acidic anion has a strong affinity for the basic cations present in the dust flux composition. Therefore, the neutralization capacities of the major acid neutralizing cations like Ca^{2+}, Mg^{2+} and NH_4^+ were determined through its neutralization factor (N_f) based on the following equation given by Satsangi (2013):

$$N_f\,(Ca^{2+}) = [Ca^{2+}] / [SO_4^{2-}] + 2[NO_3^-] \qquad N_f\,(NH_4^+) = [NH_4^+] / 2[SO_4^{2-}] + [NO_3^-]$$

$$N_f\,(Mg^{2+}) = [Mg^{2+}] / [SO_4^{2-}] + 2[NO_3^-] \qquad N_f\,(K^+) \;\; = [K^+] / 2[SO_4^{2-}] + [NO_3^-]$$

	MN	SMA	PC	JNU	N – II	CV
Nf (Ca2+)	1.29	0.25	1.29	1.29	1.23	1.8
Nf (Mg2+)	0.14	0.09	0.14	0.08	0.15	0.61
Nf (K+)	0.15	0.01	0.15	0.12	0.26	0.53
Nf (NH4+)	0.05	0.16	0.05	0.04	0.06	0
	1	1	1	1	1	1
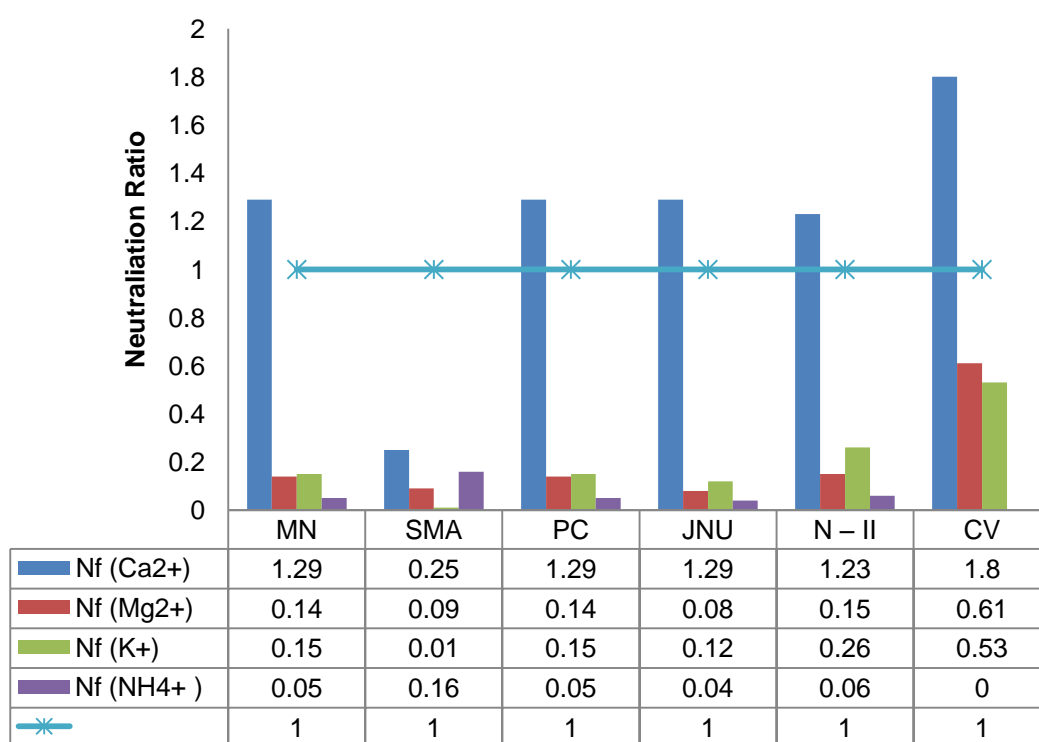
Fig.4.15.Neutralization factor (N_f) of the major basic cations at each site

Amongst all the major basic cationic bases, highest neutralization ratios were observed for Ca^{2+} at all the sites that ranged from 0.25 (SMA site) to 1.80 (CV site) (Fig.4.15). Therefore, the dominating role of Ca^{2+} in the major stoichiometric reactions required for the scavenging of the acidic precursor gases from the atmosphere cannot be ruled out. NH_4^+, on the other hand, showed the least neutralization factor, thereby, suggesting towards its absence from the stoichiometric neutralization reactions. However, owing to the high industrial emissions of ammonia over the industrial estate, a comparatively higher neutralization factor of NH_4^+ (0.16) was observed in the dustfall fluxes at SMA site.

4.4.1. Mukherjee Nagar (MN)

The dominance of N_f (Ca^{2+}) at MN site has resulted in Ca^{2+} being the major cationic base involved in controlling the fluxes of the acidic NO_3^- from the atmosphere. However, the strong affinity of SO_4^{2-} with Ca^{2+} in comparison to NO_3^- (Fig.4.16.a) has eventually resulted in a low median equivalent ratio of NO_3^-/SO_4^{2-} (0.73) in the dust fluxes.
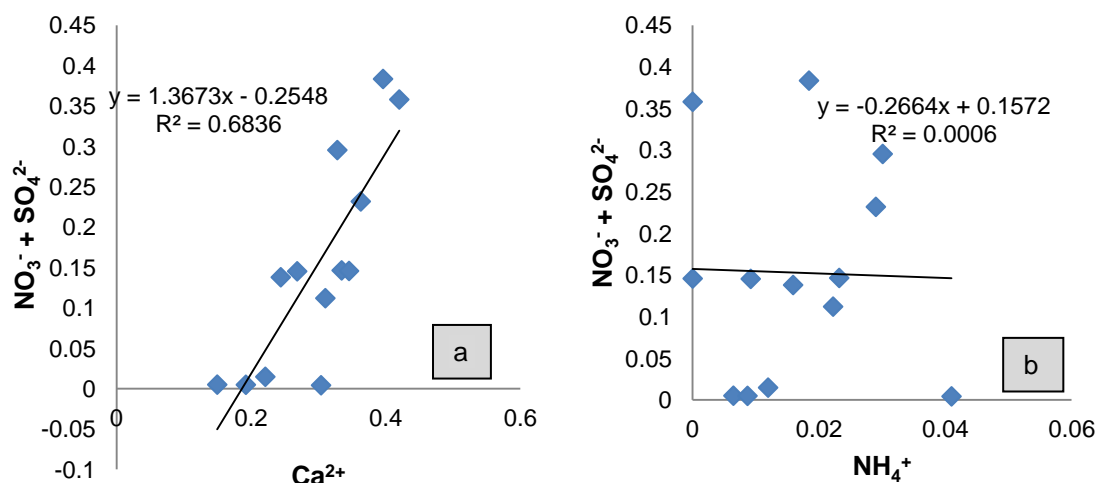
Fig.4.16. Regressions plots between a) $NO_3^- + SO_4^{2-}$ vs Ca^{2+} and b) $NO_3^- + SO_4^{2-}$ vs NH_4^+ at MN site

NH_4^+ being a weak base cation, on the other hand, showed the lowest flux values owing to the pre dominance of Ca^{2+} as a major basic cation in the dustfall fluxes. This has resulted in the minimum interference of NH_4^+ in the stoichometric

neutralization reaction required for the scavenging of NO_3^- and SO_4^{2-} through dustfall fluxes (Fig.4.16.b). Based on the rainfall intensity and scavenging patterns, Kulshrestha et al. (2009) have already demonstrated that NH_4^+ and NO_3^- mainly exist as NH_4NO_3 in the ambient particulate matter which can also be collected along with the dustfall. In order to understand the covariation of ions and their associated sources, correlation coefficients were calculated as given in the Table 4.10.

Table 4.10. Correlation matrix of Nr with the ionic components of dust fluxes at MN site

	Na^+	NH_4^+	K^+	Ca^{2+}	Mg^{2+}	F^-	Cl^-	NO_3^-	SO_4^{2-}	pH
Na^+	1									
NH_4^+	-.017	1								
K^+	.510	.141	1							
Ca^{2+}	**.802****	.165	.413	1						
Mg^{2+}	**.934****	.038	.491	**.905****	1					
F^-	.211	-.064	.093	.551	.312	1				
Cl^-	**.777****	-.168	.253	**.870****	**.784****	**.604***	1			
NO_3^-	.531	-.041	.014	**.768****	**.667***	**.774****	**.777****	1		
SO_4^{2-}	**.660***	-.023	.025	**.836****	**.750****	**.671***	**.863****	**.927****	1	
pH	**.613***	-.289	-.055	.489	**.565***	.269	**.669***	.472	**.568***	1

**. Correlation is significant at the 0.01 level (2-tailed).

*. Correlation is significant at the 0.05 level (2-tailed).

A significant positive correlation of NO_3^- with Cl^- (r=0.777), F^- (r=0.774), Ca^{2+} (r = 0.768) and Mg^{2+} (r=0.667) showed the dominance of crustal sources in regulating the deposition fluxes of NO_3^-. A strong positive correlation of Ca^{2+} with Cl^- (r=0.870), SO_4^{2-} (r=0.836) and NO_3^- (r=0.768) suggests the dominant formation of $CaCl_2$ and $CaSO_4$ in the dust fluxes along with the formation of $Ca(NO_3)_2$ under the excess Ca^{2+} condition. A weak negative correlation of NH_4^+ with the major anionic species, on the

other hand, suggests towards the near absence of NH_4^+ in the coarse mode fraction of the dust fluxes.

4.4.2. SMA Industrial Estate (SMA)

The role of Ca^{2+} in the stoichiometric neutralization reactions was observed to be limited by the excess emissions of acidic precursor gases over the industrial estate. This has eventually resulted in high deposition fluxes of NO_3^- and SO_4^{2-} irrespective of the Ca^{2+} in the dust fluxes (Fig: 4.17.a). A low median value of NO_3^-/SO_4^{2-} equivalent ratio (0.25) further suggested towards the dominance of SO_4^{2-} over NO_3^- in Ca^{2+} neutralization reactions by the dustfall fluxes.
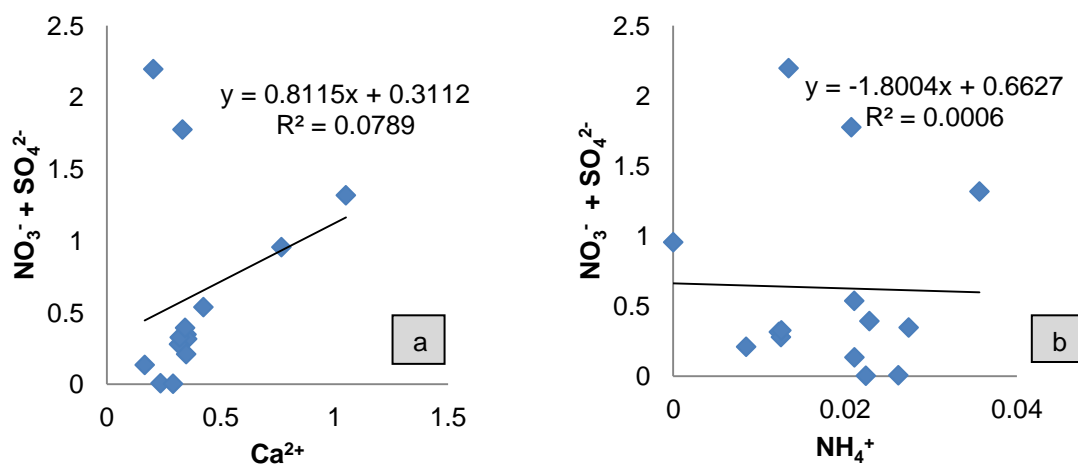
Fig.4.17. Regressions plots between a) $NO_3^- + SO_4^{2-}$ vs Ca^{2+} and b) $NO_3^- + SO_4^{2-}$ vs NH_4^+ at SMA site

Unlike the other sites, high acidic precursor gas emissions at SMA have eventually resulted in raising the neutralization factor of NH_4^+. But the scavenging of NO_3^- and SO_4^{2-} through NH_4^+ neutralization reactions remained limited owing to the weak base nature of the cation in the dust fluxes (Fig 4.17. b).

The covariance of different ions in the dust fluxes gave a significantly strong positive correlation of NH_4^+ with Cl^- (r=1), SO_4^{2-} (r=0.998), Ca^{2+} (r=0.990) and NO_3^- (r=0.984) that suggested towards the dominance of anthropogenic sources in regulating the dust fluxes of NO_3^- and SO_4^{2-} at SMA site (Table 4.11) .

Table 4.11 Correlation matrix of Nr with the ionic components of dust fluxes at SMA site

	Na^+	NH_4^+	K^+	Ca^{2+}	Mg^{2+}	F^-	Cl^-	NO_3^-	SO_4^{2-}	pH
Na^+	1									
NH_4^+	-.261	1								
K^+	-.086	.958**	1							
Ca^{2+}	-.176	.990**	.964**	1						
Mg^{2+}	-.207	.998**	.966**	.994**	1					
F^-	.503	-.222	-.217	-.187	-.199	1				
Cl^-	-.238	1.000**	.960**	.992**	.999**	-.205	1			
NO_3^-	-.265	.984**	.923**	.977**	.982**	-.081	.985**	1		
SO_4^{2-}	-.254	.998**	.951**	.991**	.997**	-.184	.998**	.990**	1	
pH	.205	.574*	.577*	.595*	.597*	-.100	.580*	.540*	.568*	1

**. Correlation is significant at the 0.01 level (2-tailed).

*. Correlation is significant at the 0.05 level (2-tailed).

A strong correlation of Ca^{2+} with Cl^- (r=0.992), SO_4^{2-} (r=0.991) and NO_3^- (r=0.977) suggests towards the possible formation of $CaCl_2$, $CaSO_4$ and $Ca(NO_3)_2$ along with NH_4Cl, $(NH_4)_2SO_4$ and NH_4NO_3 in the dust flux samples collected at SMA site.

4.4.3. Peeragarhi chowk (PC)

Being a major transport hub, the dustfall flux at PC site showed a dominance of Ca^{2+} in regulating the stoichiometric neutralization reactions required for the scavenging of NO_3^- and SO_4^{2-} through dustfall fluxes (Fig.4.18a). This has resulted in a dominance of SO_4^{2-} over NO_3^- with a median equivalence ratio of 0.60 in the dustfall fluxes despite the prevalence of NOx emission sources near the sampling site. NH_4^+, on the other hand, showed relatively weak buffering of NO_3^- and SO_4^{2-} (Fig.4.18b) owing to the low neutralization factor of NH_4^+ (0.05) in comparison to the Ca^{2+} (1.29) observed in the dust fluxes at site PC.
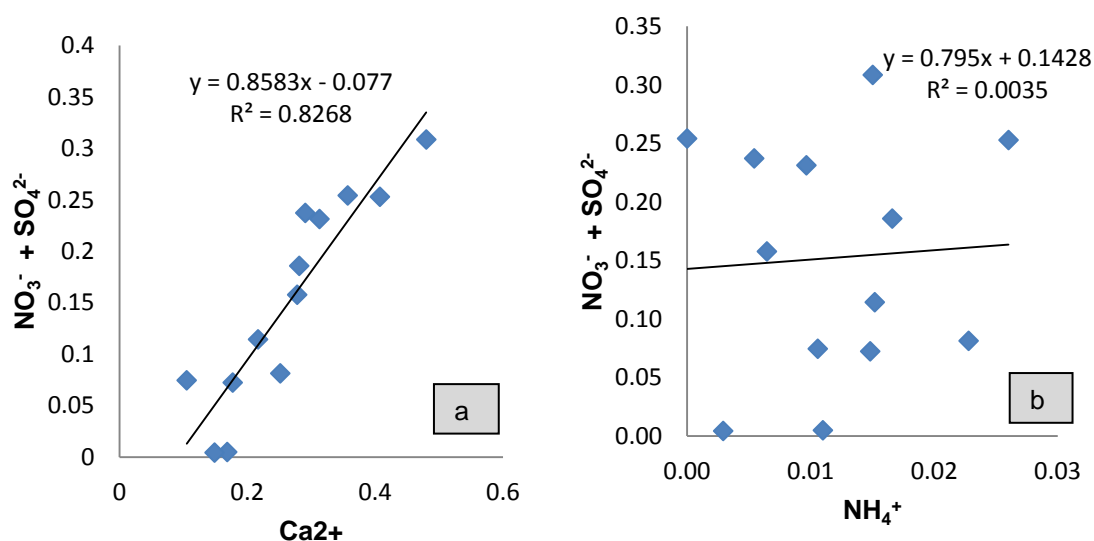
Fig. 4.18. Regressions plots between a) $NO_3^- + SO_4^{2-}$ vs Ca^{2+} and b) $NO_3^- + SO_4^{2-}$ vs NH_4^+ at PC site

The covariance of ionic composition of the dust fluxes (Table. 4.12) showed a significant positive correlation of Ca^{2+} with Mg^{2+} (r=0.917) and Cl^- (r=0.633) thereby indicating the crustal source of the dust fluxes at PC site.

Table 4.12. Correlation matrix of Nr with the ionic components of dust fluxes at PC site

	Na^+	NH_4^+	K^+	Ca^{2+}	Mg^{2+}	F^-	Cl^-	NO_3^-	SO_4^{2-}	pH
Na^+	1									
NH_4^+	.167	1								
K^+	**.719**[**]	.218	1							
Ca^{2+}	**.860**[**]	.219	.629[*]	1						
Mg^{2+}	**.950**[**]	.192	.628[*]	**.917**[**]	1					
F^-	.220	.110	.168	.597[*]	.359	1				
Cl^-	.661[*]	.464	.405	.633[*]	**.764**[**]	.260	1			
NO_3^-	**.724**[**]	.043	.551	**.869**[**]	**.792**[**]	.622[*]	.598[*]	1		
SO_4^{2-}	.654[*]	.063	.395	**.873**[**]	**.773**[**]	**.765**[**]	.660[*]	**.821**[**]	1	
pH	.519	-.367	-.010	.389	.570[*]	.151	.329	.398	.412	1

**. Correlation is significant at the 0.01 level (2-tailed).

*. Correlation is significant at the 0.05 level (2-tailed).

A strong positive correlation of NO_3^- with Ca^{2+} (r=0.869), Mg^{2+} (r=0.792) and Na^+ (r=0.724) and a comparatively stronger correlation of SO_4^{2-} with Ca^{2+} (r=0.873), Mg^{2+} (r=0.773) and Na^+ (r=0.654) suggested towards the formation of $Ca(NO_3)_2$, $CaSO_4$, $Mg(NO_3)_2$, $MgSO_4$, $NaNO_3$ and Na_2SO_4 in the dust fluxes at the site PC.

4.4.4. JNU.

Though the neutralization capacity of Ca^{2+} (1.29) showed values similar to the traffic site PC but its role in the scavenging of NO_3^- and SO_4^{2-} through dustfall remained limited (Fig 4.19a). This could be attributed to the minimum anthropogenic influence at JNU site that has resulted in the low levels of NO_3^- and SO_4^{2-} in the dust fluxes even at high Ca^{2+} levels. The equivalence ratio of NO_3^-/ SO_4^{2-} showed a median value of 0.67 thereby indicating a dominance of SO_4^{2-} over NO_3^- in the dustfall fluxes. NH_4^+ showed minimum interactions in the scavenging of NO_3^- and SO_4^{2-} (Fig.4.19.b) owing to the weak base properties of NH_4^+ ($N_f = 0.04$) in comparison to Ca^{2+} ($N_f = 1.29$).
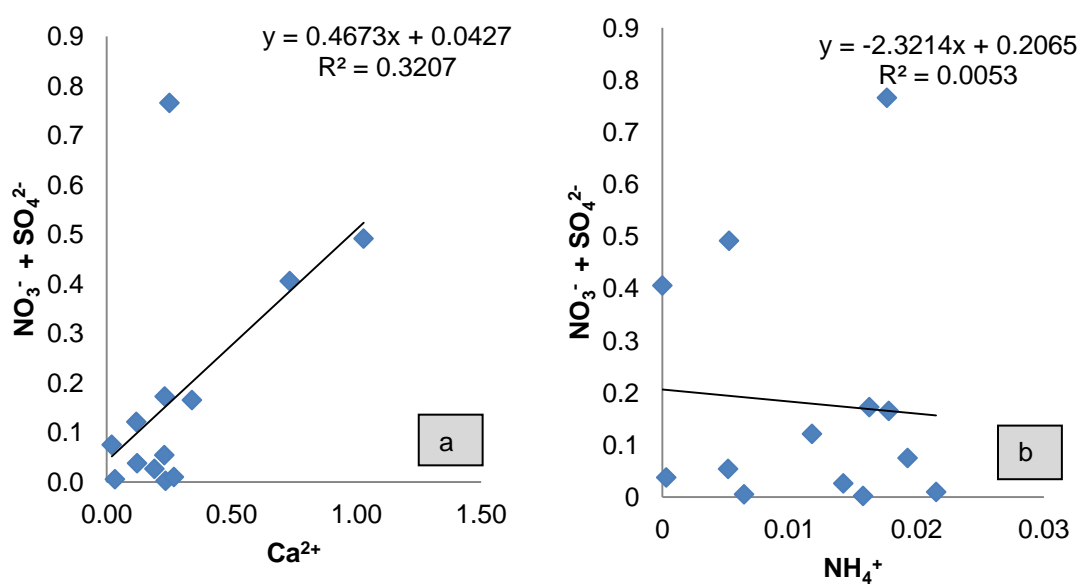
Fig.4.19 Regressions plots between a) $NO_3^- + SO_4^{2-}$ vs Ca^{2+} and b) $NO_3^- + SO_4^{2-}$ vs NH_4^+ at JNU site.

The correlation matrix (Table.4.13) showed a strong correlation of Ca^{2+} with K^+ (r= 0.892), Cl^- (r=0.861) and Na^+ (r=0.621) but a weak negative correlation with Mg^{2+} (r =-0.054).

Table 4.13. Correlation matrix of Nr with the ionic components of dust fluxes at JNU site

	Na^+	NH_4^+	K^+	Ca^{2+}	Mg^{2+}	F^-	Cl^-	NO_3^-	SO_4^{2-}	pH
Na^+	1									
NH_4^+	.195	1								
K^+	.606*	-.257	1							
Ca^{2+}	.621*	-.380	**.892****	1						
Mg^{2+}	.561*	.416	-.099	-.054	1					
F^-	.391	-.149	.425	.679*	-.072	1				
Cl^-	.577*	-.340	**.713****	**.861****	.035	**.721****	1			
NO_3^-	.557*	-.266	.478	.647*	.251	.684**	**.877****	1		
SO_4^{2-}	.566*	-.024	.587*	.485	.123	.166	.531	.442	1	
pH	.600*	-.422	**.893****	**.957****	-.126	**.714****	**.898****	**.709****	.503	1

*. Correlation is significant at the 0.05 level (2-tailed).

**. Correlation is significant at the 0.01 level (2-tailed).

This, therefore, becomes indicative towards the possible marine influence in the dust fluxes at JNU site which has eventually resulted in a significant positive correlation of SO_4^{2-} with K^+ (r=0.587) and Na^+ (r=0.566) and a strong correlation of NO_3^- with Cl^- (r=0.877), Ca^{2+} (r=0.647) and Na^+ (r=0.557). Therefore, the possible compounds in the dustfall fluxes over JNU could be suggested as K_2SO_4, Na_2SO_4, $NaNO_3$, KCl, NaCl and $Ca(NO_3)_2$.

4.4.5. Noida Phase – II (N-II)

Though Ca^{2+} showed highest neutralization factor amongst all the major cationic base at N- II site but the role of Ca^{2+} in the buffering of NO_3^- and SO_4^{2-} in the dust fluxes remained limited (Fig 4.20. a). An equivalence ratio of NO_3^-/ SO_4^{2-} showed

its median value at 0.8, thereby suggesting towards the near equivalence of NO_3^- and SO_4^{2-} in the dust fluxes. NH_4^+ showed no significant participation in the stoichiometric neutralization reaction required for the dust flux scavenging of the acidic precursor gases (Fig 4.20 b) owing to its weak base cationic properties with respect to other major cationic bases.
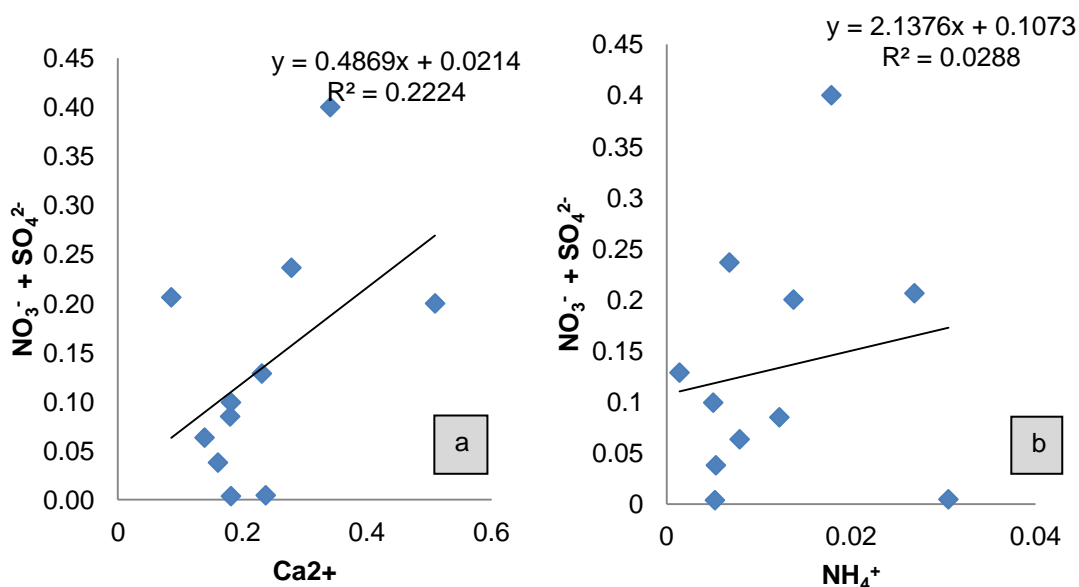
Fig.4.20. Regressions plots between a) $NO_3^- + SO_4^{2-}$ vs Ca^{2+} and b) $NO_3^- + SO_4^{2-}$ vs NH_4^+ at N-II site

The correlation matrix (Table. 4.14) showed a mixture of influences at site N–II with Na^+ showing a significant positive correlation with Cl^- (r= 0.627) and Cl^- showing a strong positive correlation with NO_3^- (r= 0.869) as well with SO_4^{2-} (r= 0.735) with the possible indication of marine influence in the dust flux scavenging. However, a strong positive correlation of K^+ with SO_4^{2-} (r=0.810) and a significant positive correlation of Mg^{2+} with NO_3^- (r=0.709) also suggests towards the possible role of crustal source contribution to the major fluxes of NO_3^- and SO_4^{2-} at N- II site. NH_4^+ however maintained a weak positive correlation with Mg^{2+} (r=0.547) as well as K^+ (r=0.512) which becomes suggestive towards its crustal sources. Therefore, the possible dominating compounds in the dust fluxes could be speculated as $Mg(NO_3)_2$, $Mg(SO_4)_2$, K_2SO_4, KNO_3 and $NaCl$.

Table 4.14. Correlation matrix of Nr with the ionic components of dust fluxes at N-II site

	Na^+	NH_4^+	K^+	Ca^{2+}	Mg^{2+}	F^-	Cl^-	NO_3^-	SO_4^{2-}	pH
Na^+	1									
NH_4^+	.316	1								
K^+	.423	.512	1							
Ca^{2+}	.360	.039	.426	1						
Mg^{2+}	.511	.547	**.711***	**.781****	1					
F^-	.282	.288	.482	.540	.553	1				
Cl^-	.627*	-.064	.403	.590	.625*	.397	1			
NO_3^-	.490	.127	.665*	.493	**.709***	.537	**.869****	1		
SO_4^{2-}	.360	.184	**.810****	.444	.638*	.564	**.735***	**.899****	1	
pH	-.656*	-.272	-.486	-.078	-.263	.108	-.249	-.270	-.235	1

*. Correlation is significant at the 0.05 level (2-tailed).
**. Correlation is significant at the 0.01 level (2-tailed).

4.4.6. Chhuchhakwas village(CV)

The rural background of the site CV has resulted in the highest $N_f(Ca^{2+})$ of the dustfall fluxes as compared to the other sites. Though a significant scavenging of the acidifying precursor gases were observed in the form of NO_3^- and SO_4^{2-} (Fig 4.21) but the low median value of NO_3^- / SO_4^{2-} equivalence ratio of 0.3 suggested towards the dominance of SO_4^{2-} over NO_3^- in the dustfall fluxes. NH_4^+, on the other hand, maintained its non-detectable values throughout the sampling period. Therefore, the significance of NH_4^+ in the dust flux scavenging properties was not established in the results and hence was not plotted against $NO_3^- + SO_4^{2-}$
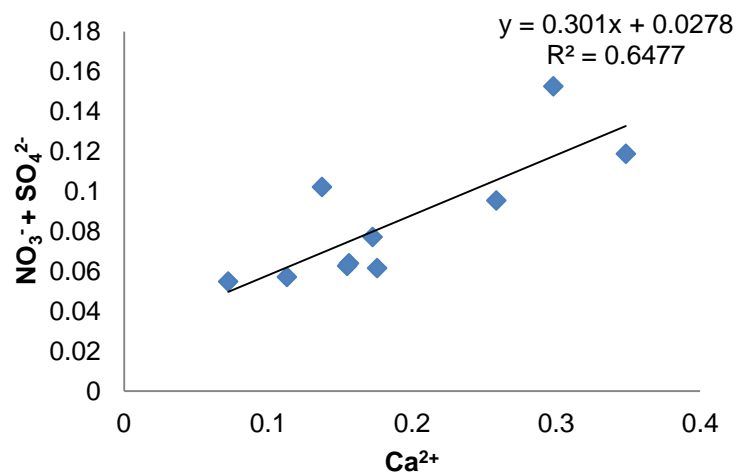
Fig.4.21. Regressions plots between NO_3^- + SO_4^{2-} vs Ca^{2+} at CV site

The covariance of different ions in the dust fluxes (Table 4.15) showed a strong correlation of Ca^{2+} with K^+ (r=0.848), F^- (r=0.844) and Mg^{2+} (r =0.743) which indicates towards the crustal sources of dust fluxes at site CV. A strong correlation of NO_3^- with F^- (r=0.795), Ca^{2+} (r=0.762) and Na^+ (r =0.709) and a strong correlation of SO_4^{2-} with Cl^- (r=0.897), Ca^{2+} (r=0.770), K^+ (r= 0.721) F^- (r=0.718) and Na^+ (r=0.616) suggested towards the dominant role of crustal sources in scavenging of the acidifying precursor gases over CV site. Therefore, the possible compounds formed in the dust fluxes could be speculated as $Ca(NO_3)_2$, $NaNO_3$, $CaSO_4$, K_2SO_4 and Na_2SO_4.

Table 4.15. Correlation matrix of Nr with the ionic components of dust fluxes at CV site

	Na^+	NH_4^+	K^+	Ca^{2+}	Mg^{2+}	F^-	Cl^-	NO_3^-	SO_4^{2-}
Na+	1								
K+	-.042	1							
Ca^{2+}	.229	**.848**[**]	1						
Mg^{2+}	-.271	**.971**[**]	**.743**[*]	1					
F^-	.518	.614	**.844**[**]	.445	1				
Cl^-	.678[*]	.527	.509	.363	.470	1			
NO_3^-	**.709**[*]	.441	**.762**[*]	.241	**.795**[**]	.645[*]	1		
SO_4^{2-}	.616	**.721**[*]	**.770**[**]	.551	**.718**[*]	**.897**[**]	**.754**[*]	1	
pH	.561	-.562	-.328	-.666[*]	-.100	.124	.181	-.054	1

*. Correlation is significant at the 0.05 level (2-tailed).

**. Correlation is significant at the 0.01 level (2-tailed).

4.5. Sources of influence on Nr dustfall fluxes

With the statistical evaluation of the data set showing a cocktail of sources contributing to the Nr fluxes over different sampling sites, there is a need for normalizing the dust flux data set with a reference crustal element. Ca^{2+} being the major base cations of dust fluxes were therefore used for delineating the crustal from the non crustal sources of interferences (Chakraborty et al., 2010; Behera et al., 2010). The Ca^{2+} normalized values were determined for the dustfall fluxes as well as for soil in order to apportion the relative abundance of source influence on the Nr fluxes (Table 4.16).

Table.4.16. Calcium normalized ionic composition of the dust and soil at each sites

	Site MN		Site SMA		Site PC		Site JNU		Site N-II		Site CV	
	Dust	**Soil**	**Dust**	**Soil**	**Dust**	**Soil**	**Dust**	**Soil**	**Dust**	**Soil**	**Dust**	**Soil**
Na^+/Ca^{2+}	0.18	1.33	0.3	0.4	0.2	0.54	0.2	0.03	0.24	1.29	0.32	0.89
NH_4^+/Ca^{2+}	0.05	ND	0.17	0.49	0.05	ND	0.12	0.06	0.06	ND	ND	ND
K^+/Ca^{2+}	0.15	0.14	0.12	0.15	0.14	0.11	0.22	0.38	0.26	0.04	0.36	0.8
Mg^{2+}/Ca^{2+}	0.06	0.51	0.12	0.18	0.06	0.08	0.08	0.11	0.08	0.24	0.16	0.11
F^-/Ca^{2+}	0.06	0.01	0.15	0.01	0.06	0.01	0.11	0.02	0.09	ND	0.08	0.03
Cl^-/Ca^{2+}	0.41	3.43	1.3	1.05	0.79	1.23	0.6	0.09	0.53	3.15	1.25	2.93
NO_3^-/Ca^{2+}	0.54	0.29	1.06	ND	0.59	0.14	0.91	0.21	0.85	0.26	0.34	0.92
SO_4^{2-}/Ca^{2+}	0.66	1.49	4.28	12.67	0.80	1.40	1.34	1.03	0.90	0.70	0.90	2.3

A comparison of Ca^{2+} normalized NO_3^- levels in dust fluxes and soil samples at SMA site showed a high NO_3^-/Ca^{2+} (1.06) in its dustfall fluxes on one hand with non-detectable levels of scavenged NO_3^- levels in its local soil on the other. This could be attributed to a complete absence of crustal source influence on the nitrate fluxes at SMA site. However, with the highest NO_3^-/Ca^{2+} in the local soil of CV site (0.34) but with low NO_3^-/Ca^{2+} (0.92) in the dustfall fluxes, the dominating interferences from the non crustal sources to Nr fluxes cannot be ruled out.

MN and PC site, on the other hand, showed similar NO_3^- enrichments in its dust flux pattern which could be attributed to its same source emissions with the relative low enrichment of soil nitrates at MN (0.29) over PC site (0.14) indicating towards its significant crustal source interference in the Nr fluxes.

Non-detectable values of NH_4^+ normalized Ca^{2+} concentrations in the local soil with a relatively higher enrichment of NH_4^+ in the dustfall fluxes, suggested towards a complete absence of crustal source contribution to the NH_4^+ fluxes at all the sites.

The crustal abundance of SO_4^{2-}, on the other hand, showed relatively higher enrichments than the dustfall counterparts, thereby indicating towards a non crustal source of contribution of SO_4^{2-} fluxes at all the sites. However, a higher enrichment of SO_4^{2-} was observed in the dustfall fluxes at N–II site which become speculative of its crustal source contribution. A relatively higher enrichment of Cl^- in the soil samples at all the sites indicated towards its non crustal abundance in the sampling regions. Baring from few exceptions, a low enrichment of K^+, Mg^{2+} and F^- in the dustfall fluxes were observed in general, thereby indicating towards its non crustal sources of influence,

4.6. Summer time fluxes of dustfall and its ionic species

Total dustfall deposition for dust load and its ionic species was estimated for all the sites as given in the Table 4.16. The calculation was done based on 90 days summer period (April–June) for the year 2015. The table represents the summer time deposition of dust that varied from 386–1042 $g/m^2/d$ during 3 months. Variations of these loadings of dust corresponded to the site characteristic and summer activities. In general, the order of ionic fluxes was noted as $Ca^{2+}>SO_4^{2-}>NO_3^->Cl^->Na^+>K^+>Mg^{2+}=F^->NH_4^+$ at MN site, $SO_4^{2-}>Cl^->NO_3^->Ca^{2+}=NH_4^+>Na^+ = K^+>F^-$ at SMA site, $Ca^{2+}>Cl^->SO_4^{2-}>NO_3^->Na^+>K^+>Mg^{2+}>NH_4^+=F^-$ at PC site, $SO_4^{2-}>Ca^{2+}>NO_3^->Cl^->K^+>Na^+>F^->Mg^{2+}=NH_4^+$ at JNU site, $Ca^{2+}>SO_4^{2-}>NO_3^->Cl^->Na^+ = K^+>Mg^{2+}=F^->NH_4^+$ at N–II site and $Cl^->Ca^{2+}>SO_4^{2-}>NO_3^->K^+>Na^+>Mg^{2+}=F^->NH_4^+$ at CV site which can be explained in similar manner as described in section 4.2.

Table 4.17. Estimation of the dustfall and its contribution to the ionic fluxes during the summer of Delhi–NCR region (2015)

Fluxes (g/m^2)	Sampling sites					
	MN	SMA	PC	JNU	N–II	CV
Dustfall	500	1042	493	597	386	927
NO_3^-	0.3 ± 0.1	1.5 ± 0.9	0.3 ± 0.05	0.3 ± 0.08	0.3 ± 0.07	0.1± 0.01
NH_4^+	0.03 ± 0.005	1.5 ±1.4	0.02 ± 0.003	0.02 ± 0.003	0.02 ± 0.005	ND
Ca^{2+}	0.5 ± 0.04	1.5 ± 0.76	0.48 ± 0.05	0.5 ± 0.14	0.4 ± 0.062	0.34 ± 0.05
Mg^{2+}	0.03 ± 0.003	0.3 ± 0.25	0.03 ± 0.005	0.02 ± 0.003	0.03 ± 0.006	0.07 ± 0.033
Na^+	0.1 ± 0.014	0.2 ± 0.06	0.09 ± 0.01	0.05 ± 0.01	0.08 ± 0.01	0.1 ± 0.02
K^+	0.08 ± 0.01	0.1 ± 0.03	0.07 ± 0.01	0.06 ± 0.01	0.09 ± 0.02	0.14 ± 0.04
SO_4^{2-}	0.4 ± 0.11	0.12 ± 0.01	0.4 ± 0.08	0.6 ± 0.25	0.3 ± 0.1	0.28 ± 0.04
Cl^-	0.3 ± 0.07	6.00 ± 5.3	0.4 ± 0.07	0.2 ± 0.05	0.2 ± 0.044	0.371 ± 0.05
F^-	0.03 ± 0.009	0.09 ± 0.03	0.03 ± 0.004	0.024 ± 0.005	0.03 ± 0.005	0.03 ± 0.004

4.7. Morphological and particle size distribution of the dust

Morphological assessment of the dustfall samples were carried out with the help of Scanning Electron Microscope (SEM). The SEM image for all the samples were acquired at the magnification of 500x. The most common shapes observed in the images were spherical, irregular, tubular, platy, long and prismatic, porous, crystalline and rhombic shape (Fig.4.23) owing to the geology and wind direction being the major controller of the mineralogy and morphology of the air borne dust (Zarasvandi et al., 2011). The tubular and rhomboidal shape in the morphological analysis of the dust may be present due to calcite and illite originating from the crustal sources. Presence of flaky agglomeration confirmed the occurrence of Ca^{2+} dominated reactions in the atmospheric dust (Gao et al., 2001) which along with the presence of irregular and spherical shapes also confirmed the presence of biological materials in the dust sample (Pachauri et al., 2013).
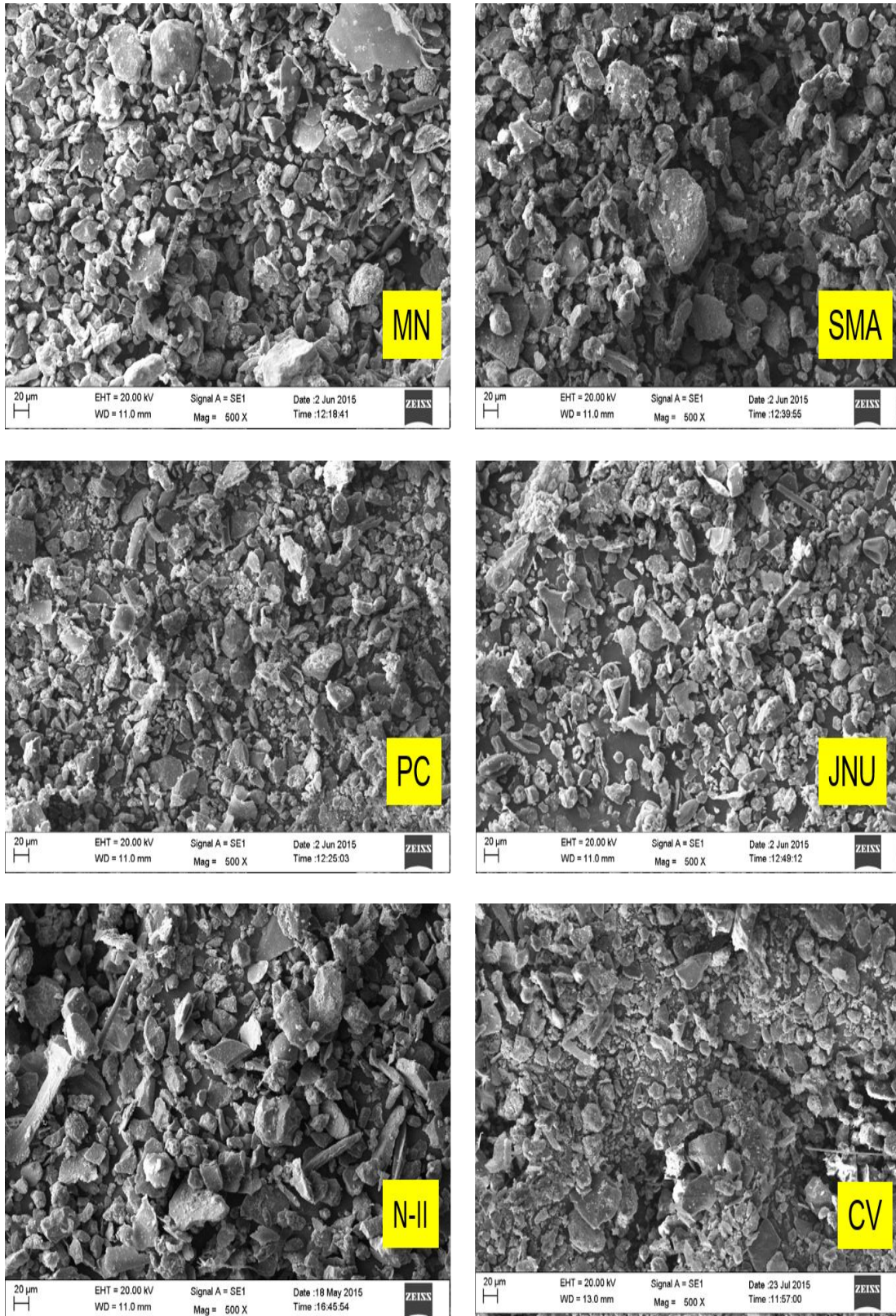
Fig.4.22. SEM Image of dust samples at each site (Magnification, 500x).

The SEM image of the dustfall samples were subjected to particle size distribution by using ImageJ and R software for the selected sampling sites (Fig 4.23–4.28). Image data were analysed for different size range of diameter from <2.5μm to >10μm. The data showed a modal distribution with the maximum frequency of the particle diameter being <2.5μm (Table.4.17). 90%, 89%, 89%, 85%, 85% and 82% of the dustfall fluxes were present in <2.5μm particle size range at CV, JNU, N- II, SMA, MN and PC site respectively. This gives a clear indication towards the role of anthropogenic activities in the crustal and non crustal derived dust fluxes (Srivastava et al., 2007).

Table.4.17. Particle size distribution of the dustfall at each sampling sites

Size range of Particulate matter	Number of Particles					
	MN	SMA	PC	JNU	N-II	CV
≤ 2.5μm	2971	3116	4087	3573	4481	1827
2.5-10 μm	437	445	768	408	440	188
>10 μm	104	92	157	26	96	18
Total No. of Particle	3512	3653	5012	4007	5017	2033

(n=2, Number of Image analysed through ImageJ Software)

Fig.4.23. Particle size analysis and their distribution of the dustfall flux particulates at MN site (Fig. a, b); Fig.a, overall particle size distribution of the dust: Fig. b, particle size distribution from <2.5μm to >10μm.

Fig.4.24. Particle size analysis and their distribution of the dustfall flux particulates at SMA site (Fig. a, b); Fig.a, overall particle size distribution of the dust: Fig. b, particle size distribution from <2.5µm to >10µm.

Fig.4.25. Particle size analysis and their distribution of the dustfall flux particulates at PC site (Fig. a, b); Fig.a, overall particle size distribution of the dust: Fig. b, particle size distribution from <2.5μm to >10μm.
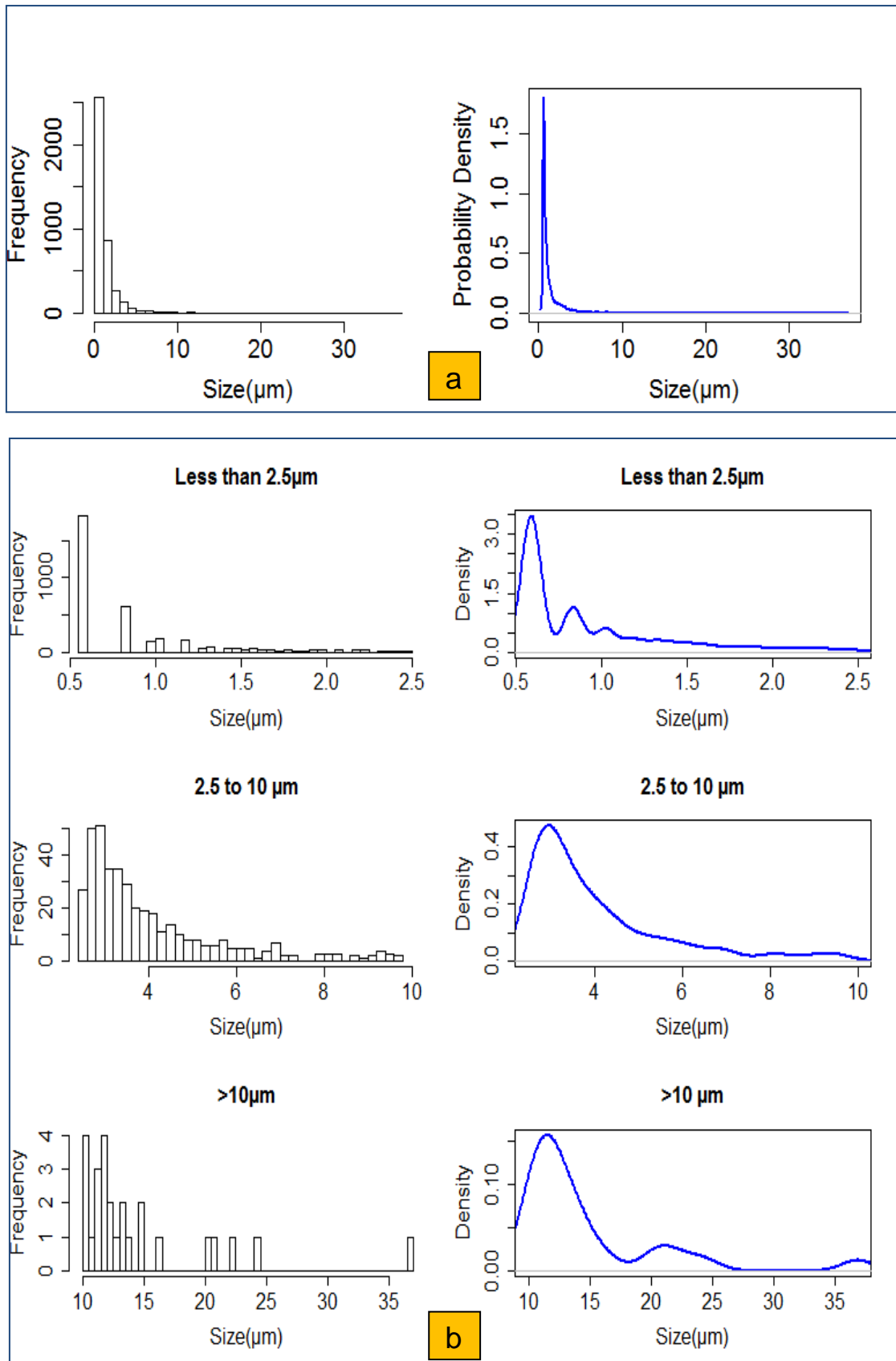
Fig.4.26. Particle size analysis and their distribution of the dustfall flux particulates at JNU site (Fig. a, b); Fig.a, overall particle size distribution of the dust: Fig. b, particle size distribution from <2.5µm to >10µm.
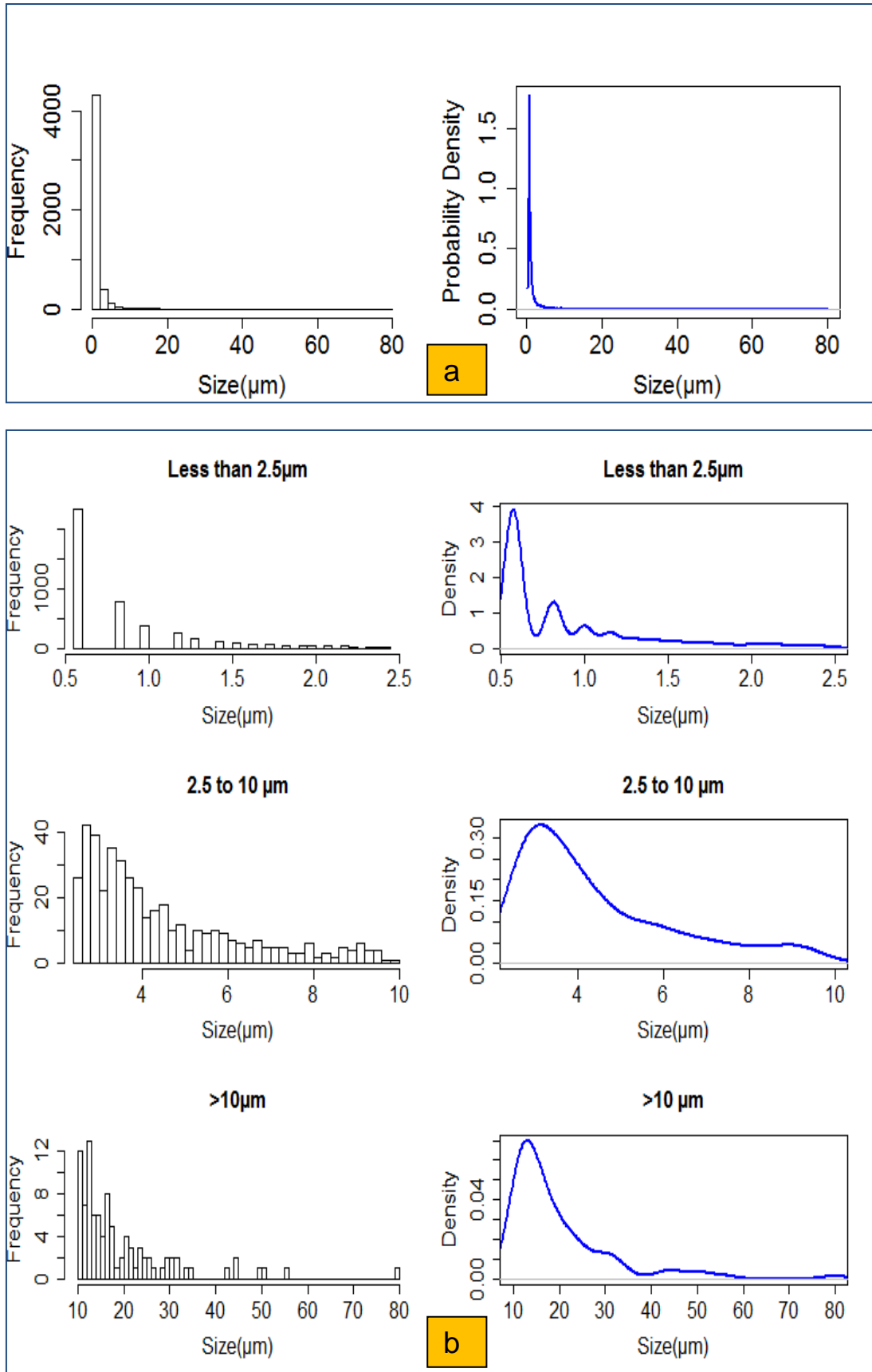
Fig.4.27. Particle size analysis and their distribution of the dustfall flux particulates at N-II site (Fig. a, b); Fig.a, overall particle size distribution of the dust: Fig. b, particle size distribution from <2.5µm to >10µm.
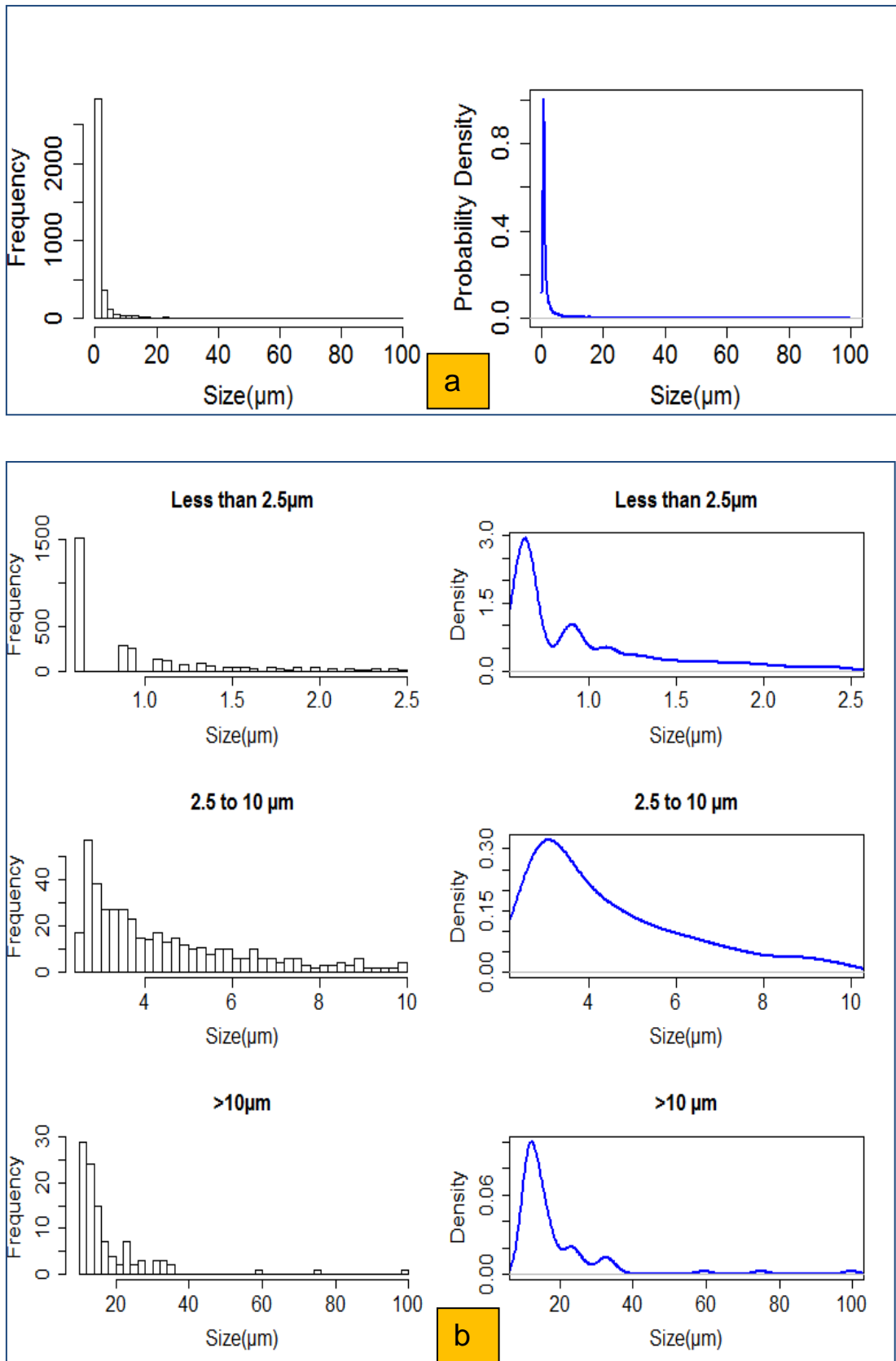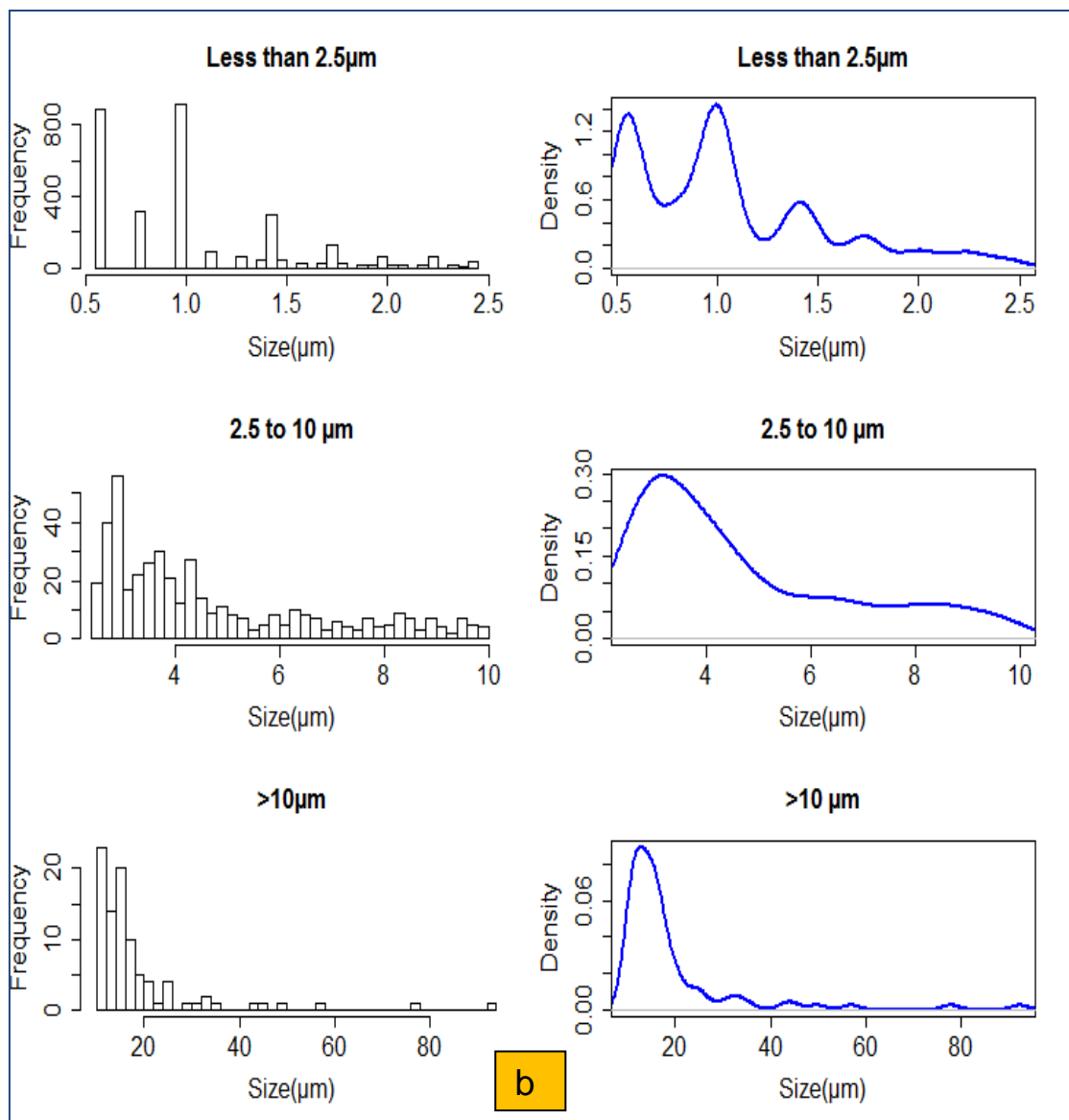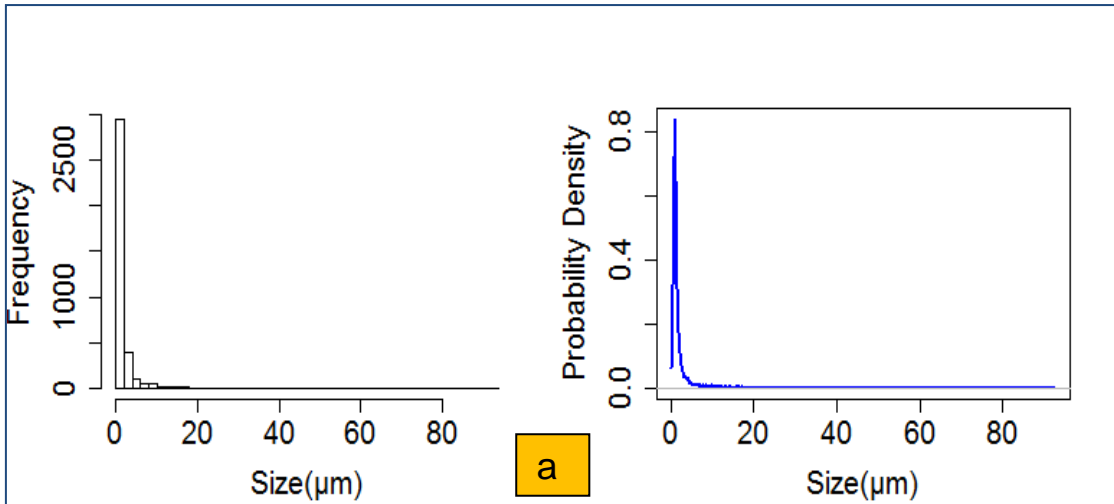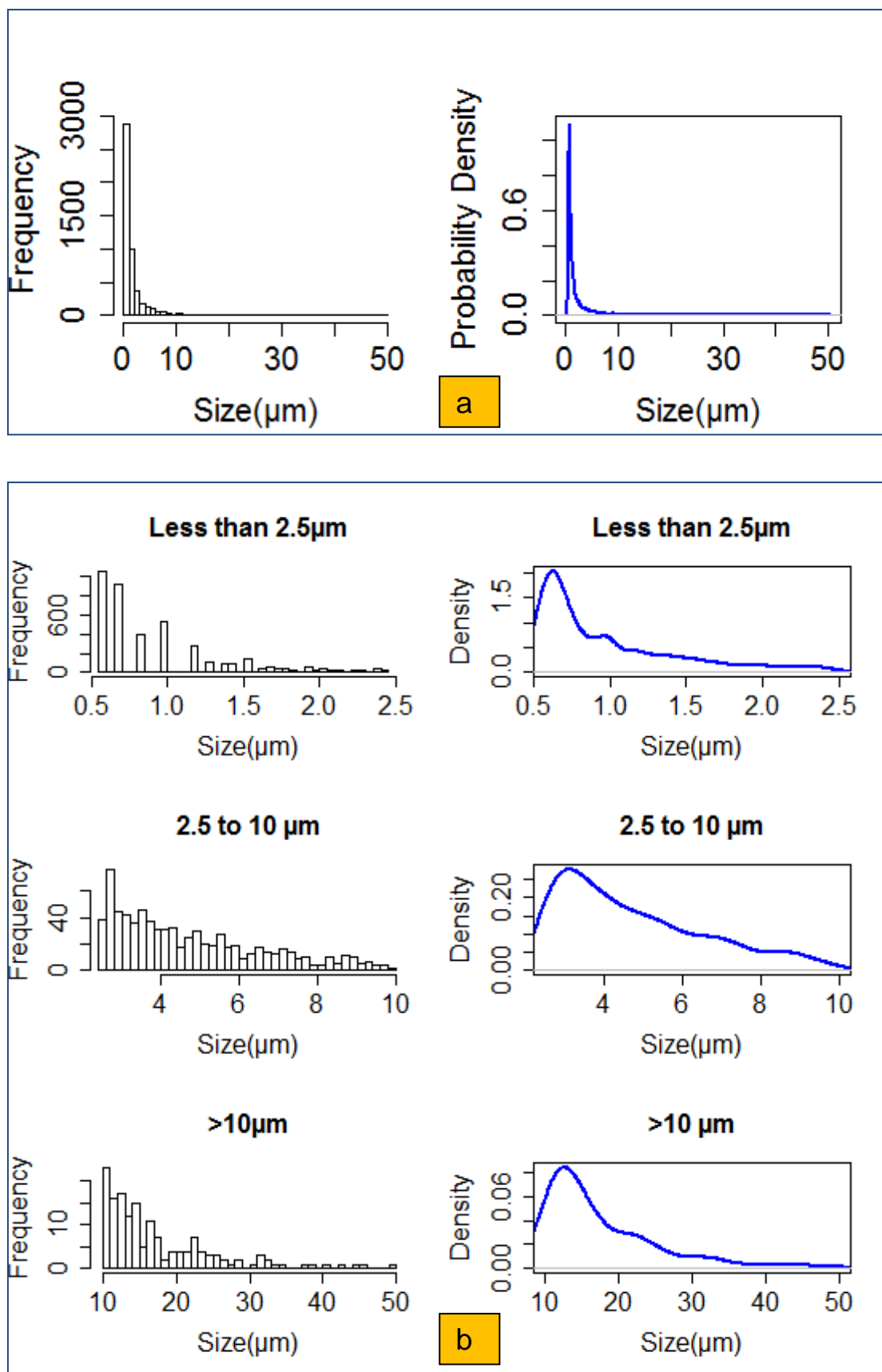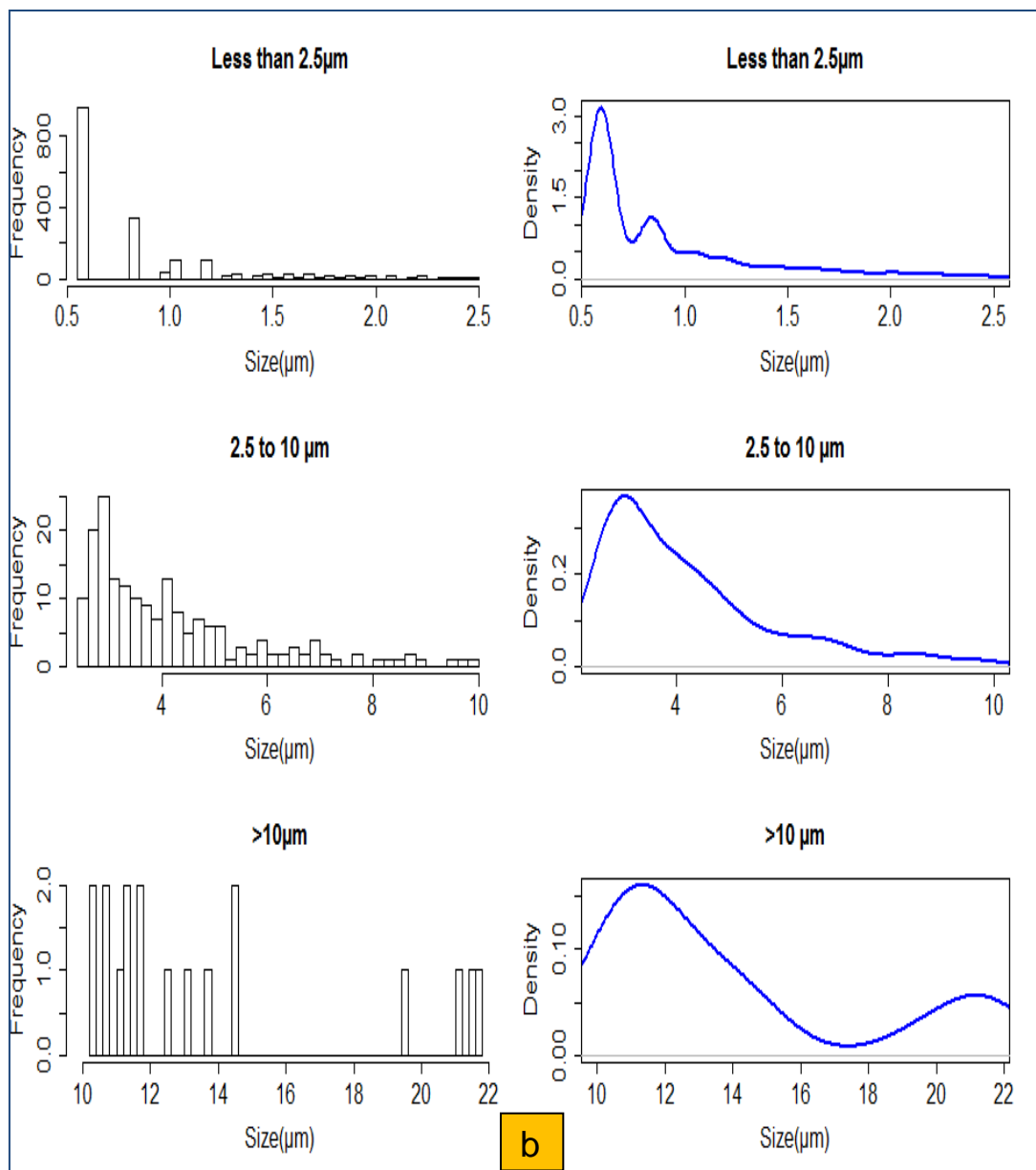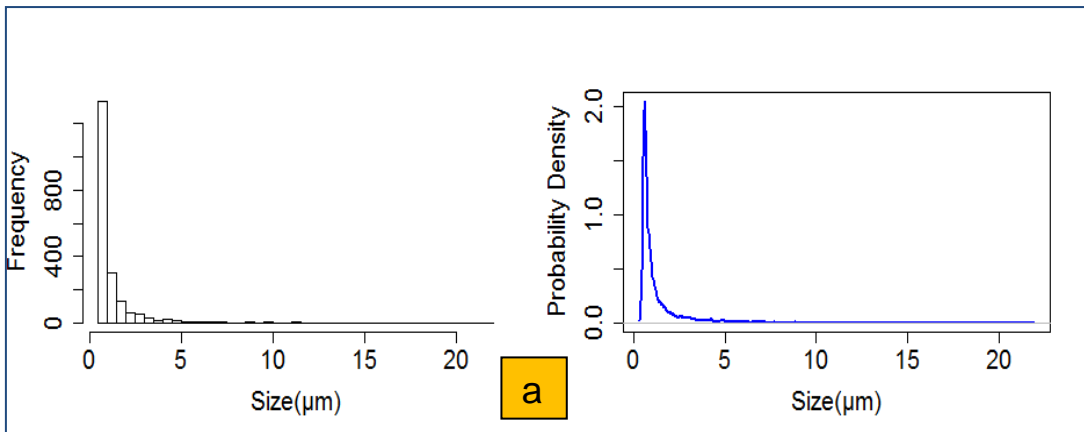
Fig.4.28. Particle size analysis and their distribution of the dustfall flux particulates at CV site (Fig. a, b); Fig.a, overall particle size distribution of the dust: Fig. b, particle size distribution from <2.5μm to >10μm.

4.8. Elemental analysis of the dust

Elemental Dispersive X–Ray spectroscopy analysis was done for deriving the elemental composition of the dustfall fluxes. A total of 13 elements were analyzed for their compositional percentages in the sample (Fig. 4.30-4.35). Owing to the large percentage of the oxygen in the overall elemental composition, the calculations were deducted for the relative oxygen abundances in the dust flux composition. Carbon and silicon were observed to be in large amounts along with the oxygen thereby suggesting the presence of C and Si in their oxide forms in the dust fluxes. High fractions of carbons were observed at the rural CV site (93%) and residential MN site (72%) which indicates towards the presence of major carbon sources. High fractions of Si at the sub urban N–II site (63%) and traffic PC site (31%) suggests towards the dominating crustal sources contributing to the fractions of dustfall fluxes. JNU, on the other hand, showed the highest fraction of Fe (45%) in the dustfall fluxes. Heavy metal composition of Fe (10%), Al (9%), Cu (1%), Zn (1%) at the traffic PC site confirmed the vehicular emissions in the contribution of the dust fluxes. Fractions of Ca were also observed in the dust fluxes at MN (3%), SMA (3%), PC (12%), JNU (2%), N – II (4%) and CV (1%) site thereby confirming the contribution of crustal sources in the dustfall.
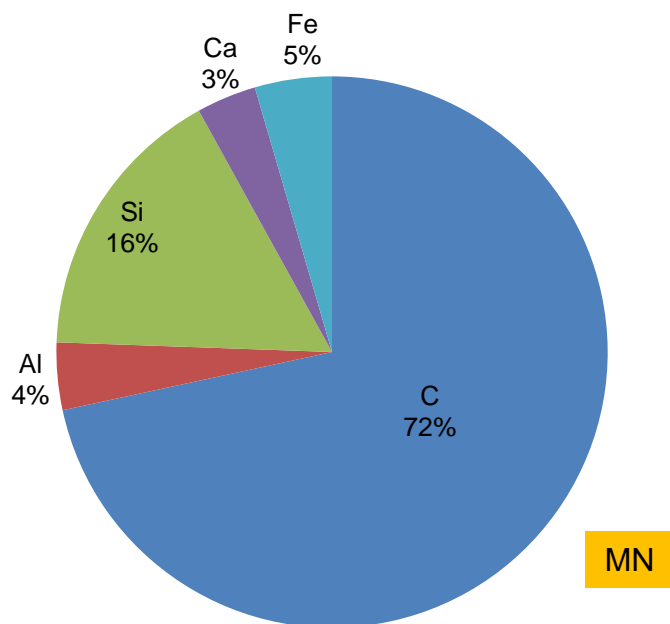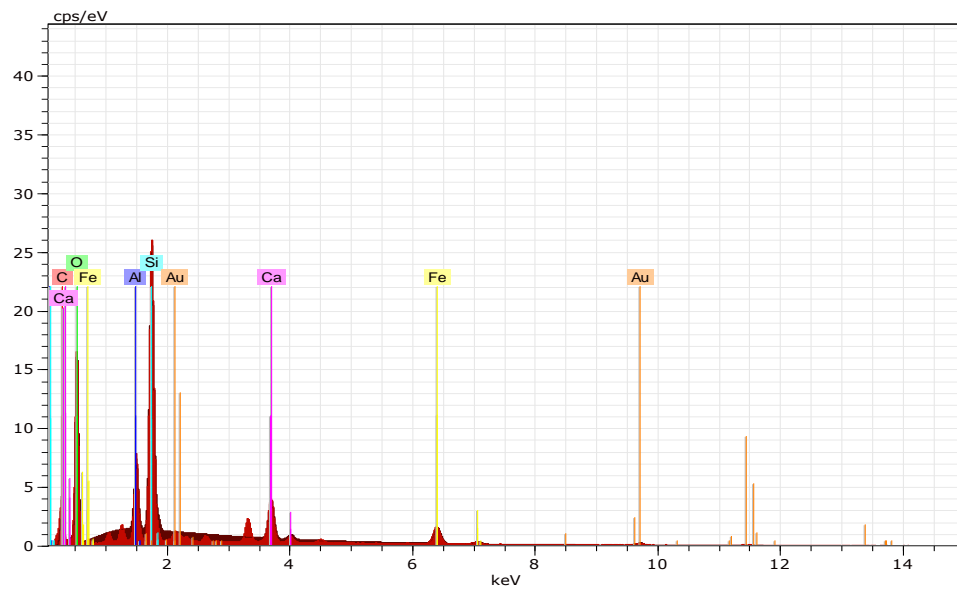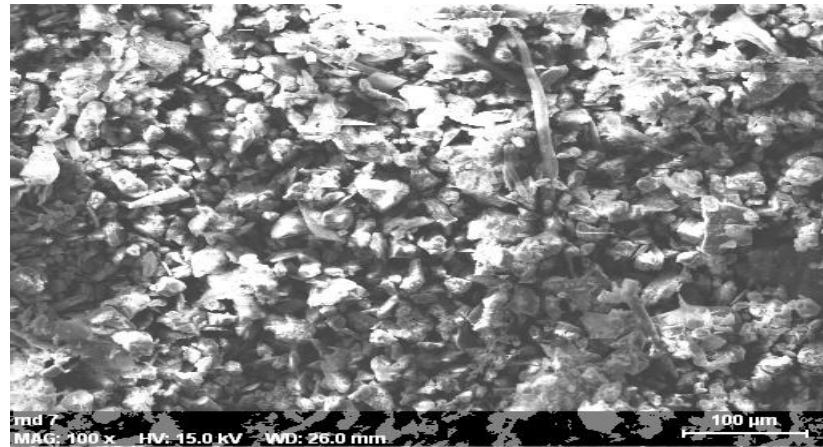
Fig. 4.29. Elemental composition of the dust at MN site
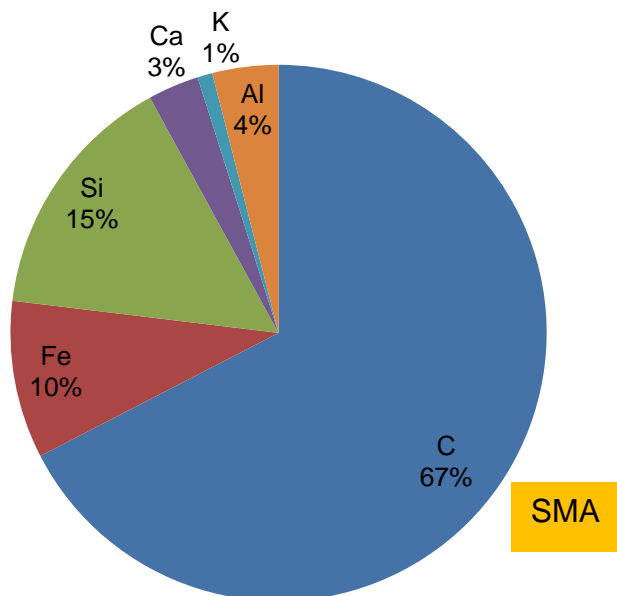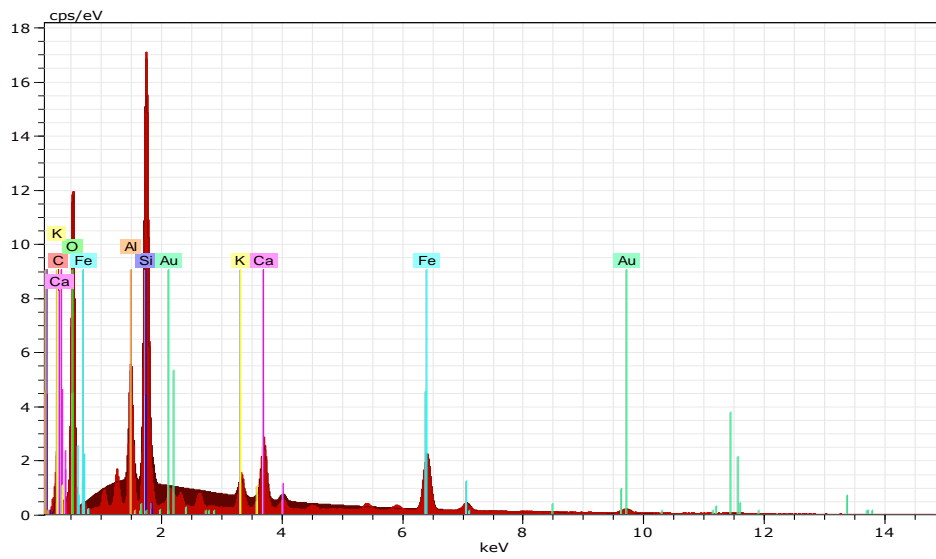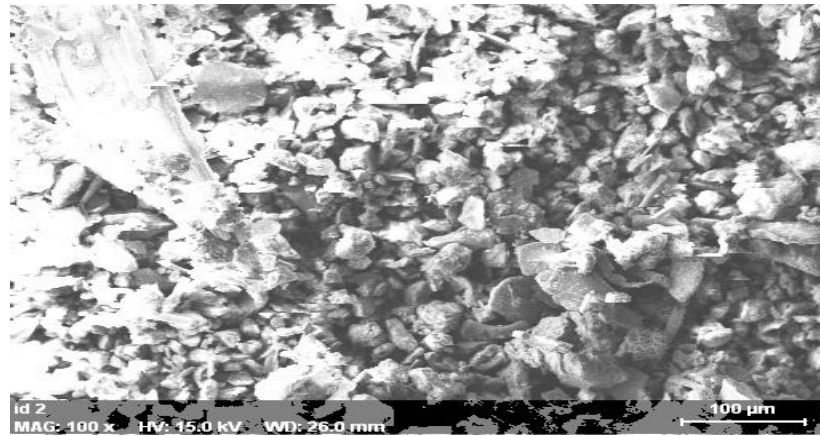
Fig. 4.30. Elemental composition of the dust at SMA site
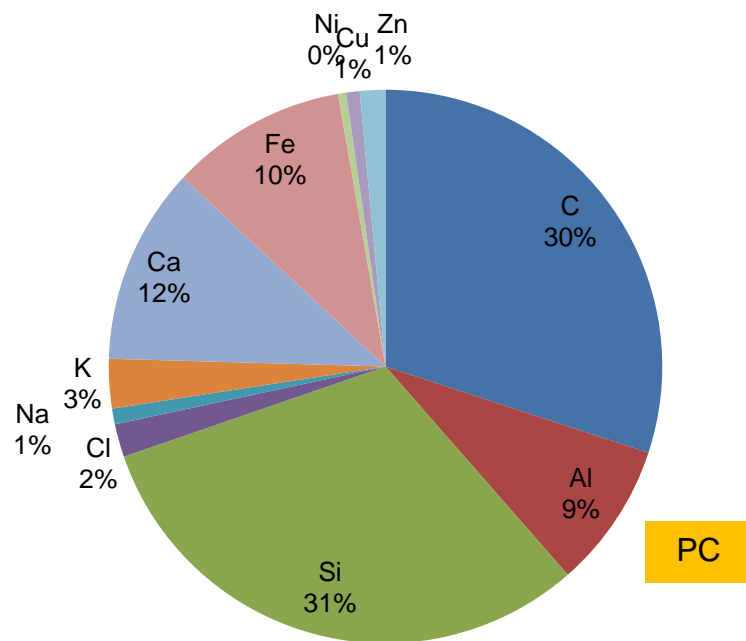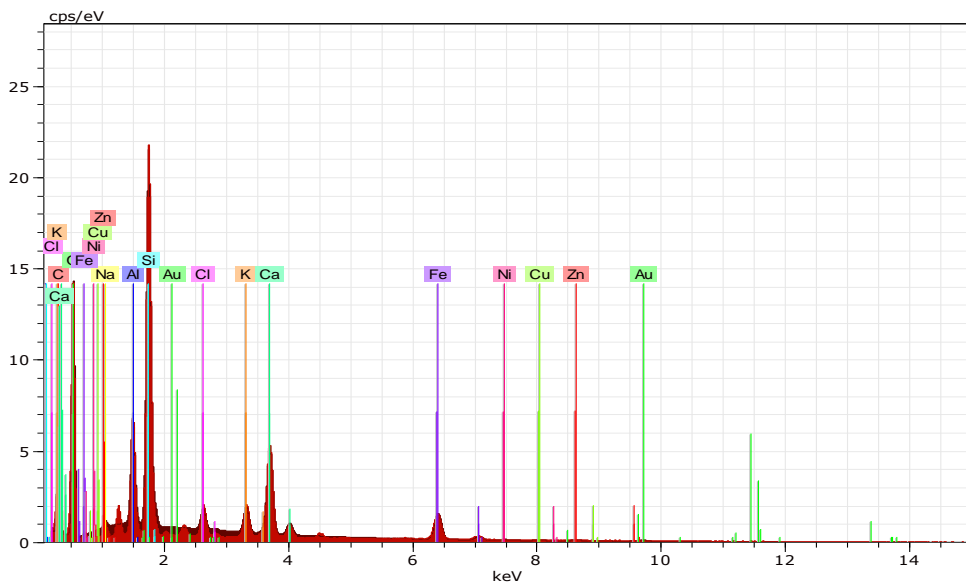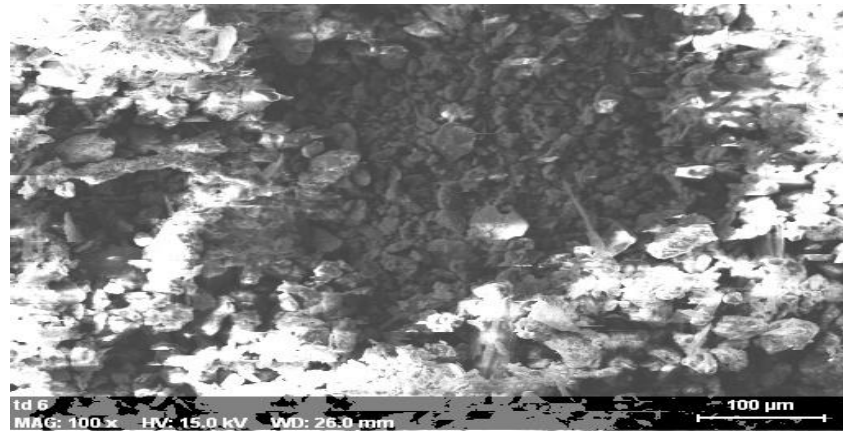
Fig. 4.31. Elemental composition of the dust at PC site
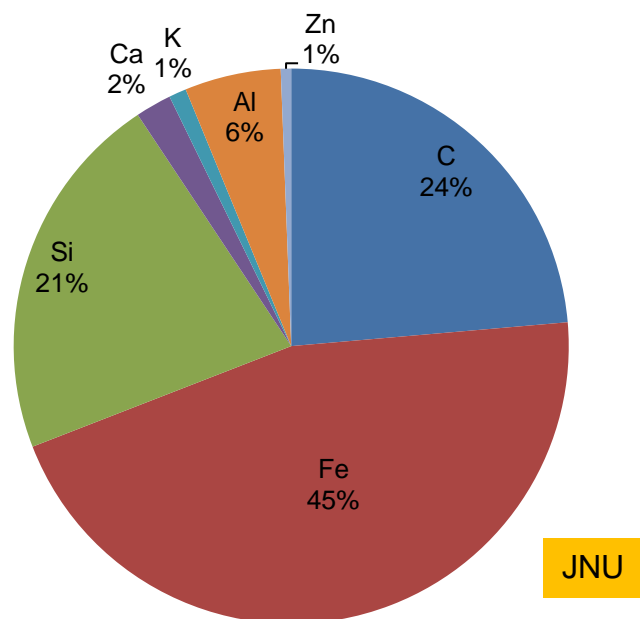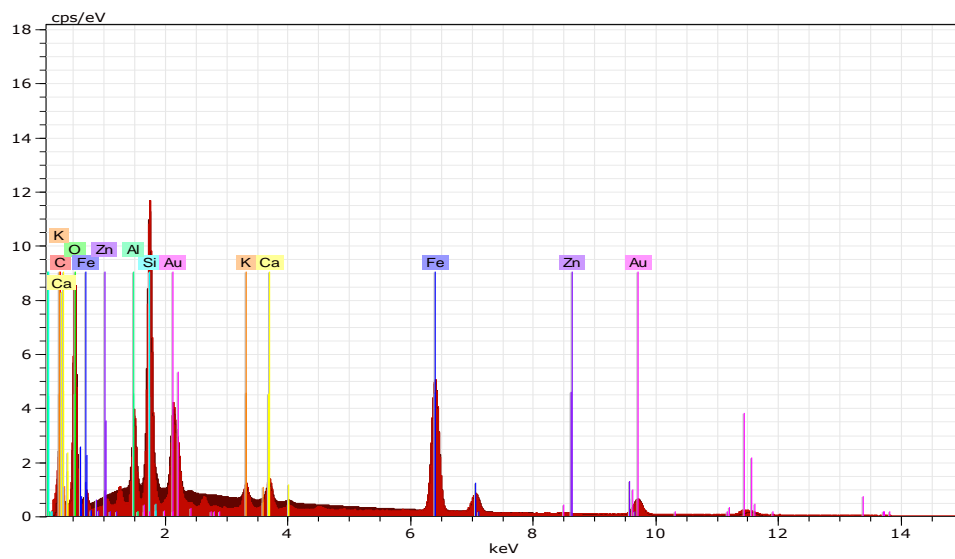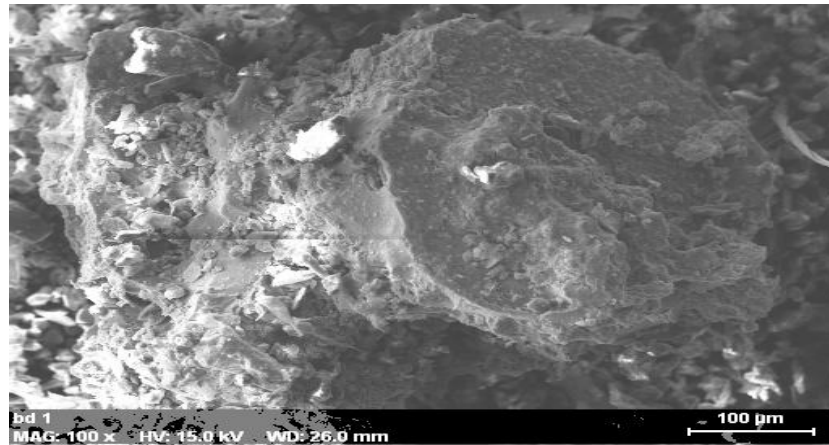
Fig. 4.32. Elemental composition of the dust at JNU site
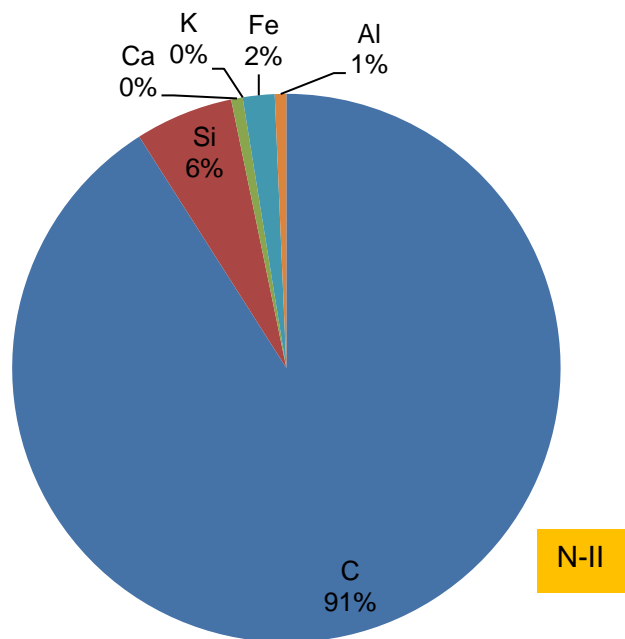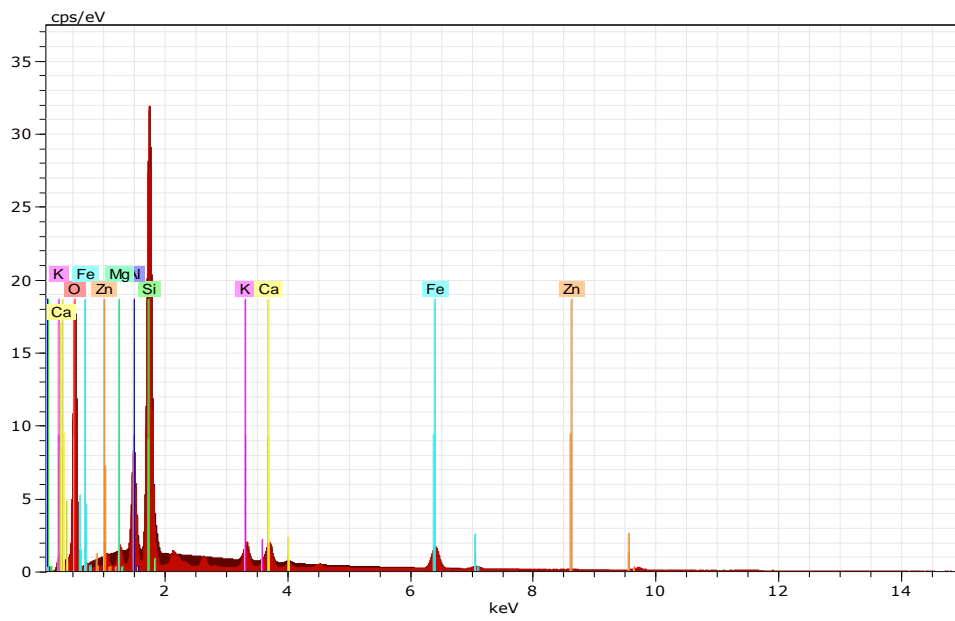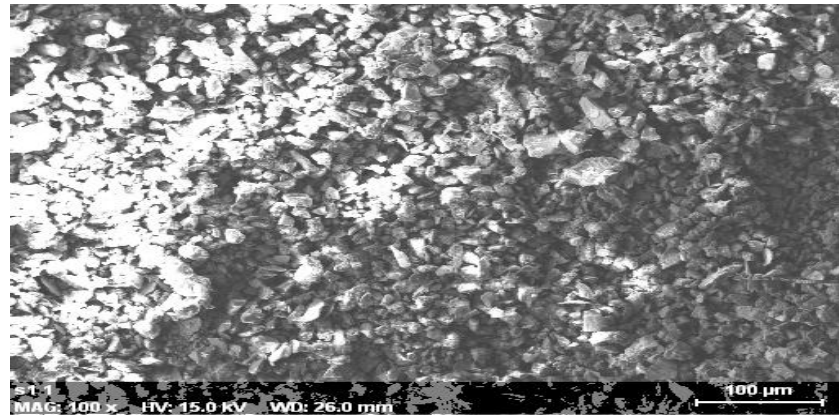
Fig. 4.33. Elemental composition of the dust at N-II site
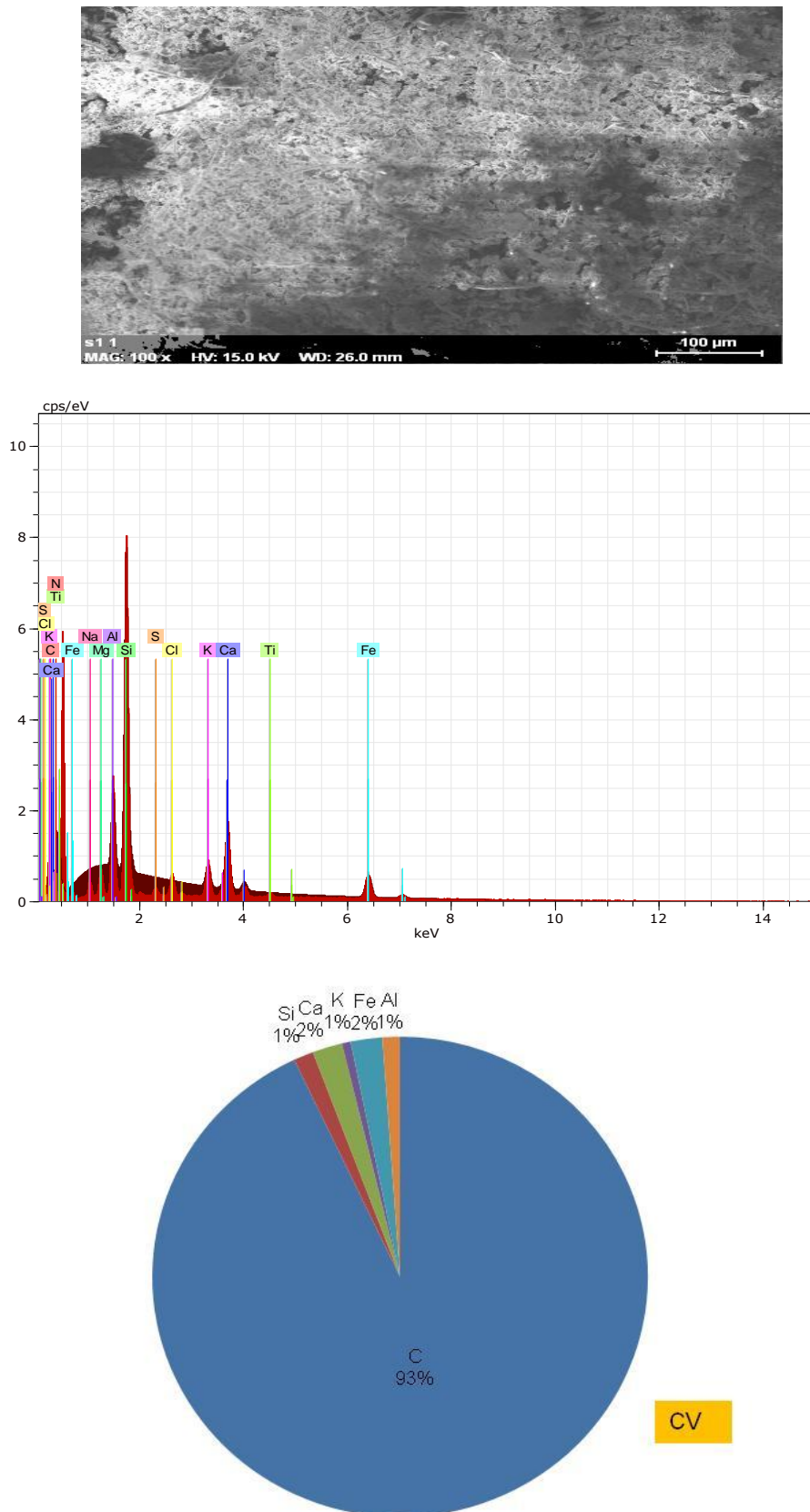
Fig.4.34. Elemental composition of the dust at CV site

Chapter 5
Conclusions

Conclusions

The rising Nr emission from the expanding industrial and agricultural sectors in India has eventually resulted in its consequent interaction with the removal mechanism of the atmospheric dust rich in $CaCO_3$. The study was, therefore, focussed on the Nr fluxes through dustfall mechanism over Delhi–NCR region that has been characterized by its changing dynamics of its different land use pattern through rapid urbanization. Dustfall fluxes varied in the range of $81 - 5584 mg/m^2/d$ which was observed to be highest at the industrial SMA site (1157 ± 345 mg/m^2/d) followed by the soil re-suspended dustfall fluxes observed at the rural CV site (1029 ± 215 mg/m^2/d). Lowest dust fluxes were observed at N–II site (428 ± 95 mg/m^2/d) owing to the well built concrete surfaces of its commercial land use pattern. However, a similar pattern in the dustfall fluxes were observed at residential MN site (555 ± 115 mg/m^2/d) and at traffic PC site (548 ± 71 mg/m^2/d) as well. This could be attributed to the construction activities involved in the urban sprawling of the already populated residential MN site and high road dust emissions observed at PC site. JNU site being a typical urban forest showed a comparatively higher value in its dustfall fluxes (664 ± 264 mg/m^2/d) amongst the other urban sampling locations owing to the untimely construction and renovation activity of the campus during the sampling duration. Total dustfall during summer months (April–June) for the period of 90 days has been 50, 104, 49, 60, 39 and 93 mg/m^2 at MN, SMA, PC, JNU, N–II and CV site, respectively.

A further insight into the ionic composition of the dust fluxes revealed the effect of the pollution sources over the different land use pattern. Ca^{2+} remained the dominant base cation with its average flux values that ranged from 3.8 ± 0.6 mg/m^2/d at CV site to 16.2 ± 8.4 mg/m^2/d at SMA site. This has resulted in the high dust fluxes of SO_4^{2-} that ranged from 3.1 mg/m^2/d at CV site to 132.73 mg/m^2/d at SMA site. The relative abundance of Ca^{2+} and SO_4^{2-} in the dustfall fluxes, on the other hand, has eventually resulted in variable fluxes of oxidized Nr (NO_3^-) and reduced Nr (NH_4^+) depending upon the meteorological parameters at each site of different characteristics.

Owing to the high Nr emissions from the industrial activities and its losses from refrigeration units, a high average flux of NO_3^- (16.45±10.17 mg/m^2/d) and NH_4^+ (16.33±16 mg/m^2/d) was observed at the SMA site. Despite the presence of heavy vehicular traffic condition at the PC site, its NO_3^- (3.39±0.61 mg/m^2/d) and NH_4^+ (0.22±0.04 mg/m^2/d) fluxes were observed to be relatively lower than the residential MN site. This could be attributed to the bottleneck traffic situation of the heavily encroached narrow road lanes along with the poor sewerage condition of the MN site that has resulted in high values of NO_3^- (3.59±0.61 mg/m^2/d) and NH_4^+ (0.22±0.04 mg/m2/d) fluxes. Absence of any major source of Nr emissions near JNU has lead to lower values of NO_3^- (2.98±0.84 mg/m^2/d) and NH_4^+ (0.21±0.04 mg/m^2/d) dust fluxes in comparison to the other urban sampling locations. On comparison of Nr fluxes at JNU with the suburban (N- II) and rural site (CV) of the study area, a relatively higher Nr fluxes of NO_3^- (3.36±0.78 mg/m^2/d) and NH_4^+ (0.22± 0.05 mg/m^2/d) were observed at the N–II site. This could be attributed to the frequency of power cuts in NCR resulting in an increased use of diesel generators which along with the biogenic emissions and increased biomass burning of the suburban land use pattern has contributed to its relatively higher Nr fluxes. CV being a rural site showed the lowest dustfall fluxes of NO_3^- (1.24±0.16 mg/m^2/d) owing to its minimum exposure to the anthropogenic disturbances.

Statistical evaluation of the data set with the correlation matrices and ion balance regression plots revealed the dominance of Ca^{2+} in the dustfall flux stoichiometric neutralization reactions that has resulted in a low median equivalence ratio of NO_3^-/ SO_4^{2-} at all the sites. This suggests towards the high affinity of Ca^{2+} for SO_4^{2-} over NO_3^- with the eventual dependence of NO_3^- scavenging reactions on the relative abundances of Ca^{2+} and SO_4^{2-} in the dustfall fluxes. Therefore, NO_3^- were speculated to be present as $Ca(NO_3)_2$ at MN site, NH_4NO_3 and $Ca(NO_3)_2$ SMA site, $Ca(NO_3)_2$, $Mg(NO_3)_2$ and $NaNO_3$ at PC site, $NaNO_3$ and $Ca(NO_3)_2$ at JNU site, $Mg(NO_3)_2$ and KNO_3 at N − II site and as $Ca(NO_3)_2$ and $NaNO_3$ at CV site. NH_4^+, on

the other hand, showed weak correlations with the ionic composition of the dust fluxes, thereby indicating towards it near absence in the coarse mode particulate phases.

Crustal interferences could be attributed for increased scavenging of NO_3^- at MN and PC site based on their respective Ca^{2+} normalized ratios in their soil as well as in the dustfall fluxes. The morphological and elemental analysis of the dust samples further confirmed the relative contribution of crustal sources at each site with carbon, silicon and calcium providing the major contribution to the dustfall fluxes of reactive nitrogen species.

References

References

Andreae, M. O. (1995). Climatic effects of changing atmospheric aerosol levels. *World survey of climatology*, *16*, 347-398.

Anderson, N., Strader, R., & Davidson, C. (2003). Airborne reduced nitrogen: ammonia emissions from agriculture and other sources. *Environment International*, *29*(2), 277-286.

Aneja, V. P., Schlesinger, W. H., Erisman, J. W., Behera, S. N., Sharma, M., & Battye, W. (2012). Reactive nitrogen emissions from crop and livestock farming in India. *Atmospheric Environment*, *47*, 92–103. doi:10.1016/j.atmosenv.2011.11.026

Ansari, A. S., & Pandis, S. N. (2000). The effect of metastable equilibrium states on the partitioning of nitrate between the gas and aerosol phases. *Atmospheric Environment*, *34*(1), 157–168. doi:10.1016/S1352-2310(99)00242-3

Arimoto, R., Kim, Y. J., Kim, Y. P., Quinn, P. K., Bates, T. S., Anderson, T. L., & Sokolik, I. N. (2006). Characterization of Asian dust during ACE-Asia. *Global and Planetary change*, *52*(1), 23-56.

Arsene, C., Olariu, R. I., & Mihalopoulos, N. (2007). Chemical composition of rainwater in the northeastern Romania, Iasi region (2003–2006). *Atmospheric Environment*, *41*(40), 9452-9467.

Balakrishna, G., & Pervez, S. (2009). Source apportionment of atmospheric dust fallout in an urban-industrial environment in India. *Aerosol and Air Quality Research*, *9*(3), 359–367. doi:10.4209/aaqr.2008.12.0065

Bardouki, H., Liakakou, H., Economou, C., Sciare, J., Smolík, J., Ždímal, V., et al. (2003). Chemical composition of size-resolved atmospheric aerosols in the eastern Mediterranean during summer and winter. *Atmospheric Environment*, *37*(2), 195–208. doi:10.1016/S1352-2310(02)00859-2

Bari, A., Ferraro, V., Wilson, L. R., Luttinger, D., & Husain, L. (2003). Measurements of gaseous HONO, HNO3, SO2, HCl, NH3, particulate sulfate and PM2.5 in New York, NY. *Atmospheric Environment*, *37*(20), 2825–2835. doi:10.1016/S1352-2310(03)00199-7

Baron, J. S., Rapporteur, M. B., Adams, M., Agboola, J. I., Allen, E. B., Bealey, W. J., et al. (2014). Nitrogen Deposition, Critical Loads and Biodiversity, 465–480. doi:10.1007/978-94-007-7939-6

Bauer, S. E. (2004). Global modeling of heterogeneous chemistry on mineral aerosol surfaces: Influence on tropospheric ozone chemistry and comparison to observations. *Journal of Geophysical Research*, *109*(D2), 1–17. doi:10.1029/2003JD003868

Bauer, S. E., Koch, D., Unger, N., Metzger, S. M., Shindell, D. T., & Streets, D. G. (2007). Nitrate aerosols today and in 2030: a global simulation including aerosols and tropospheric ozone. *Atmospheric Chemistry and Physics*, *7*(19), 5043–5059. doi:10.5194/acp-7-5043-2007

Bayesian, H. Journal of Environmental Statistics.

Berkowitz, C. M., Jobson, T., Jiang, G., Spicer, C. W., & Doskey, P. V. (2004). Chemical and meteorological characteristics associated with rapid increases of O_3 in Houston, Texas. *Journal of Geophysical Research D: Atmospheres*, *109*(10), 1–12. doi:10.1029/2003JD004141

Bory, A., Dulac, F., Moulin, C., Chiapello, I., Newton, P. P., Guelle, W., & Bergametti, G. (2002). Atmospheric and oceanic dust fluxes in the northeastern tropical Atlantic Ocean: how close a coupling?. In *Annales Geophysicae* (Vol. 20, No. 12, pp. 2067-2076).

Budhavant, K. B., Rao, P. S. P., Safai, P. D., Gawhane, R. D., Raju, M. P., Mahajan, C. M., & Satsangi, P. G. (2012). Atmospheric Wet and Dry Depositions of Ions over an Urban Location in South-West India. *Aerosol and Air Quality Research*, *12*(4), 561–570. doi:10.4209/aaqr.2011.12.0233

Bradshaw, J., Davis, D., Grodzinsky, G., Smyth, S., Newell, R., Sandholm, S., & Liu, S. (2000). Observed distributions of nitrogen oxides in the remote free troposphere from the NASA global tropospheric experiment programs. *Reviews of Geophysics*, *38*(1), 61-116.

Calvo, a. I., Alves, C., Castro, a., Pont, V., Vicente, a. M., & Fraile, R. (2013). Research on aerosol sources and chemical composition: Past, current and emerging issues. *Atmospheric Research*, *120-121*, 1–28. doi:10.1016/j.atmosres.2012.09.021

Chakraborty, a, Gupta, T., & Site, a S. (2009). Chemical Characterization of Submicron Aerosol in Kanpur Region: a Source Apportionment Study, 87–90.

Chin, M., Diehl, T., Ginoux, P., & Malm, W. (2007). Intercontinental transport of pollution and dust aerosols: implications for regional air quality. *Atmospheric Chemistry and Physics*, *7*(21), 5501-5517.

Chung, C. S., Hong, G. H., Kim, S. H., Lim, J. H., Park, J. K., & Yang, D. B. (1998). Shore based observation on wet deposition of inorganic nutrients in the Korean Yellow Sea coast. *The Yellow Sea*, *4*(1), 30-39.

Committee, S. A., Adopted, T. S., Meeting, I., & November, T. S. (2010). Technical Manual on Dry Deposition Flux Estimation in East Asia, (November).

Das, R., Das, S. N., & Misra, V. N. (2005). Chemical composition of rainwater and dustfall at Bhubaneswar in the east coast of India. *Atmospheric Environment*, *39*(32), 5908–5916. doi:10.1016/j.atmosenv.2005.06.030

Dentener, F. J., Carmichael, G. R., Zhang, Y., Lelieveld, J., & Crutzen, P. J. (1996). Role of mineral aerosol as a reactive surface in the global troposphere. *Journal of Geophysical Research: Atmospheres (1984–2012)*, *101*(D17), 22869-22889.

Duce, R. A., Liss, P. S., Merrill, J. T., Atlas, E. L., Buat-Menard, P., Hicks, B. B.,& Zhou, M. (1991). The atmospheric input of trace species to the world ocean. *Global biogeochemical cycles*, *5*(3), 193-259.

Duce, R. a, LaRoche, J., Altieri, K., Arrigo, K. R., Baker, a R., Capone, D. G., et al. (2008). Impacts of atmospheric anthropogenic nitrogen on the open ocean. *Science (New York, N.Y.)*, *320*(5878), 893–897. doi:10.1126/science.1150369

Ellis, R. a., Murphy, J. G., Markovic, M. Z., Vandenboer, T. C., Makar, P. a., Brook, J., & Mihele, C. (2011). The influence of gas-particle partitioning and surface-atmosphere exchange on ammonia during BAQS-Met. *Atmospheric Chemistry and Physics*, *11*(1), 133–145. doi:10.5194/acp-11-133-2011

Endo, T., Yagoh, H., Sato, K., Matsuda, K., Hayashi, K., Noguchi, I., & Sawada, K. (2011). Regional characteristics of dry deposition of sulfur and nitrogen compounds at EANET sites in Japan from 2003 to 2008. *Atmospheric Environment*, *45*(6), 1259–1267. doi:10.1016/j.atmosenv.2010.12.003

Erickson, D. J., Seuzaret, C., Keene, W. C., & Gong, S. L. (1999). A general circulation model based calculation of HCl and ClNO2 production from sea salt dechlorination: Reactive Chlorine Emissions Inventory. *Journal of Geophysical Research: Atmospheres (1984–2012)*, *104*(D7), 8347-8372.

Erisman, J. W., Bleeker, a., Galloway, J., & Sutton, M. S. (2007). Reduced nitrogen in ecology and the environment. *Environmental Pollution*, *150*(1), 140–149. doi:10.1016/j.envpol.2007.06.033

Fairlie, T. D., Jacob, D. J., Dibb, J. E., Alexander, B., Avery, M. a., Van Donkelaar, a., & Zhang, L. (2010). Impact of mineral dust on nitrate, sulfate, and ozone in transpacific Asian pollution plumes. *Atmospheric Chemistry and Physics*, *10*(8), 3999–4012. doi:10.5194/acp-10-3999-2010

Fenn, M. E., Ross, C. S., Schilling, S. L., Baccus, W. D., Larrabee, M. a., & Lofgren, R. a. (2013). Atmospheric deposition of nitrogen and sulfur and preferential canopy consumption of nitrate in forests of the Pacific Northwest, USA. *Forest Ecology and Management*, *302*, 240–253. doi:10.1016/j.foreco.2013.03.042

Fischer, E., Pszenny, A., Keene, W., Maben, J., Smith, A., Stohl, A., & Talbot, R. (2006). Nitric acid phase partitioning and cycling in the New England coastal atmosphere. *Journal of Geophysical Research: Atmospheres (1984–2012)*, *111*(D23).

Galloway, J. N., Levy, H., & Kashibhatla, P. S. (1994). Year 2020 - Consequences of Population-Growth and Development on Deposition of Oxidized Nitrogen. *Ambio*, *23*(2), 120–123.

Galloway, J. N. (1998). The global nitrogen cycle: Changes and consequences. *Environmental Pollution*, *102*(SUPPL. 1), 15–24. doi:10.1016/S0269-7491(98)80010-9

Galloway, J. N., Dentener, F. J., Capone, D. G., Boyer, E. W., Howarth, R. W., Seitzinger, S. P., et al. (2004). *Nitrogen cycles: past , present , and future*.

Galloway, J. N., Townsend, A. R., Erisman, J. W., Bekunda, M., Cai, Z., Freney, J. R., et al. (2008). Transformation of the nitrogen cycle: recent trends, questions, and potential solutions. *Science (New York, N.Y.)*, *320*(5878), 889–892. doi:10.1126/science.1136674

Gao, Y., & Anderson, J. R. (2001). Characteristics of Chinese aerosols determined by individual-particle analysis. *Journal of Geophysical Research: Atmospheres (1984–2012)*, *106*(D16), 18037-18045

Gerecke, A., Thielmann, A., Gutzwiller, L., & Rossi, M. J. (1998). The chemical kinetics of HONO formation resulting from heterogeneous interaction of NO2 with flame soot. *Geophysical Research Letters*, *25*(13), 2453-2456

Gong, S. L. (2003). Characterization of soil dust aerosol in China and its transport and distribution during 2001 ACE-Asia: 2. Model simulation and validation. *Journal of Geophysical Research*, *108*(D9), 1–13. doi:10.1029/2002JD002633

Goossens, D. (2006). Aeolian deposition of dust over hills: the effect of dust grain size on the deposition pattern. *Earth surface processes and landforms*, *31*(6), 762-776

Granat, L., Norman, M., Leck, C., Kulshrestha, U. C., & Rodhe, H. (2002). Wet scavenging of sulfur compounds and other constituents during the Indian Ocean Experiment (INDOEX). *Journal of Geophysical Research: Atmospheres*, *107*(19). doi:10.1029/2001JD000499

Gupta, G. P., Kumar, B., Singh, S., & Kulshrestha, U. C. (2015). Urban climate and its effect on biochemical and morphological characteristics of Arjun (*Terminalia arjuna*) plant in National Capital Region Delhi. *Chemistry and Ecology*, (July 2015), 1–15. doi:10.1080/02757540.2015.1043286

Hoffmann, C., Funk, R., Wieland, R., Li, Y., & Sommer, M. (2008). Effects of grazing and topography on dust flux and deposition in the Xilingele grassland, Inner Mongolia. *Journal of Arid Environments*, *72*(5), 792-807.

Im, U., Christodoulaki, S., Violaki, K., Zarmpas, P., Kocak, M., Daskalakis, N., et al. (2013). Atmospheric deposition of nitrogen and sulfur over southern Europe with focus on the Mediterranean and the Black Sea. *Atmospheric Environment*, *81*(x), 660–670. doi:10.1016/j.atmosenv.2013.09.048

Jain, M., Kulshrestha, U. ., Sarkar, a. ., & Parashar, D., (2000). Influence of crustal aerosols on wet deposition at urban and rural sites in India. *Atmospheric Environment*, *34*(29-30), 5129–5137. doi:10.1016/S1352-2310(00)00350-2

Keene, W. C., Pszenny, A. A., Maben, J. R., & Sander, R. (2002). Variation of marine aerosol acidity with particle size. *Geophysical research letters*, *29*(7), 5-1.

Kondo, Y., Morino, Y., Fukuda, M., Kanaya, Y., Miyazaki, Y., Takegawa, N., et al. (2008). Formation and transport of oxidized reactive nitrogen, ozone, and secondary organic aerosol in Tokyo. *Journal of Geophysical Research: Atmospheres*, *113*(21), 1–23. doi:10.1029/2008JD010134

Krueger, B. J., Grassian, V. H., Cowin, J. P., & Laskin, a. (2004). Heterogeneous chemistry of individual mineral dust particles from different dust source regions: The importance of particle mineralogy. *Atmospheric Environment*, *38*(36), 6253–6261.doi:10.1016/j.atmosenv.2004.07.010

Kubilay, N., Nickovic, S., Moulin, C., & Dulac, F. (2000). An illustration of the transport and deposition of mineral dust onto the eastern Mediterranean. *Atmospheric Environment*, *34*(8), 1293–1303. doi:10.1016/S1352-2310(99)00179-X

Kulshrestha, U. C., Sarkar, a. K., Srivastava, S. S., & Parashar, D. C. (1996). Investigation into atmospheric deposition through precipitation studies at New Delhi (India). *Atmospheric Environment*, *30*(24), 4149–4154. doi:10.1016/1352-2310(96)00034-9

Kulshrestha, U. C., Saxena, A., Kumar, N., Kumari, K. M., & Srivastava, S. S. (1998). Chemical composition and association of size-differentiated aerosols at a suburban site in a semi-arid tract of India. *Journal of Atmospheric Chemistry*, *29*(2), 109-118.

Kulshrestha, U. C., Kulshrestha, M. J., Sekar, R., Sastry, G. S. R., & Vairamani, M. (2003). Chemical characteristics of rainwater at an urban site of south-central India. *Atmospheric Environment*, *37*(21), 3019–3026. doi:10.1016/S1352-2310(03)00266-8

Kulshrestha, U. C. (2009). Atmospheric dust in India-A natural geo-engineering tool to combat climate change. *ENVIS Newsletter SES JNU ISSN-0974-1364*, *14*(3), 2-5.

Kulshrestha, U. (2013). Encyclopedia of Environmental Management. *Gas*, *6*(7), 8

Kulshrestha, M. J., Singh, R., Duarah, R., & Rao, P. G. (2014). Influence of crustal aerosols on wet deposition at a rural site of North-East India. *International Journal of Environmental Studies*, *71*(4), 510-525

Kulshrestha, U. C., Kulshrestha, M. J., Satyanarayana, J., & Reddy, L. A. K. (2014). Atmospheric deposition of reactive nitrogen in India. In *Nitrogen Deposition, Critical Loads and Biodiversity* (pp. 75-82). Springer Netherlands

Kumar, A., Sarin, M. M., & Sudheer, A. K. (2008). Mineral and anthropogenic aerosols in Arabian Sea–atmospheric boundary layer: Sources and spatial variability. *Atmospheric Environment*, *42*(21), 5169-5181

Kumar, A., Sudheer, A. K., & Sarin, M. M. (2008). Chemical characteristics of aerosols in MABL of Bay of Bengal and Arabian Sea during spring inter-monsoon: a comparative study. *Journal of earth system science*, *117*(1), 325-332

Kumar, A., & Sarin, M. M. (2009). Mineral aerosols from western India: Temporal variability of coarse and fine atmospheric dust and elemental characteristics. *Atmospheric Environment*, *43*(26), 4005–4013. doi:10.1016/j.atmosenv.2009.05.014

Kumar, A., & Sarin, M. M. (2010). Atmospheric water-soluble constituents in fine and coarse mode aerosols from high-altitude site in western India: Long-range transport and seasonal variability. *Atmospheric Environment*, *44*(10), 1245–1254. doi:10.1016/j.atmosenv.2009.12.035

Lawrence, C. R., & Neff, J. C. (2009). The contemporary physical and chemical flux of aeolian dust: A synthesis of direct measurements of dust deposition. *Chemical Geology*, *267*(1-2), 46–63. doi:10.1016/j.chemgeo.2009.02.005

Lefer, B. L., Talbot, R. W., & Munger, J. W. (1999). Nitric acid and ammonia at a rural northeastern US site. *Journal of Geophysical Research: Atmospheres (1984–2012)*, *104*(D1), 1645-1661.

Li, K. H., Song, W., Liu, X. J., Shen, J. L., Luo, X. S., Sui, X. Q., et al. (2012). Atmospheric reactive nitrogen concentrations at ten sites with contrasting land use in an arid region of central Asia. *Biogeosciences*, *9*(10), 4013–4021. doi:10.5194/bg-9-4013-2012

Liao, H., Adams, P. J., Chung, S. H., Seinfeld, J. H., Mickley, L. J., & Jacob, D. J. (2003). Interactions between tropospheric chemistry and aerosols in a unified general circulation model. *Journal of Geophysical Research: Atmospheres (1984–2012)*, *108*(D1), AAC-1.

Marticorena, B., & Bergametti, G. (1996). Dust Emissions, *23*(15), 1921–1924.

Martin, D., Bergametti, G., & Strauss, B. (1990). On the use of the synoptic vertical velocity in trajectory model: validation by geochemical tracers. *Atmospheric environment. Part A. General Topics*, *24*(8), 2059-2069.

Matsumoto, K., Minami, H., Uyama, Y., & Uematsu, M. (2009). Size partitioning of particulate inorganic nitrogen species between the fine and coarse mode ranges and its implication to their deposition on the surface ocean. *Atmospheric Environment*, *43*(28), 4259–4265. doi:10.1016/j.atmosenv.2009.06.014

Maxwell-Meier, K., Weber, R., Song, C., Orsini, D., Ma, Y., Carmichael, G. R., & Streets, D. G. (2004). Inorganic composition of fine particles in mixed mineral dust-pollution plumes observed from airborne measurements during ACE-Asia. *Journal of Geophysical Research D: Atmospheres*, *109*(19), 1–20. doi:10.1029/2003JD004464

Metzger, S., Mihalopoulos, N., & Lelieveld, J. (2006). Importance of mineral cations and organics in gas-aerosol partitioning of reactive nitrogen compounds: case study based on MINOS results. *Atmospheric Chemistry and Physics*, *6*(9), 2549-2567

Mian Chin, Diehl, T., Ginoux, P., & Malm, W. (2007). Intercontinental transport of pollution and dust aerosols: implications for regional air quality. *Atmospheric Chemistry and Physics Discussions*, *7*(3), 9013–9051. doi:10.5194/acpd-7-9013-2007

Norman, M., Das, S. N., Pillai, a. G., Granat, L., & Rodhe, H. (2001). Influence of air mass trajectories on the chemical composition of precipitation in India. *Atmospheric Environment*, *35*(25), 4223–4235. doi:10.1016/S1352-2310(01)00251-5

O'Hara, S. L., Clarke, M. L., & Elatrash, M. S. (2006). Field measurements of desert dust deposition in Libya. *Atmospheric Environment*, *40*(21), 3881-3897

Okin, G. S., & Gillette, D. A. (2001). Distribution of vegetation in wind-dominated landscapes: Implications for wind erosion modeling and landscape processes. *Journal of Geophysical Research: Atmospheres (1984–2012)*, *106*(D9), 9673-9683

Pachauri, T., Singla, V., Satsangi, A., Lakhani, A., & Maharaj Kumari, K. (2013). SEM-EDX characterization of individual coarse particles in Agra, India. *Aerosol and Air Quality Research*, *13*(2), 523–536. doi:10.4209/aaqr.2012.04.0095

Pandey, S. K., Tripathi, B. D., & Mishra, V. K. (2008). Dust deposition in a sub-tropical opencast coalmine area, India. *Journal of environmental management*, *86*(1), 132-138.

Parashar, D. C., Kulshrestha, U. C., & Jain, M. (2001). Precipitation and aerosol studies in India. *Environmental monitoring and assessment*, *66*(1), 47-61

Pillai, A. G., Naik, M. S., Momin, G. A., Rao, P. S. P., Safai, P. D., Ali, K., & Granat, L. (2001). Studies of wet deposition and dustfall at Pune, India. *Water, Air, and Soil Pollution*, *130*(1-4), 475-480

Pitts, B. F., & Pitts, J. N. (2000). Chemistry of the upper and lower atmosphere: Theory, experiments and applications

Prospero, J. M., & Lamb, P. J. (2003). African droughts and dust transport to the Caribbean: Climate change implications. *Science*, *302*(5647), 1024-1027

Ramanathan, V., Crutzen, P. J., Lelieveld, J., Mitra, a. P., Althausen, D., Anderson, J., et al. (2001). Indian Ocean Experiment: An integrated analysis of the climate forcing and effects of the great Indo-Asian haze. *Journal of Geophysical Research*, *106*(D22), 28371. doi:10.1029/2001JD900133

Rastogi, N., & Sarin, M. M. (2005). Long-term characterization of ionic species in aerosols from urban and high-altitude sites in western India: Role of mineral dust and anthropogenic sources. *Atmospheric Environment*, *39*(30), 5541–5554. doi:10.1016/j.atmosenv.2005.06.011

Rastogi, N., & Sarin, M. (2006). Atmospheric abundances of nitrogen species in rain and aerosols over a semi-arid region: sources and deposition fluxes. *Aerosol and Air Quality Research*, *6*(4), 406-417.

Ravi Krishna, R. (2012). Current atmospheric aerosol research in India. *Current Science*, *102*(3), 440–451

Reddy, L. A. K., Kulshrestha, U. C., Satyanarayana, J., Kulshrestha, M. J., & Moorthy, K. K. (2008). Chemical characteristics of PM10 aerosols and airmass trajectories over Bay of Bengal and Arabian Sea during ICARB. *Journal of earth system science*, *117*(1), 345-352

Reis, S., Pinder, R. W., Zhang, M., Lijie, G., & Sutton, M. a. (2009). Reactive nitrogen in atmospheric emission inventories, 7657–7677. doi:10.5194/acp-9-7657-2009

Rengarajan, R., Sarin, M. M., & Sudheer, a. K. (2007). Carbonaceous and inorganic species in atmospheric aerosols during wintertime over urban and high-altitude sites in North India. *Journal of Geophysical Research: Atmospheres*, *112*(21), 1–16. doi:10.1029/2006JD008150

Rengarajan, R., Srinivas, B., & Sarin, M. M. (2010). Atmospheric deposition of reactive nitrogen over continental sites and oceanic regions of India : A review, 1–14

Ruijrok, W., Davidson, C. I., & Nicholson, W. (1995). Dry deposition of particles. *Tellus B*, *47*(5), 587-601.

Russell, K. M., Keene, W. C., Maben, J. R., Galloway, J. N., & Moody, J. L. (2003). Phase partitioning and dry deposition of atmospheric nitrogen at the mid-Atlantic US coast. *Journal of Geophysical Research: Atmospheres (1984–2012)*, *108*(D21)

Salam, A., Bauer, H., Kassin, K., Ullah, S. M., & Puxbaum, H. (2003). Aerosol chemical characteristics of a mega-city in Southeast Asia (Dhaka–Bangladesh). *Atmospheric Environment*, *37*(18), 2517-2528

Satsangi, A., Pachauri, T., Singla, V., Lakhani, A., & Maharaj Kumari, K. (2013). Water soluble ionic species in atmospheric aerosols: Concentrations and sources at agra in the indo-gangetic plain (IGP). *Aerosol and Air Quality Research*, *13*(6), 1877–1889. doi:10.4209/aaqr.2012.08.0227

Satsangi, G. S., Lakhani, a., Khare, P., Singh, S. P., Kumari, K. M., & Srivastava, S. S. (2002). Measurements of major ion concentration in settled coarse particles and aerosols at a semiarid rural site in India. *Environment International*, *28*(1-2), 1–7. doi:10.1016/S0160-4120(01)00122-2

Seinfeld, J. H., Carmichael, G. R., Arimoto, R., Conant, W. C., Brechtel, F. J., Bates, T. S., & Zhang, X. Y. (2004). ACE-ASIA-Regional climatic and atmospheric chemical effects of Asian dust and pollution. *Bulletin of the American Meteorological Society*, *85*(3), 367-380

Seinfeld, J. H., & Pandis, S. N. (2012). *Atmospheric chemistry and physics: from air pollution to climate change*. John Wiley & Sons

Sellegri, K., Gourdeau, J., Despiau, S., & Putaud, J. P. (2001). Chemical composition of marine aerosol in a Mediterranean coastal zone during the FETCH experiment. *Journal of geophysical research*, *106*(D11), 12023-12037

Shen, Z., Caquineau, S., Cao, J., Zhang, X., Han, Y., Gaudichet, A., & Gomes, L. (2009). Mineralogical characteristics of soil dust from source regions in northern China. *Particuology*, *7*(6), 507-512

Shen, Z., Wang, X., Zhang, R., Ho, K., Cao, J., & Zhang, M. (2011). Chemical composition of water-soluble ions and carbonate estimation in spring aerosol at a semi-arid site of Tongyu, China. *Aerosol and Air Quality Resarch*, *11*(4), 360-368

Simpson, D., Butterbach-Bahl, K., Fagerli, H., Kesik, M., Skiba, U., & Tang, S. (2006). Deposition and emissions of reactive nitrogen over European forests: A modelling study. *Atmospheric Environment*, *40*(29), 5712–5726. doi:10.1016/j.atmosenv.2006.04.063

Singh, S., & Kulshrestha, U. C. (2012). Abundance and distribution of gaseous ammonia and particulate ammonium at Delhi, India. *Biogeosciences*, *9*(12), 5023–5029. doi:10.5194/bg-9-5023-2012

Singh, S., & Kulshrestha, U. C. (2014). Rural versus urban gaseous inorganic reactive nitrogen in the Indo-Gangetic plains (IGP) of India. *Environmental Research Letters*, *9*(12), 125004. doi:10.1088/1748-9326/9/12/125004

Smith, A. M., Keene, W. C., Maben, J. R., Pszenny, A. A., Fischer, E., & Stohl, A. (2007). Ammonia sources, transport, transformation, and deposition in coastal New England during summer. *Journal of Geophysical Research: Atmospheres (1984–2012)*, *112*(D10)

Song, C. H., & Carmichael, G. R. (2001). Gas-particle partitioning of nitric acid modulated by alkaline aerosol. *Journal of Atmospheric Chemistry*, *40*(1), 1–22. doi:10.1023/A:1010657929716

Spokes, L. J., Yeatman, S. G., Cornell, S. E., & Jickells, T. D. (2000). Nitrogen deposition to the eastern Atlantic Ocean. The importance of south-easterly flow. *Tellus, Series B: Chemical and Physical Meteorology*, *52*(1), 37–49. doi:10.1034/j.1600-0889.2000.00062.x

Squizzato, S., Masiol, M., Brunelli, a., Pistollato, S., Tarabotti, E., Rampazzo, G., & Pavoni, B. (2013). Factors determining the formation of secondary inorganic aerosol: A case study in the Po Valley (Italy). *Atmospheric Chemistry and Physics*, *13*(4), 1927–1939. doi:10.5194/acp-13-1927-2013

Sullivan, R. C., Guazzotti, S. a., Sodeman, D. a., & Prather, K. a. (2006). Direct observations of the atmospheric processing of Asian mineral dust. *Atmospheric Chemistry and Physics Discussions*, *6*(3), 4109–4170. doi:10.5194/acpd-6-4109-2006

Sutton, M. a., Erisman, J. W., Dentener, F., & Möller, D. (2008). Ammonia in the environment: From ancient times to the present. *Environmental Pollution*, *156*(3), 583–604. doi:10.1016/j.envpol.2008.03.013

Tegen, I., & Fung, I. (1994). Modeling of mineral dust in the atmosphere: Sources, transport, and optical thickness. *Journal of Geophysical Research: Atmospheres (1984–2012)*, *99*(D11), 22897-22914

Tegen, I., & Fung, I. (1995). Contribution to the atmospheric mineral aerosol load from land surface modification. *Journal of Geophysical Research: Atmospheres (1984–2012)*, *100*(D9), 18707-18726

Tegen, I., Harrison, S. P., Kohfeld, K. E., Engelstaedter, S., & Werner, M. (2002). Emission of soil dust aerosol: Anthropogenic contribution and future changes. *Geochimica Et Cosmochimica Acta*, *66*(15A), A766

Tørseth, K., Aas, W., Breivik, K., Fjæraa, A. M., Fiebig, M., Hjellbrekke, A. G., & Yttri, K. E. (2012). Introduction to the European Monitoring and Evaluation Programme (EMEP) and observed atmospheric composition change during 1972–2009. *Atmospheric Chemistry and Physics*, *12*(12), 5447-5481

Uno, I., Uematsu, M., Hara, Y., He, Y. J., Ohara, T., Mori, A., & Bandow, H. (2007). Numerical study of the atmospheric input of anthropogenic total nitrate to the marginal seas in the western North Pacific region. *Geophysical Research Letters*, *34*(17)

Usher, C. R., Michel, A. E., & Grassian, V. H. (2003). Reactions on Mineral Dust Reactions on Mineral Dust. *New York*, *103*(November), 4883–4940. doi:10.1021/cr020657y

Van Vuuren, D. P., Bouwman, L. F., Smith, S. J., & Dentener, F. (2011). Global projections for anthropogenic reactive nitrogen emissions to the atmosphere: An assessment of scenarios in the scientific literature. *Current Opinion in Environmental Sustainability*, *3*(5), 359–369. doi:10.1016/j.cosust.2011.08.014

Venkataraman, C., Reddy, C. K., Josson, S., & Reddy, M. S. (2002). Aerosol size and chemical characteristics at Mumbai, India, during the INDOEX-IFP (1999). *Atmospheric Environment*, *36*(12), 1979-1991.

Verma, S. K., Deb, M. K., Suzuki, Y., & Tsai, Y. I. (2010). Ion chemistry and source identification of coarse and fine aerosols in an urban area of eastern central India. *Atmospheric Research*, *95*(1), 65-76

Vet, R., Artz, R. S., Carou, S., Shaw, M., Ro, C. U., Aas, W., et al. (2014). A global assessment of precipitation chemistry and deposition of sulfur, nitrogen, sea salt, base cations, organic acids, acidity and pH, and phosphorus. *Atmospheric Environment*, *93*, 3–100. doi:10.1016/j.atmosenv.2013.10.060

Wallace, J. M., & Hobbs, P. V. (2006). *Atmospheric science: an introductory survey* (Vol. 92). Academic press

Walworth, J. (2013). Nitrogen in Soil and the Environment, (2), 3–5.

Who. (1999). Chapter 1 - Dust : Definitions and Concepts. *Hazard Prevention and Control in the Work Environment: Airborne Dust*, 1–96

Wu, F., Zhang, D., Cao, J., Zhang, T., & An, Z. (2014). Background-like nitrate in desert air. *Atmospheric Environment*, *84*(x), 39–43. doi:10.1016/j.atmosenv.2013.11.043

Zarasvandi, A., Carranza, E. J. M., Moore, F., & Rastmanesh, F. (2011). Spatio-temporal occurrences and mineralogical–geochemical characteristics of airborne dusts in Khuzestan Province (southwestern Iran). *Journal of geochemical exploration*, *111*(3), 138-151

Zdanowicz, C. M., Zielinski, G. A., & Wake, C. P. (1998). Characteristics of modern atmospheric dust deposition in snow on the Penny Ice Cap, Baffin Island, Arctic Canada. *Tellus B*, *50*(5), 506-520

Zellweger, C., Forrer, J., Hofer, P., Nyeki, S., Schwarzenbach, B., Weingartner, E., et al. (2002). Partitioning of reactive nitrogen (NO_y) and dependence on meteorological conditions in the lower free troposphere. *Atmospheric Chemistry and Physics Discussions*, *2*(6), 2259–2296. doi:10.5194/acpd-2-2259-2002

Zhang, X. Y., Arimoto, R., Zhu, G. H., Chen, T., & Zhang, G. Y. (1998). Concentration, size-distribution and deposition of mineral aerosol over Chinese desert regions. *Tellus B*, *50*(4), 317-330

Zhang, D., Iwasaka, Y., Shi, G., Zang, J., Matsuki, A., & Trochkine, D. (2003). Mixture state and size of Asian dust particles collected at southwestern Japan in spring 2000. *Journal of Geophysical Research: Atmospheres (1984–2012)*, *108*(D24)